KU LEUVEN

FACULTEIT INGENIEURSWETENSCHAPPEN

# Photochemical Recovery of Europium from Rare Earth Mixtures

Daphne Havaux

Thesis submitted for the degree of
Master of Science in
Chemical Engineering, option
Environmental engineering

**Thesis supervisors:**
Prof. dr. ir. T. Van Gerven
Prof. dr. K. Binnemans

Academic year 2013 – 2014

**Master of Science in Chemical Engineering**

KU LEUVEN

FACULTEIT INGENIEURSWETENSCHAPPEN

# Photochemical Recovery of Europium from Rare Earth Mixtures

Daphne Havaux

Thesis submitted for the degree of
Master of Science in
Chemical Engineering, option
Environmental engineering

**Thesis supervisors:**
Prof. dr. ir. T. Van Gerven
Prof. dr. K. Binnemans

**Assessors:**
Prof. dr. ir. R. Dewil
M. Baka

**Mentor:**
B. Van den Bogaert

Academic year 2013 – 2014

# Foreword

I would like to take this opportunity to express my sincerest gratitude and recognition towards all the people who supported me during this Master Thesis year.
First of all, my recognition goes out to my supervisors, Prof. Dr. Ir. Tom Van Gerven and Prof. Dr. Koen Binnemans, who guided me through this most challenging project with their knowledge and enthusiasm. The advice and assistance they gave me during our monthly meetings were of great value to keep me motivated and to lead me into the right direction.
A special word of thanks goes out to my daily supervisor, Bart Van den Bogaert, from whom I received a lot of help and encouragement. Thank you, Bart, for the support and patient guidance during this year. Please know that your helpfulness, your availability to answer my questions and your quick and productive responses were profoundly appreciated.
Furthermore, I would like to express my gratitude to all the people who assisted me in the lab and helped creating a pleasant work environment, in particular Michèle Vanroelen, who carried out the ICP-MS measurements, and Jeroen Jacobs, for helping me with the determination and interpretation of the crystal structures.
In addition, I owe a lot to my fellow students for offering me friendships for live and for making my study period in Leuven an unforgettable experience.
Last but certainly not least, I am very much obliged to my family, especially to my parents and my sister Valérie, for constantly supporting me and for being there whenever I needed them.

*Daphné Havaux*

# Table of Contents

# Abstract

The rare earths encounter an increasing popularity in today's society due to their usage in numerous high tech and modern applications. Some of these metals are scarce as their name suggests, while their demand continues to rise by cause of their economic, strategic and geopolitical relevance. World's largest rare earth producer, China, is responsible for more than 90 % of the global rare earth supply. However, since it faces increasing domestic demands, China is currently restricting its export. Consequentially, the global market suffers from a critical shortage of rare earths. The limited availability has caused a positive incentive in the search for sustainable recycling methods and alternative separation techniques. The photochemical separation of rare earths is entirely in line with this purpose of 'urban mining'. This thesis examines the various parameters that affect the photochemical separation of rare earth elements in an aqueous solution, with the aim that this technology can contribute to the recycling of industrial waste streams such as the relevant europium/yttrium -mixtures present in lamp phosphors.

This innovative separation technique consists of two main parts: the selective photochemical reduction of europium(III), followed by the chemical separation. The absorption of UV-light, originating from low-pressure mercury lamps (LPML) with main light output at 185 and 254 nm, induces the transfer of an electron from the ligands to the central europium(III)-ion via a ligand-to-metal charge-transfer (LMCT-band). Europium(III) is hereby selectively reduced to the divalent europium(II). Subsequently, the divalent europium is removed from the solution by precipitation as insoluble $EuSO_4$. Strictly speaking, the selectivity of the separation arises from the specificity of the redox reaction through the LMCT-bands. Europium(III) has a water-to-europium charge transfer band at 188 nm, which corresponds to the light output at 185 nm of the LPML. In addition, sulfate, next to its role as a precipitating agent, creates an extra sulfate-to-europium LMCT-band at 240 nm, which overlaps with the 254 nm output of the light source. Additives can therefore generate new absorption bands and thereby allow us to work at longer (i.e. more energy-efficient) wavelengths.

The influence of chemical and spectral parameters was identified and evaluated in terms of separation efficiency and selectivity. A so-called scavenger is added to the mixtures, i.e. an organic compound that neutralizes reactive hydroxyl radicals which are formed along with the photochemical reduction reaction. These radicals cause an undesirable back reaction via oxidation of divalent europium. Isopropanol and formic acid were tested as scavenger. With regard to formic acid, shorter illumination times are required to achieve the same europium removal. This can be attributed to the absorption of light by formic acid at 260 nm, thereby forming reactive radicals which cause an additional reduction of europium(III). The main disadvantage of this scavenger is its strong acidity, which causes the need to work at low pH (0-1). Isopropanol, on the other hand, has no additional photochemical reducing effect, but allows higher pH. This leads to better results in terms of illumination times since the pH of the aqueous phase influences the speed of the photochemical reaction.

An increase in the basicity from pH 0 to pH 4 leads to faster reactions. This observation has been linked to the presence of protons at low pH, which promote the unwanted oxidation of divalent to trivalent europium. Additionally, divalent europium is more stable in less acidic media. pH values higher than or equal to 6 cause hydrolysis, which leads to hydroxide precipitation of all the rare earths, so that no selective separation can be achieved. The most efficient separation was therefore obtained at pH 4.

Next to the equimolar mixtures, (synthetic simulated) industrial europium/yttrium-mixtures with different molar ratios were also investigated. The higher the excess of yttrium, the slower the europium removal takes place. However, longer illumination times yield the same removal-percentage (> 90 %) and selectivity (~ 100 %) for europium. Consequently, the excess of yttrium only induces a kinetic effect that entails an additional difficulty with regard to the reduction of illumination times. A possible way to tackle this problem is to use stronger lamps with higher irradiance. This leads to faster reactions and allows shorter residence times. High and homogeneous irradiances, corresponding to the absorption band of the forward reaction (185 and 254 nm), accelerate the reaction. Analogously, low irradiances for the photochemical backward reaction (at 366 nm) increase the efficiency of the separation.

The experiments clearly indicate that the photochemical technique works and that it is characterized by high efficiency and selectivity. Pure $EuSO_4$ precipitation was obtained without co-precipitation of other rare earths. Therefore, we can conclude that the selective photochemical reduction of europium(III) is a promising technique to remove europium from rare earths mixtures in a very efficient manner. This technique has great potential to be used in the recycling of europium in waste streams of lamp phosphors and could thus provide an answer to the current scarcity of europium.

# Samenvatting

De zeldzame aarden winnen aan belangstelling in onze huidige samenleving omwille van hun talrijke toepassingsmogelijkheden in o.m. hoogtechnologische en duurzame sectoren. Zoals hun naam doet vermoeden, zijn sommige van deze metalen schaars. Vanwege hun economisch, strategisch en geopolitiek belang blijft de vraag ernaar echter toenemen. China produceert 90 % van alle zeldzame aarden, maar kampt met een stijgende binnenlandse vraag. Daarom voert China hoe langer hoe minder zeldzame aarden uit, en dreigt er een nakend tekort aan zeldzame aarden op de wereldmarkt. De beperkte beschikbaarheid veroorzaakt een positieve stimulans in het onderzoek naar duurzame recyclagemethoden en alternatieve scheidingstechnieken. De fotochemische scheiding van zeldzame aarden kadert volledig in deze visie van stadsmijnbouw. Deze masterproef onderzoekt de verschillende parameters die de fotochemische scheiding van zeldzame aarden in een waterige oplossing beïnvloeden, zodanig dat deze technologie kan bijdragen tot de recyclage van industrieel relevante afvalstromen, zoals europium/yttrium-mengsels uit lampfosforen.

Deze innovatieve scheidingstechniek bestaat uit twee belangrijke delen: de selectieve fotochemische reductie van europium(III), gevolgd door een chemische scheiding. De absorptie van UV-licht, afkomstig van lage druk kwiklampen die hun voornaamste lichtoutput bij 185 en 254 nm hebben, veroorzaakt een elektronenoverdracht van liganden naar europium(III) via een ladingsoverdrachtband (*charge-transfer band)*. Europium(III) wordt hierbij selectief gereduceerd naar tweewaardig europium(II). Vervolgens wordt tweewaardig europium uit de oplossing verwijderd door precipitatie als onoplosbare $EuSO_4$. Met andere woorden, de selectiviteit van de scheiding vloeit voort uit de specificiteit van de redoxreacties via de CT-banden. Driewaardig europium bezit een water-naar-europium ladingsoverdrachtband bij 188 nm, die goed overeenkomt met de lichtoutput van lage druk kwiklampen bij 185 nm. Daarnaast creëert sulfaat, naast zijn rol als neerslagreagens om het tweewaardig europium te verwijderen, een extra ladingsoverdrachtband van sulfaat-naar-europium bij 240 nm. De invloed van chemische en lichtbronparameters werd in kaart gebracht en geëvalueerd op vlak van scheidingsefficiëntie en selectiviteit.

Aan de mengsels wordt een zogenaamde “scavenger” toegevoegd, een organische

verbinding die hydroxylradicalen, gevormd bij de fotochemische reductie, neutraliseert. Deze radicalen veroorzaken immers een ongewenste terugreactie via oxidatie van tweewaardig europium. Zowel isopropanol als mierenzuur werden getest als scavenger. Met betrekking tot mierenzuur kwam men tot de vaststelling dat dit kortere belichtingstijden vereist om dezelfde europium-verwijdering te verwezenlijken. Mierenzuur absorbeert namelijk licht bij 260 nm en vormt hierbij reactieve radicalen die een additionele reductie van driewaardig europium veroorzaken. Het grote nadeel van deze scavenger is de sterke zuurheid, waardoor steeds bij lage pH (0–1) gewerkt moet worden. Isopropanol daarentegen heeft geen extra reducerende werking, maar laat hogere pH-waarden toe, wat leidt tot betere resultaten inzake belichtingstijd.

De pH van de waterige fase beïnvloedt de snelheid van de fotochemische reactie. Een stijging van de pH van 0 tot 4 leidt tot snellere reacties. Deze waarneming is gekoppeld aan de aanwezigheid van protonen bij lage pH die de ongewenste terugoxidatie van divalent tot trivalent europium promoten. Bij lage pH waarden is tweewaardig europium ook minder stabiel. pH-waarden hoger dan 6 veroorzaken hydrolyse, wat leidt tot hydroxide-neerslag van alle zeldzame aarden, waardoor er geen selectieve scheiding bereikt kan worden. De efficiëntste scheiding werd bijgevolg bekomen bij pH 4.

Naast equimolaire mengsels werden er ook (synthetisch gesimuleerde) industriële europium/yttrium-mengsels bij verschillende molaire verhoudingen onderzocht. Hoe hoger de overmaat aan yttrium, des te trager de europium-verwijdering plaatsvindt. Langere belichtingstijden geven evenwel dezelfde verwijderingspercentages (> 90 %) en selectiviteit (~ 100 %) voor europium. Bijgevolg veroorzaakt de overmaat aan yttrium slechts een kinetisch effect dat een extra moeilijkheid met zich meebrengt inzake het reduceren van belichtingstijden. Een mogelijke oplossing hiervoor is het gebruik van intensere lampen met een hogere irradiantie. Dit leidt tot snellere reacties, een noodzakelijke voorwaarde om in de toekomst om te schakelen van batch naar continue systemen. Hoge en homogene irradianties, overeenkomend met de absorptieband van de voorwaartse reactie (185 en 254 nm), versnellen de reactie. Bijkomend zullen lage irradianties bij de fotochemische terugwaartse reactie (bij 366 nm) een vermindering in belichtingstijd in de hand werken en de efficiëntie nog verhogen.

De experimenten tonen zonder enige twijfel aan dat de fotochemische techniek werkt en gekenmerkt wordt door een hoge efficiëntie en selectiviteit. Zuivere $EuSO_4$ neerslag werd bekomen zonder co-precipitatie van andere zeldzame aarden. Deze techniek heeft aldus een groot potentieel om ingezet te worden in de recyclage van europium uit europium-yttrium afvalstromen van lampfosforen en kan op die manier een antwoord bieden aan de huidige schaarste aan europium.

# List of Figures and Tables

## List of Figures

## List of Tables

# List of Abbreviations and Symbols

| | |
|---|---|
| RE | Rare Earth |
| REEs | Rare Earth Elements |
| Z | Atomic number |
| LREE | Light Rare Earth Element |
| HREE | Heavy Rare Earth Element |
| HEV | Hybrid electric vehicle |
| $E^0$ | Reduction potential |
| $e^-$ | Electron |
| at.% | Atom percentage |
| WTO | World Trade Organisation |
| D | Distribution ratio |
| $c_{org}$ | RE concentration in the organic phase |
| $c_{aq}$ | RE concentration in the aqueous phase |
| ß | Separation factor |
| DEHPA | Di(2-ethylhexyl)phosphoric acid |
| CT-band | Charge-transfer band |
| LMCT | Ligand-to-metal charge-transfer |
| LPML | Low pressure mercury lamp |
| HPML | High pressure mercury lamp |
| LED | Light emitting diode |
| ICP-MS | Inductively coupled plasma mass spectrometry |
| PQ | PlasmaQuad |
| ppm | Parts per million |
| ppb | Parts per billion |
| vol% | Volume percentage |
| TXRF | Total reflection X-ray fluorescence |
| UV-Vis Spectroscopy | Ultraviolet-visible spectroscopy |
| $I_0$ | Intensity of the reference beam |
| I | Intensity of the detector beam |
| A | Absorbance |
| ε | Molar extinction coefficient |
| HSE | Health, safety and environment |
| RSD | Relative standard deviation |
| $K_{sp}$ | Solubility product |
| $[REE]_{initial}$ | Initial (before illumination ) rare earth concentration |
| $\varepsilon_r$ | Dielectric constant |
| R | Universal gas constant |
| T | Absolute temperature |
| p | Partial pressure |

| | |
|---|---|
| n | Number of moles |
| F | Faraday constant |
| λ | Wavelength |
| $pH_{initial}$ | pH before addition of scavenger |
| $pH_{final}$ | pH after addition of scavenger |
| THF | Tetrahydrofuran |
| HMPA | Hexamethylfosforamide |

# 1. Introduction

Due to their unique magnetic, catalytic and phosphorescent properties, rare earths are utilized in a wide range of applications going from high-tech electronic devices to green-energy and medical applications. Rare earths are highly analogous in chemical characteristics. A keynote property is that these metals are typically found in a trivalent oxidation state. The rare earth element europium has a stable divalent state in water as well and will be highlighted regarding its chemical properties in chapter two. Emphasis is put on the use of europium in lamp phosphors in chapter three, considering that some of the europium containing mixtures used in the experimental part of this master thesis, are based on the chemical composition of commercial lamp phosphors.

The name 'rare earths' is misleading, as these metals are fairly abundant in the earth's crust. Rare earths are however scarce on the global supply market, as will be elucidated in chapter four. The shortage of these precious metals causes economic and political concerns. Consequently, governments focus attention on the research of new recycling and separation technologies. As will be elaborated in chapter five, there is an important chemical similarity between the different rare earth elements, causing the separation of a rare earth mixture into usable fractions to be time-consuming and expensive. Separation is currently carried out by solvent extraction in which hundreds of extraction stages are required in order to reach the purity requirements of most applications. Other separation techniques exploit differences in oxidation state in order to selectively remove the non-trivalent elements. The selective reduction/oxidation techniques can be realized in a chemical, electrochemical or photochemical way.

In this master thesis, emphasis is put on the photochemical separation technique whereby the photochemical reduction is linked with a separation stage. Concretely, the absorption of light transfers an electron from a complexing ligand to the central rare earth ion, thereby reducing the trivalent rare earth element to the divalent state. The final separation is

obtained by exploiting the different chemical properties of the divalent element compared to the trivalent REE in the mixture. This will be explained in more detail in chapter six.

The actual goal is to investigate the influences of the separation of $Eu^{3+}$-containing rare earth mixtures, by the photochemical reduction of europium to $Eu^{2+}$, followed by precipitation as $EuSO_4$. The photochemical separation efficiency and selectivity is explored by varying different parameters in chapter nine. The experimental part can be subdivided in two main discussions. In the first place, the *chemical parameters* are varied: e.g. the concentration of the precipitating agent, the pH of the aqueous solution, the type of scavenger and the molar ratios of rare earths. Secondly, the *spectral parameters*, such as the spectral irradiance, the region of wavelength emission, the homogeneity and distance of irradiation, are investigated with regard to their influence on the thermodynamics and kinetics of the separation.

Photochemical redox separation requires further research to overcome the existing barriers, such as the long illumination times. The (spectral) influences need to be further characterised when targeting commercial and industrial applications, as will become clear in chapter ten. However, due to its outstanding selectivity, very efficient separations can be performed. This makes photochemical separation a very promising technique for the recycling of rare earths.

This master thesis is part of the research activities done within 'Research Platform for the Advanced Recycling and Re-use of Rare Earths' ($RARE^3$) [1]. This is a KU Leuven project that focuses on innovative and sustainable recycling processes for rare earths, joined with inventive separation technologies.

# 2. Rare Earths

## 2.1 Rare Earth Elements

The rare earth elements (REEs) are a group of chemical elements containing the 15 lanthanides from lanthanum to lutetium (atomic number Z = 57-71), together with scandium (Z = 21) and yttrium (Z = 39) shown in the periodical table in Figure 1 [2]. A distinction is made between the light rare earth elements (LREEs): La-Eu & Sc, and the less abundant heavy rare earth elements (HREEs): Gd-Lu & Y.

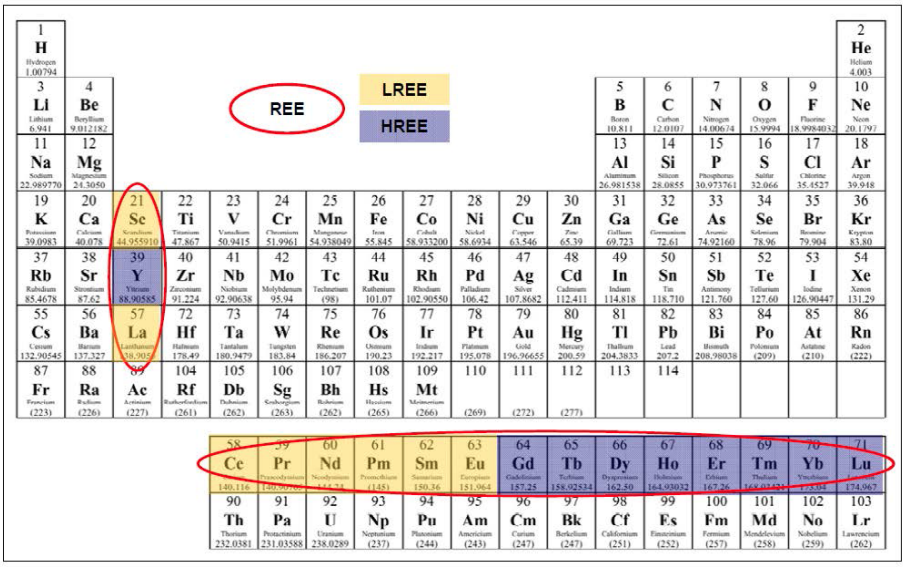


**Figure 1: The 17 REEs in the Periodic Table [2].**

The lanthanide group shows similar chemical properties due to the specific atomic configuration of the rare earths. There is a gradual filling of electrons in the 4f orbitals as more protons are added to the nucleus of the lanthanides. The main difference with the other metals is that the valence electrons are not situated in the outermost shell, but in the 4f orbitals, resulting in a shielding of the 4f electrons by the filled 5s and 5p orbitals. The rather stable outer shell configuration of the lanthanides leads to similar chemical properties of the rare earths and hence difficulties in their separation [3].

Rare earths are typically present as trivalent ions in aqueous solutions. However, in addition to the trivalent oxidation state, Ce, Pr and Tb exhibit the tetravalent state and Sm, Eu and Yb occur in the divalent state as well [4].

Rare earths are used in many applications, enhancing a low-carbon future, particularly in the renewable energy and transportation sectors [5]. Permanent magnets containing rare earths (neodymium and dysprosium) are for instance used in wind turbine generators and electric and hybrid vehicle technologies (HEV's). Furthermore, rare earths are used as catalysts for increasing gasoline yield or as additives (mainly cerium) to reduce sulfur oxide emissions ($SO_x$) for fluid catalytic cracking in petroleum refining [2]. Another 'green application' of rare earths is the usage in fluorescent lighting in order to lower green house gas emissions and energy use compared to incandescent light bulbs [5].

## 2.2 Europium

In this section, emphasis is put on one of the REEs, more precisely europium, considering that the experimental part of this master thesis covers the photochemical separation of rare earth mixtures containing europium.

### 2.2.1 Properties

Europium is a member of the lanthanide group with the symbol Eu and atomic number 63. Europium has the second lowest melting point and the lowest density of all lanthanides [6]. It is considered as a light rare earth. The electronic configuration of the europium atom is $[Xe]4f^76s^2$. Hence, the electron shell configurations of Eu(II) and Eu(III) are $[Xe]4f^7$ and $[Xe]4f^6$ respectively.

As already mentioned, europium does not only have a stable trivalent oxidation state, but a divalent state as well. Eu(III) has a high standard redox potential in water, namely $Eu(III) + e^- \rightarrow Eu(II)$; $E^0 = -0.34V$ [4]. This reflects the stability of the divalent state due to the half-filled 4f subshell. Both oxidation states of europium have luminescent properties. Europium plays a crucial role in the fluorescent lightning sector. It is used in high-energy efficiency lighting applications that lower green house gas emissions and energy use compared to incandescent light bulbs. The fluorescent properties of europium and its applications will be discussed more accurately and thoroughly in chapter three.

### 2.2.2 Occurrence

Europium has a low abundance in nature; it is present in the earth's crust at a concentration of about 1.8 grams per tonne [7]. To put this in perspective, the crustal abundance of europium is almost as abundant as tin [8]. It is not found free in nature, but in several minerals. These minerals are typically depleted or enriched in europium compared to that of other rare earths. This is known as the europium anomaly [9] [10]. This partition difference is attributed to the stable divalent state of europium that causes differences in tendency to be incorporated in the minerals [10]. An overview of the europium composition of the different rare earth-containing ores is illustrated in Table 1 in mass percentage [10]. Please notice that the composition of a specific ore varies according to the location. Commercially, europium is mainly obtained by solvent extraction to isolate the individual rare earth from the ore, which generally contains multiple lanthanides. Refinement to pure metal is difficult with the conventional separation methods, taking into account the chemical similarity of the REEs [11].

**Table 1: Ores containing europium [10]**

| Ore | Europium content (%) |
|---|---|
| Monazite | 0.10 |
| Bastnäsite | 0.12 |
| Xenotime | 0.20 |

Europium (together with dysprosium, neodymium, terbium and yttrium) is defined by the U.S. Department of Energy (DOE) as critical on the short-term (until 2015) and critical on the mid-term (2015-2025) (Figure 2 and Figure 3) [12]. The term 'critical' is based on the importance to clean-energy and on the supply risk [12].

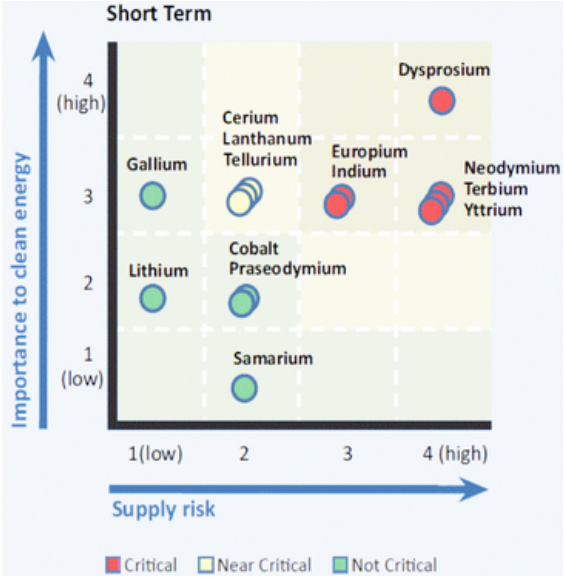


**Figure 2: Criticality matrix for the short-term (present-2015) [12].**

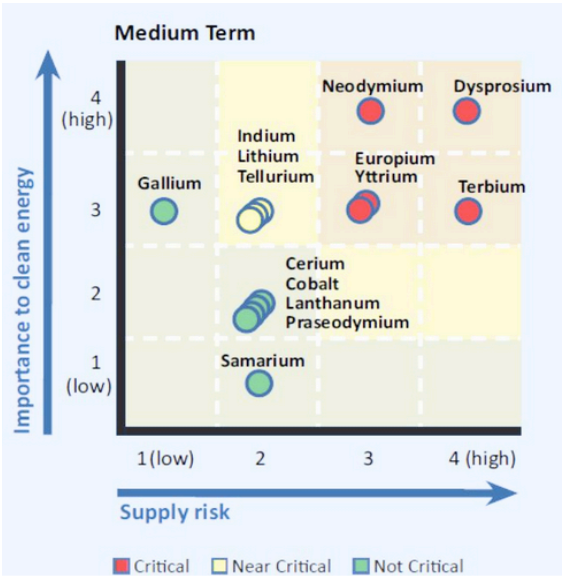


**Figure 3: Criticality matrix for the medium term (2015-2025) [12].**

# 3. Applications of Europium

High purity europium offers a great market importance due to its wide range of substantial applications. It is used in display materials such as field emission displays and laser devices, in euro banknotes as a security measure (Figure 4) [13], but also in lighting applications such as tricolor fluorescent lamps [14]. Focus is put on the latter in the following sections, taking into consideration that some REE mixtures that are used in the experimental part of the master thesis are based on commercial REE mixtures applied in lamp phosphors.

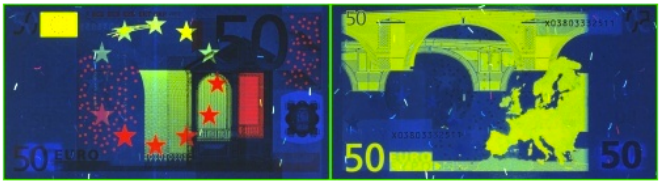

**Figure 4: Euro banknotes containing europium [13].**

## 3.1 Lamp Phosphors

### 3.1.1 Components

A lamp phosphor is visualized in Figure 5 [15] showing the different components of the lamp. The cathode is made out of coiled tungsten filaments. The glass tube is filled with inert gas argon and a small quantity of mercury. The amount of mercury in a fluorescent lamp ranges between 3.5 to 15 mg, depending on the type of fluorescent lamp, the manufacturer, and the date of manufacturing of the fluorescent lamp [16].

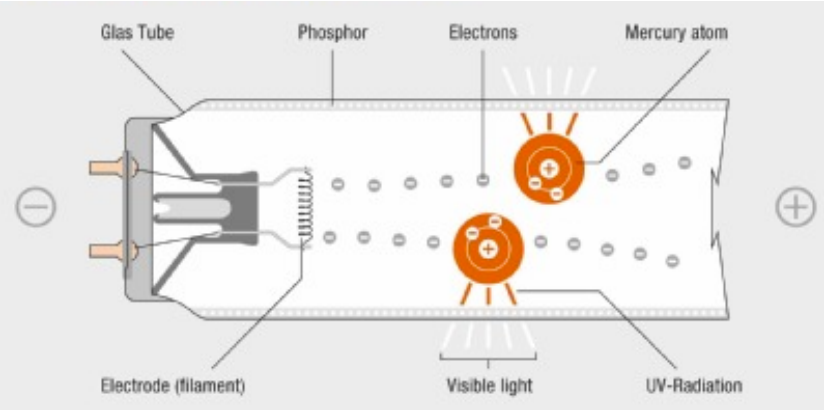


**Figure 5: Illustration of a fluorescent lamp [15].**

The inside of the lamp is coated with multiple layer coatings. The glass is firstly coated with a barrier layer containing alumina ($Al_2O_3$), followed by a second layer of phosphor coating [17]. The barrier layer is a good protector of the glass against the attack of mercury vapor, because it retards the take-up of mercury by the glass. It enables the reduction of the amount of mercury that is needed in the lamp, which is an environmental concern. Additionally, it is a good UV reflector in the sense that UV which penetrates the rare earth phosphor layer, is reflected by the alumina and has a second chance to be reabsorbed by the rare earth phosphor coating [11].

### 3.1.2 Working Principle

Firstly, electrical energy is converted into invisible UV radiation: when current flows into the electrodes, electrons are emitted. This causes an excitation of mercury atoms that emit their characteristic UV radiation (predominately at 254 nm and 185 nm) [18]. Secondly, the incident UV-energy is absorbed by the triphosphor coating and converted into visible UV light.

## 3.2 Phosphors

It became clear from the previous section that the triphosphor coating is crucial for converting the UV light to visible light in the lamp phosphors. The characteristics and composition of the coating will be stated next.

### 3.2.1 Luminescence

The luminescent materials are called phosphors and are mostly solid inorganic materials consisting of a host lattice that is intentionally doped during synthesis with impurities called activators. The activator concentration is generally low considering the fact that at high concentrations the efficiency of the luminescence process sometimes decreases due to concentration quenching [19]. Additionally, the activator ions are commonly quite expensive. The absorption of energy takes place via the doped material or exceptionally through the host lattice. Sometimes secondary dopants, i.e. sensitizers, are used to absorb the exciting radiation when the absorption of energy by the primary activators is too weak [20]. The emission practically always originates from the impurities [17].

Figure 6 displays the energy level diagram of divalent and trivalent europium ions. The horizontal lines represent narrow energy states of the 4f levels and the triangles indicate the levels from which radiative transitions can occur [20].

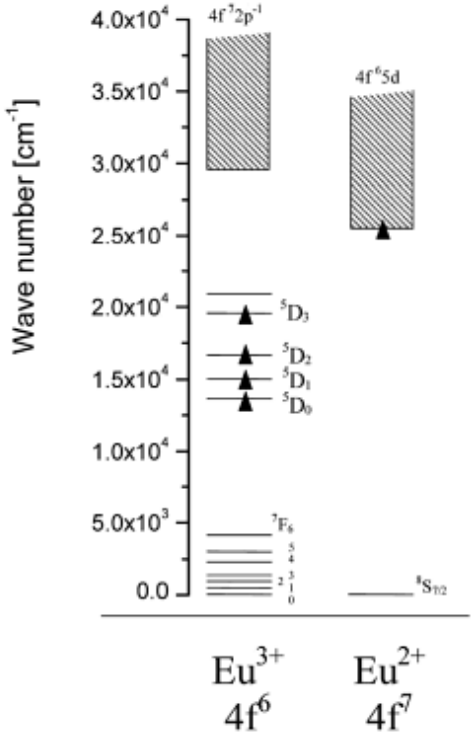


**Figure 6: Energy level diagram of $Eu^{3+}$ and $Eu^{2+}$ [20].**

The theory of luminescence can be briefly summarized as follows; the activator is in the lowest energy state, namely the ground state, at low temperatures. When the activator absorbs energy, a transition to an excited non-equilibrium vibrational level occurs. The optical centre undergoes anharmonic vibrational motion and relaxes while radiating weak

electromagnetic radiation, called hot luminescence. This takes place at high speed and can only be detected within picoseconds after excitation [21]. The common type of luminescence occurs after hot luminescence, when the energy distribution between the sublevels of the excited states has attained a quasi-equilibrium character [22]. This is characterized by emitting a photon with a typical wavelength that can be observed as light with a specific color.

### 3.2.2 Triphosphor

The three primary colors for the human visual system have narrow emission bands that are centered at 450 nm for blue, 550 nm for green and 610 nm for the red color. When lamps emit white light that correspond with these bands (red, blue and green) and the rest of the spectrum is left nearly empty, the human eye will perceive high brightness per Watt and good color rending [23]. This is the case for RE triphosphors where white light is obtained by mixing blue-, green- and red-emitting phosphors. The triphosphors are made nowadays by blending $BaMgAl_{10}O_{17}$: $Eu^{2+}$ for the blue color, green emitting (La,Ce)$PO_4$: $Tb^{3+,}$ and the red emitting europium doped yttria; $Y_2O_3$: $Eu^{3+}$. The peak wavelength emissions of a triphosphor are shown in Figure 7 [21].

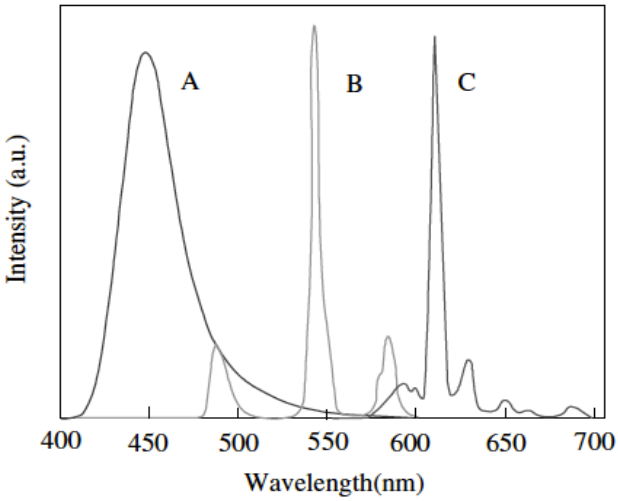


**Figure 7: Emission spectra of the phosphors in the triphosphor blend.**
**A: blue $(Sr, Ca)_5(PO_4)_3$ Cl: $Eu^{2+}$, B: green LaPO4: $Tb3^+$ and C: red $Y_2O_3$: $Eu^{3+}$[21].**

Emission A, B and C correspond with blue $(Sr, Ca)_5(PO_4)_3$ Cl: $Eu^{2+}$, green $LaPO_4$: $Tb^{3+}$ (green) and red $Y_2O_3$: $Eu^{3+}$respectively. Please notice that the blue color of the triphosphor of Figure 7 is composed of $(Sr,Ca)_5(PO_4)_3Cl$: $Eu^{2+}$ and not of the usual $BaMgAl_{10}O_{17}$: $Eu^{2+}$. The green

and blue phosphors have varied since the 1960s while europium-doped yttria is used as red phosphor since the beginning of the tricolor blend fluorescent lamps. The compositions of the triphosphor blend can be adjusted and thereby vary the light temperature of the emitted light [17].

### 3.2.3 Red emitting Phosphor: Europium-doped Yttria

Mixtures containing yttrium and europium in the experimental part of the master thesis are based on the red emitting phosphor, and hence will be discussed in more detail. $Y_2O_3$: $Eu^{3+}$ (YOX: $Eu^{3+}$): trivalent europium activated yttria phosphor is the generally used red-emitting triphosphor for lamps.

The red phosphor is the dominant component by weight of the triphosphor blend (approximately 60 %) [24]. Yttria forms a perfect refractory matrix in rare earth-doped material due to its favorable thermomechanical properties such as high melting point, high chemical stability, low thermal expansion and high dielectric breakdown strength [25]. It is a host for trivalent europium, meaning that $Y^{3+}$ is substituted by $Eu^{3+}$ in the $Y_2O_3$ lattice. Usually five to ten atom percentage (at.%) of yttrium is changed into europium. It is possible to go up to 50 at.% of europium in the phosphors, but this is economically not viable. Doping less than 3 at.% of $Eu^{3+}$ is not suitable because the charge transfer band of europium won't be intense enough to absorb all the UV radiation in a phosphor lamp . The peak of the charge transfer band is located at approximately 240 nm while the mercury atoms in the phosphor lamp emit their characteristic UV radiation at 254 nm, so this is at the tail of the absorption band [20].

The excitation and emission of the trivalent europium is due to optical transitions within the discrete levels of the 4f shell. The deep lying 4f-electrons of europium(III) are substantially shielded from the environment and the host lattice by the outer electrons in the $5s^2$ and $5p^6$ orbitals, which have a higher energy than the 4f orbitals [21]. Consequently the f-f emission spectra consist of sharp lines [26]. In the $Y_2O_3$:$Eu^{3+}$ emission spectrum visible in Figure 7, two types of transitions are present: $^5D_0 \rightarrow {}^7F_1$ is a weak magnetic dipole (MD) transition and the intense $^5D_0 \rightarrow {}^7F_2$ is an electric dipole (ED) transition [27].

# 4. Need for Recycling

## 4.1 Rare Earths Occurrence and Mining

Despite their name, the rare earths are relatively abundant in the earth crust compared to other metals. The lanthanides with low atomic number occur in greater abundance in nature than the ones with higher atomic number. This is due to the nucleus synthesis of the elements in the core of supernovas by atomic fusion; higher atomic numbers require higher temperatures and pressures and are thus not as easily formed as compared to the lighter ones [3]. REEs rarely occur in concentrated form, which makes them economically quite challenging to exploit. Besides, REEs never occur as individual elements but as mixtures in the ores. For some applications rare earths can be used in mixtures, such as in mischmetal or oxide catalysts. However, optical, electronic and magnetic applications require mostly individual pure lanthanides [3]. For instance, REEs used in phosphors must be 99.99 % pure since the presence of impurities can deform the colour characteristics [12]. The RE production is expensive and potentially damaging to the environment [28]. Accordingly, the limited supply of the minerals in the marketplace is not a result of scarcity, but of economic and environmental concerns [29]. Additionally, co-mining of REE ores gives rise to a surplus of the more abundant elements [30]. The market demands are not in balance with the occurrence of REEs in the most common ores, considering that many applications do not use REEs in mixture but rather high purity elements. This is known as the balance-problem [31].

## 4.2 Market

Currently, China produces over 90 % of the world's rare earth elements. China has invested in the development of rare earth processing techniques since the 1960s [32] and has gained a lot of knowledge on not only extraction of rare earth oxides from ores, but also in the downstream processes [5]. Despite the large production of REEs, China has only 37 % of the world's proven reserves [33]. Other places containing significant rare earth minerals are the

United States, Canada, Australia, India and Brazil [33]. Nevertheless, many countries do not have economical or operational primary deposits on their territory and need to rely on import and recycling of REEs. China is dominating the market by tightening control of rare earth exports by export quotas. In 2010, China imposed a 40 % cut in export quotas, saying it wanted to preserve its resources and diminish pollution. This caused an increase in global rare earth prizes and gave Chinese companies a competitive advantage. In March 2014, the world trade organisation (WTO) claimed that China's export restrictions were in violation with the global trade rules. China appealed against this WTO panel report in April 2014 [34] [35]. In the meantime, countries whose high-tech industry is reliant on the rare earth imports are most impacted by the export restrictions [32]. Consequently, the development of a green sustainable low carbon economy, based on rare earth applications, is affected as well. Production at non-Chinese mines are enhanced; mines in Australia, Brazil, Canada, Malawi, the United States, and Vietnam are expected to be operational in less than five years. Nevertheless the start-up of new mines entails technical difficulties, regulatory barriers and capital costs. Additionally, China will continue to dominate the market of the most scarce and expensive heavy rare earths [36]. That is why research for substitution options, efficient use of rare earths and recycling possibilities (urban mining) should be reinforced to tackle the supply vulnerability [37].

## 4.3 Increasing Demand

Rare earth consumption is large and growing rapidly [38]. The past 40 years, there was a large growth in applications for REEs. The availability of REEs is at risk despite the fact that the industrial demand for the REEs is relatively small in tonnage compared to other metals such as copper and iron. The shortage of some low-abundant RE entails an increase in cost price. It disturbs the market and slows down the further development of clean energy applications [39].

## 4.4 Conclusion

As a matter of fact, until 2011 less than 1 % of the REEs were actually recycled [5]. This was mainly due to an inefficient collection of waste-streams together with technological obstacles [5]. RE recycling from waste products has mainly been carried out in a laboratory

environment, but much work still needs to be done to develop recycling processes to an economical state on an industrial scale [40]. However, the End-of-Life recycling techniques and final REE recovery are indispensable and essential to handle the supply problem; efficient and environmentally friendly separation technologies will lower the REE cost and reduce the impact of mining and processing. They will lead to a diversification in suppliers and in this way lower the dependency on China's resources [12]. This is also crucial to prevent unnecessary waste of rare earths. More research efforts need to be done to optimize existing processes for the commercial recycle of RE applications. Besides, new inventive techniques need to be considered and explored to meet the point of issue of the supply risk and to respond to it with sustainable and green counter measures.

# 5. Separation of Rare Earths

Multiple rare earth elements occur together in extensive mineral deposits throughout the world. Furthermore, REE applications include many materials and a mixture of different rare earth elements [41]. Separation into individual elements and purification is necessary to meet the high purity requirements for industrial applications. The likeness in chemical properties, especially for neighbouring rare earths, hinders the separation and purification into the desirable concentrations (> 99.99 %) [4]. The conventional separation method is solvent extraction, but it is not efficient for separating neighbouring elements. More research efforts are required to optimize the existing processes for the commercial separation methods. Besides, new inventive techniques need to be considered and explored. Selective reduction techniques are part of the promising innovative separation techniques, by making selective removal of europium in europium-containing rare earth mixtures possible. The method exploits the stable divalent oxidation state of europium. The reduction of trivalent europium can be realized in a chemical, -electrochemical or photochemical way. The conventional and reductive separation methods will be discussed below.

## 5.1 Conventional Method: Solvent Extraction

### 5.1.1 Single-Stage Extraction

Solvent extraction is a separation technique that is based on the different distribution of the rare earths between two immiscible phases, an organic and an aqueous phase, due to differences in ionic radius and electrostatic interactions with the extractants. The extractant combines differently with the several REE elements by forming compounds that are more soluble and thus show greater affinity with the organic phase. The solvent ensures a good contact with the aqueous phase, because the extractant is usually too viscous to be used without solvent [42]. The extraction efficiency is expressed by the distribution ratio *D* that is calculated by equation (1).

$$D = \frac{c_{org}}{c_{aq}} \quad (1)$$

The symbols $c_{org}$ and $c_{aq}$ stand for the equilibrium concentration of respectively RE in the organic phase and aqueous phase. D is a measure for the affinity of the dissolved RE in both phases. If the distribution ratio differs from one, the RE has different activity coefficients in both phases [43]. The separation factor $\beta$ is a measure for the separation selectivity between the rare earths and is defined in equation (2).

$$\beta = \frac{D_A}{D_B} \quad (2)$$

$D_A$ and $D_B$ are the distribution coefficients of respectively rare earth A and rare earth B. For the separation of rare earth mixtures, a high selectivity is required, which means a high separation factor with respect to the other metals in the solution.

### 5.1.2 Drawback

The similarity of the adjacent trivalent lanthanide cations causes the separation factor to be very low for solvent extraction, making their mutual separation very difficult. The highest average separation factor, namely 2.5, for single stage extraction of adjacent lanthanides can be obtained by using di(2-ethylhexyl)phosphoric acid (DEHPA) as extractant. Therefore, a multiple-stage countercurrent solvent extraction system is required to purify the rare earths to the desirable concentrations, which makes the process rather complicated and laborious [44]. In a multistage continuous countercurrent process, the aqueous stream leaving the first extraction unit is fed to the next unit as aqueous feed, while the organic phase moves continuously in countercurrent direction. Today the preparation of high purity products at Rhodia requires more than 1300 mixer-settlers for very high purity requirements [45], [46]. Additionally, solvent extraction requires a large amount of organic solvents and chemicals, which could harm the environment. Synergistic extraction and ionic liquid could possibly improve the separation efficiency and decrease the environmental impact of solvent-extraction [41]. Nevertheless, the development of new separation methods to reduce environmental pollution is absolutely necessary.

## 5.2 Selective Reduction Separation Techniques

Rare earths are typically present as trivalent ions in aqueous solutions. Cerium and terbium however can be selectively oxidized, and some rare earths can be reduced: Sm, Eu, Tm and Yb. Among these, Eu(III) has the highest standard redox potential in water:
$Eu(III) + e^- \rightarrow Eu(II)$; $E^0 = -0.34V$ [4]. This reflects the stability of the divalent state due to the half-filled 4f subshell. This enables a selective reduction of Eu(III) to its divalent state in aqueous solution, followed by europium(II) sulfate precipitation. The selective reduction facilitates the separation from a mixture containing other trivalent REEs. Please notice that the selective reduction method is only applicable for elements with a stable divalent oxidation state and that it needs to be combined with other separation techniques for further purification of the remaining trivalent rare earth mixture.
This master thesis puts emphasis on the reduction of europium(III). The reduction reaction can be accomplished by various techniques, such as chemical reduction, electrochemical reduction or photochemical irradiation [47] [48].

### 5.2.1 Chemical Reduction

The reduction reaction is carried out by zinc powder according to equation (3). The reduction potential for $Zn^{2+}/Zn$ is -0.763V [47].

$$2Eu^{3+}_{(aq)} + Zn_{(s)} \rightleftharpoons 2Eu^{2+}_{(aq)} + Zn^{2+}_{(aq)} \quad (3)$$

This technique requires the use of a significant amount of $Zn^{2+}$ that eventually must be separated from europium. An unwanted competitive reaction with the reduction reaction (equation (3)) is the formation of hydrogen gas according to equation (4). The hydrogen gas bubbles can prevent the full reduction of Eu(III) by isolating the europium solution from the zinc surface. There is a formation of a passive layer on pure zinc, which decreases europium recovery [49]. Moreover, the hydrogen gas production also creates a significant fire hazard.

$$2H^{+}_{(aq)} + Zn_{(s)} \rightleftharpoons Zn^{2+}_{(aq)} + H_{2(g)} \quad (4)$$

$$\Delta E^{0}_{298K} = 0.76V \quad (5)$$

To decrease the competition between the two parallel reactions, the zinc is usually covered by a thin layer of mercury [4]. The reduction reaction with zinc amalgam (known as the Jones reductor) is carried out in a Jones column [50]. Due to the high hydrogen evolution overpotential of mercury in aqueous solution, the rate of hydrogen evolution on mercury is

slow. The presence of mercury hinders the formation of a zinc oxide coating. However, the environmental problems and concerns related to the disposal of zinc amalgam residues are serious issues [48]. Other drawbacks are the lack of flexibility of the system and the transfer of not only mercury, but also zinc into the solution. Zinc interferes with the following separations of the rare earths by coagulation of the zinc powder [51], thereby causing inconvenience in operation [52]. Additionally, the consumption of the reductor is high and the process must be repeated many times. For that reason, it is time consuming. The final, obtained purities and yields are rather low [53].

### 5.2.2 Electrochemical Reduction

Another approach to reduce trivalent europium is via electrochemical way, thus by applying a current in an electrolytic cell. The aqueous solution containing a mixture of trivalent rare earths amongst which Eu(III), is located in the cathodic compartment. It is separated from the anodic compartment by a cation exchange membrane. The cathode is usually fabricated from graphite, titanium, platinum or glassy-carbon. The anode and anolyte can vary. The anolyte releases oxygen at the anode over the course of the electrolysis. The predominant electrode reactions involved are equation (6) and (7). Equation (8) dominates at the anode [54].

**Cathode:**

$$Eu^{3+} + e^- \rightleftharpoons Eu^{2+} \quad (6)$$

$$2H^+ + 2e^- \rightleftharpoons H_2 \quad (7)$$

**Anode:**

$$2H_2O \rightleftharpoons O_2 + 4H^+ + 4e^- \quad (8)$$

Electrochemical reduction of Eu(III) does not produce Zn(II) impurities, unlike chemical reduction. It also proceeds faster than chemical reduction [55]. High purity europium is obtained and the method is amenable to countercurrent operation [3]. However, the yields and degrees of conversion are commonly insufficient and there is a direct consumption of energy [51] [56].

### 5.2.3 Photochemical Reduction

Photochemical reduction occurs by the absorption of a photon that originates from a light source. The absorption of light transfers an electron from the complexing ligand (such as water or sulfate) to the central rare earth ion. Since photochemical reduction is the topic of the experimental part of this master thesis, it is covered in more detail in the next chapter.

This technique has extensive advantages: firstly, it is an attractive option from an environmental point of view. The major advantage is that spectral selectivity can be exploited; there are very little spectral interferences from other REE at the wavelength involved, and only europium(III) will be reduced. Hence, very high selectivity can be obtained when choosing an appropriate wavelength. Moreover, the main reactants for photochemical and electrochemical reduction reactions are the usage of electrons instead of consuming (and further disposing) large amounts of chemicals (such as organic solvents and extractants that are needed for solvent extraction) [57]. Compared to the selective chemical reduction by usage of reducing agent zinc or zinc amalgam, the photochemical method needs no additional reducing agent, namely the electrons originate from the ligands such as water, and is therefore free from contamination. On the other hand, it needs to be considered that a significant amount of organic compounds, namely scavengers, are needed for the photochemical method to inhibit the backward reaction, i.e. the oxidation of europium(II) [58].

# 6. Photochemical Separation

Photochemical reaction of rare earths consists of the absorption of photons, originating from the light source, by the reactants [48]. This takes place in the charge transfer band (CT-band) and corresponds with the electron transition from the ligands or environment to the metal, i.e. a ligand-to-metal charge-transfer (LMCT). The excited state changes the chemical properties of the reactants. This enables reactions that would be thermodynamically impossible without irradiation [59]. The charge transfer band energy position is related to the electronegativity of the ligand, the ligand-to metal ion distance and the electron affinity of the rare earth ion. The latter depends on the degree of occupation of the f-shell of the rare earth ion. For instance, the charge transfer corresponding with the reduction of Eu(III) to Eu(II) will appear at relatively low energy compared to RE ions that are not easily reduced. This is due to the $4f^6$ configuration of Eu(III), which will easily gain one electron in order to attain the more stable half full subshell ($4f^7$) configuration [60].

In aqueous solutions, most of the non-trivalent REEs are unstable with main exceptions of $Eu^{2+}$ and $Ce^{4+}$. Besides, in some non-aqueous media, additional non-trivalent REE are stabilized such as $Sm^{2+}$, $Yb^{2+}$ and $Tb^{4+}$ [61]. It is essential to use optimal light sources that emit monochromatic light at the specific and particular wavelength at which the desired RE ion is oxidized/reduced.

## 6.1 Light Sources

Photochemical reactions can be carried out with different sources of irradiation, such as lasers, high-pressure mercury lamps (HPML), low-pressure mercury lamps (LPML) and Light Emitting Diodes (LEDs). Any photon source may be used as long as it is capable of operating at the wavelength within the charge-transfer band of the metal to be separated [58]. The different irradiation sources vary in region of wavelength emission and in power and the light may be pulsed or continuous [48]. The region of wavelength is crucial for the selectivity, as opposed to the photon density (i.e. power of the light), which does not have an

effect on the reaction selectivity. It is expected that the speed of the reaction will be reduced when the power is too low compared to the metal concentration and solution volume [57].

### 6.1.1 Lasers

Excimer lasers are possible light sources to induce photochemical reduction of Eu(III). An excimer is an excited dimer. In general, a combination of a noble gas such as argon, xenon or krypton and a reactive gas such as fluorine or chlorine is used in excimer lasers. An electrical current flows through the laser medium and induces an excited state of the dimer. Electronic transitions between the excited state and the ground state occur, giving rise to laser light in the UV spectrum. The region of emission depends on the composition of the used dimer: an overview of excimer lasers with their respective emission wavelength is reflected in Figure 8. The solid blocks indicate commercially important wavelengths [62].

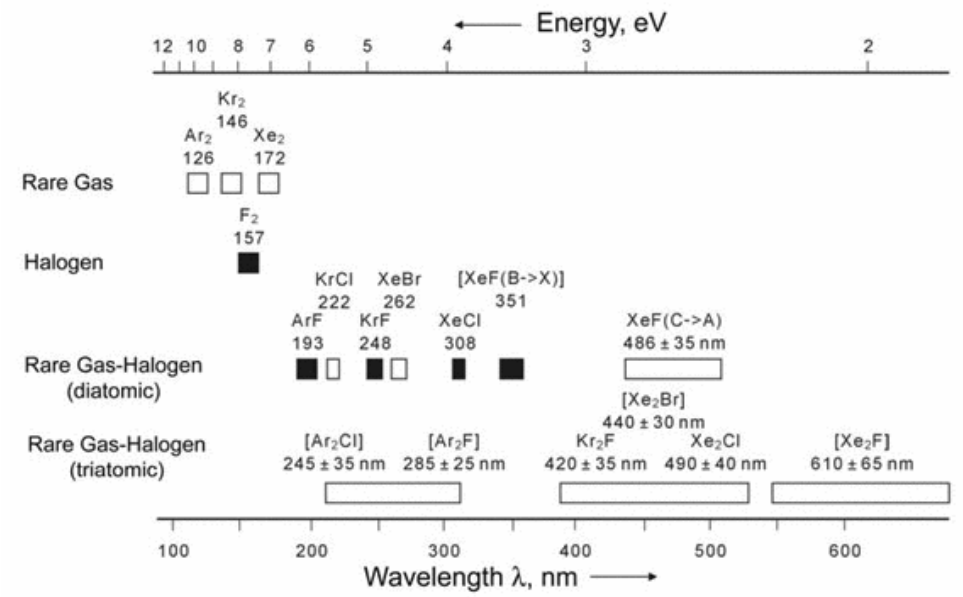


**Figure 8: Different excimer lasers with corresponding photon energy [62].**

The lasers are generally of high power and can emit short-wavelength radiation [48]. The main inconveniences are the significant cost increase and the uneasiness in workability [52].

### 6.1.2 Low and High Pressure Mercury Lamp

Mercury lamps can also be used as illuminating source for the photochemical reduction of europium. These are lamps in which light is produced by an electric arc between two electrodes, in an ionized mercury-vapor atmosphere [63]. During the gas discharge, the

mercury is excited by the current flow and emits excitation energy in the form of characteristic radiation [15] [64]. The optimum pressure of metal vapor is below $10^{-5}$ bar in LPML and between one and 200 bar in HPML. Higher power densities can be obtained in the HPML [65]. The LPML has a high-energy emission meaning lower wavelength photon emission compared to the HPML. To be specific, the LPML has got emission peaks at 185 and 254 nm while HPML emits at 310 and 365 nm [48]. The mercury lamps have some disadvantages, namely environmental pollution considering the presence of mercury and also the shortfall in energy-efficiency. The latter is related to the significant heat production (cooling may be required), the relative short lifetime of the lamp and the emission of light at different wavelengths.

### 6.1.3 Light Emitting Diodes

Light Emitting Diodes consists of semiconductors doped with impurities in order to form a p-n junction device. Electrical power is converted into optical power when electrons radiatively recombine with holes in the valence band, releasing energy in the form of photons [21]. The wavelength of the light that is emitted by the LED is determined by the band-gap across which the recombination takes place [11]. One of the key advantages is that LEDs emit quasi-monochromatic light. Fine-tuning of the LED is possible in order to emit at the specific oxidation/reduction wavelength of the target rare earth ion. Additionally, LEDs emit less heat than the conventional light sources and are consequently considered as energy-efficient. Additional advantages over the traditional light sources are the longer lifetime, smaller size and faster switching [11] [21].

## 6.2 Working Principle

As stated before, the choice of the light source is dependent on the specific wavelengths needed for selective oxidation/reduction of a certain target RE ion. Various lamps will be used in the experimental part of the master thesis to determine the influence of the irradiance on the photochemical reduction of europium, namely two immersed 11 W lamps and a set of non-immersed lamps: one 11 W lamp with reflector, two 40 W lamps and one 60 W lamp.

The main emphasis is put on the immersed LPML of 11 W with dominant emission peaks at 185 nm and 254 nm. Its irradiance profile is visible in Figure 9. The irradiance is expressed in $\mu W/(cm^2 . nm)$. Please notice that the output at wavelengths below 200 nm cannot be detected due to limitations of the irradiance measuring set.

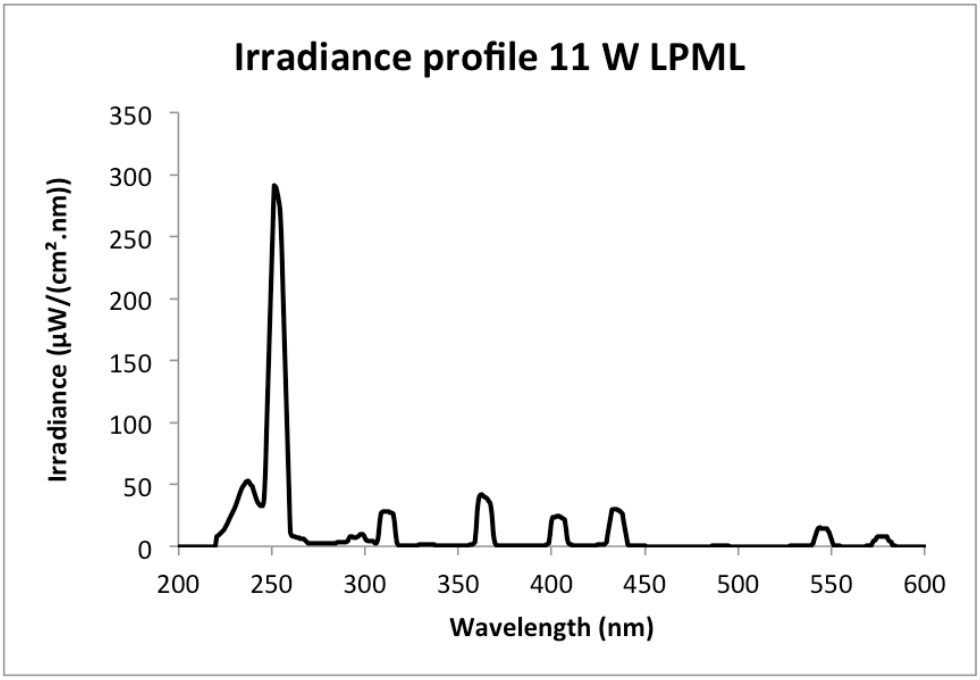


**Figure 9: Irradiance profile of the 11 W-submerged LPML.**

The following reduction reaction occurs when the RE mixture containing Eu(III) is irradiated (equation (9)). An electron is transferred from a complexing ligand such as water to the Eu(III) ion. The charge transfer band from $H_2O$ to Eu(III) is located at 188 nm [48]. Please notice that the 11 W LPML has its main emission peaks at 185 nm and 254 nm. Since the absorption happens at the tail of the emission peak of the 11 W LPML, there will be higher losses in irradiation efficiency compared to light sources that have their emission peaks at the exact absorption wavelength.

$$\left[Eu\left(H_2O\right)_n\right]^{3+} \underset{}{\overset{188\ nm}{\rightleftharpoons}} \left[Eu\left(H_2O\right)_{n-1}\right]^{2+} + OH^{\bullet} + H^{+} \qquad (9)$$

Light with wavelength around 188 nm only promotes the forward reduction reaction while the backward oxidation of europium occurs at 366 nm (equation (10)) [20].

$$2Eu^{2+} + 2H^{+} \xrightarrow{366\ nm} 2Eu^{3+} + H_2 \qquad (10)$$

The backward oxidation reaction needs to be minimized by:

**1.** destroying the $OH^{\bullet}$ radical

**2.** removing the divalent europium ion from the solution

**3.** using light sources which only irradiate at the wavelengths involved for the forward reduction reaction.

**1. Destroying the $OH^{\cdot}$ radical**

A scavenger is added for the destruction of the hydroxyl radical. Otherwise, the $OH^{\cdot}$ radical will react with Eu(III) and consequently oxidize it back to Eu(II) [57]. The choice of the scavenger depends on the kind of radicals produced. It is also important that the scavenger does not negatively interfere with the primary photo-reduction of Eu(III) [57]. Several scavengers are in use for the photo-redox reactions in aqueous media, e.g. formic acid, isopropyl alcohol and isopropyl formate. These scavengers capture the hydroxyl radical and form other more stable radicals according to equations (11), (12) and (13). Other compounds than formic acid, isopropyl alcohol and isopropyl formate can be used as well in aqueous media, as long as the scavenger contains a carbon atom bond to a free hydrogen atom that will be used for the formation of water. Secondly, the carbon atom of the scavenger needs to be bonded to a group that will stabilize the remaining radical (such as an hydroxyl group, methyl group or an double bonded oxygen).

$$HCOOH + OH^{\cdot} \rightarrow H_2O + C^{\cdot}OOH \quad (11)$$

$$(CH_3)_2 CHOH + OH^{\cdot} \rightarrow H_2O + (CH_3)_2 C^{\cdot}OH \quad (12)$$

$$HCOOCH(CH_3)_2 + OH^{\cdot} \rightarrow H_2O + C^{\cdot}OOCH(CH_3)_2 \quad (13)$$

The organic radical formed in equation (11), (12) and (13) will typically combine to form more stable species or cause further reduction of Eu(III). This will be discussed in more detail in the experimental part of the master thesis that investigates the influence of the scavenger on the photochemical reduction of europium.

**2. Europium removal**

Eu(II) is removed from the solution by adding a selective precipitating agent. If Eu(II) is not removed from the solution it can back-react according to equation (10) and hence no separation is obtained [57]. A sulfate source such as $(NH_4)_2SO_4$, $K_2SO_4$, $Na_2SO_4$,$NaHSO_4$ or $H_2SO_4$ can be used for precipitation [66]. These will react according to equation (14) or equation (15).

$$Eu^{2+} + HSO_4^- \rightarrow EuSO_4 \downarrow + H^+ \quad (14)$$

$$Eu^{2+} + SO_4^{2-} \rightarrow EuSO_4 \downarrow \quad (15)$$

Adding $SO_4^{2-}$ before the irradiation allows a homogenous formation of insoluble $EuSO_4$ precipitate. It should be noted that $SO_4^{2-}$ provokes an additional reducing effect [48] [59]. The irradiating light induces the electron donation from the sulfate anion to Eu(III) and therefore initiates the extra formation of Eu(II) according to equation (16) and (17). The charge transfer transition from $SO_4^{2-}$ to Eu(III) has its maximum at 240 nm. Also here the reaction happens at the tail of the absorption band since the LPML emits at 254 nm [67].

$$SO_4^{2-} \xrightarrow{240\ nm} O^{\bullet}SO_3^- + e^- \quad (16)$$

$$Eu^{3+} + e^- \rightarrow Eu^{2+} \quad (17)$$

Accordingly, additives can therefore generate new absorption bands and thereby allow us to work at longer (i.e. more energy-efficient) wavelengths [58]. However, the reactions with the sulfate precipitating agent are not clearly defined in the literature and there remains some confusion. The $O^{\bullet}SO_3^-$ radical is formed in equation (16). There are various pathways for recombination of this sulfate radical. As stated in equation (18), the $O^{\bullet}SO_3^-$ radical can recombine with a $H^{\bullet}$ radical that is formed during the photochemical decomposition of the scavenger HCOOH (equation(11)). Besides, the $O^{\bullet}SO_3^-$ radical can recombine with another $O^{\bullet}SO_3^-$ radical to form the peroxidisulfate anion $S_2O_8^{2-}$ according to equation (19). Peroxydisulfate is a strong oxidant, which can cause the unwanted oxidation of the divalent europium ion back to its trivalent state. Another possible reaction (equation (20)) is the reaction of the $O^{\bullet}SO_3^-$ radical with water to form $HSO_4^-$ and a hydroxyl radical. Due to the excess of water the latter will occur with highest probability. Beware that these reactions are assumptions and have not yet been confirmed by literature reports or experiments yet.

$$O^{\bullet}SO_3^- + H^{\bullet} \rightarrow HSO_4^- \quad (18)$$

$$2O^{\bullet}SO_3^- \rightarrow S_2O_8^{2-} \quad (19)$$

$$O^{\bullet}SO_3^- + H_2O \rightarrow HSO_4^- + OH^{\bullet} \quad (20)$$

**3. Suppress the photochemical back-reaction**

As stated in equation (10), the backward oxidation of europium occurs at 366 nm. It is obvious that the re-oxidation can be minimized by using light sources that only emit at the wavelengths inducing the forward reduction reaction (i.e. 188 nm and 240 nm). Important

to mention is that the immersed 11 W LPML also emits light at 366 nm. As can be seen in Figure 9, this band is far less intense than the high emission at 250 nm for the forward reduction reaction. However, the extinction coefficients of Eu(II) is higher than for the charge transfer band of Eu(III) [59], [68], so a considerable loss in efficiency is expected since light of 366 nm will give rise to partial oxidation of divalent europium. This major disadvantage already points out the advantage of monochromatic light compared to polychromatic light sources. By usage of UV filters, only the optimal wavelength range for the forward reaction can be isolated and this enhances the selectivity and the efficiency of the separation. Additionally, at higher pH, less $H^+$-ions will be present in the mixture and hence the oxidation reaction will be disfavoured according to equation (10).

# 7. Techniques and Equipment

## 7.1 Inductively Coupled Plasma Mass Spectrometry

The concentrations of the RE ions are measured with the inductively coupled plasma mass spectrometry (ICP-MS) of the type Thermo X-series, PlasmaQuad (PQ) 2.

### 7.1.1 Working Principle

Figure 10 illustrates the working principle of the ICP-MS. Samples are nebulized into a fine aerosol and introduced into the ICP torch. The ICP plasma is in fact argon plasma that is sustained by electric currents produced by electromagnetic induction. The high energetic plasma ionizes the elements in the sample. The ions are extracted and introduced into the mass-spectrometer as an ion beam, via the interface that consists of a pair of cones, the sampler and the skimmer [69]. The skimmer is located sequentially behind the sampler cone. A vacuum is maintained between the two, with an even lower vacuum behind the skimmer. This set-up maximizes the number of ions entering the mass spectrometer as a narrow axial beam, while minimizing the gas dragged along with the ions [70]. The ion beam is focused and transmitted via a lens system towards the quadrupole mass analyzer that is kept under high vacuum. In here, the ions are separated by their specific mass to charge ratio by the electrostatic filter that is established in the quadrupole. DC voltages are applied to opposite pairs of the rods in combination with RF voltages, which causes oscillation of the ions and a corkscrew motion. Only ions with a certain mass-to charge ratio reach the detector at a given instant in time while the other ions collide with the rods [69]. This corresponds with the qualitative REEs determination. Ions emerging from the quadrupole are detected and counted with an electron multiplier, resulting in a quantitative determination.

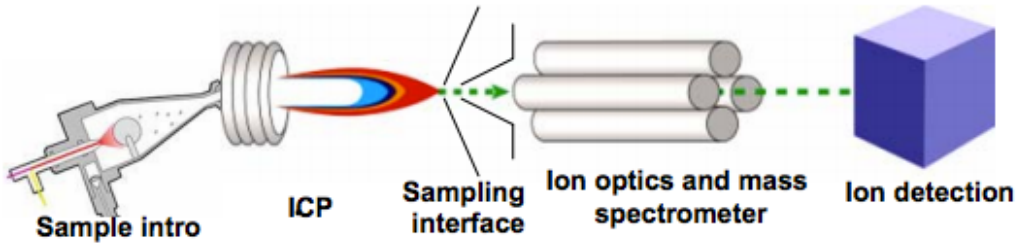


**Figure 10: Working principle of ICP-MS [70].**

### 7.1.2 Sample Preparation

The sample preparation for ICP-MS consists of the standard preparation and the sample dilution. In general, the maximal measurable concentration on ICP-MS is 2000 ppb; every 10 mL of sample needs to contain 2 vol% $HNO_3$. The unknown REEs concentrations are calculated through the standard curve. The standard curve is generated by plotting the detector response versus the concentration of the corresponding REEs standard samples with known concentration [71]. The concentrations of the standards must lie within the range of the expected unknown concentrations. Europium, samarium, gadolinium and yttrium standards are available as 1000 ppm. The calibration curve is formed with nine calibrating points (10-25-50-100-250-500-1000-1500 and 2000 ppb) by diluting the standards with Milli-Q water, taking into account the 2 vol% of $HNO_3$. Several blanks are included that consist of 2 vol% $HNO_3$ in Milli-Q water. The samples with unknown REEs concentration are diluted until each of the expected sample concentrations lies in the measurable interval of ICP-MS and contains 2 vol% $HNO_3$.

## 7.2 Total Reflection X-ray Fluorescence

A second method for measuring the RE ions concentrations is with Total Reflection X-ray Fluorescence (TXRF) of the type Bruker S2 Picofox. The advantage of TXRF compared with ICP-MS is the high measuring range and the internal calibration.

### 7.2.1 Working Principle

The working principle of TXRF is reflected in Figure 11 [72]. An X-ray beam is generated by an air-cooled X-ray tube with molybdenum target. The 50W generator can be switched on by the corresponding software command of the controlling computer. The spectral distribution and geometry of the X-ray tube radiation is modified to a narrow energy range

by a multilayer monochromator. The resulting X-ray beam strikes on the center of a polished quartz glass sample carrier and is totally reflected due to the very small angle (< 0.1°) between excitation beam and surface of the sample carrier. This is in accordance with Snell's law that describes the correlation between the angle of light incidence and its refraction at an interface between two different isotropic media [73]. As a result of the total reflection, the absorption and scattering of the X-ray beam in the sample matrix are minimized, increasing the element measurement sensitivity. Subsequently, the semiconductor detector collects the characteristic X-ray fluorescence radiation that is emitted by the sample, resulting in a qualitative element determination. Quantification of the element concentration requires the addition of a standard. The unknown concentrations of the elements in the samples are obtained by calibrating them to the known concentration of the standard. The software displays a spectrum, showing how many X-ray quanta were counted at a specific energy range [74].

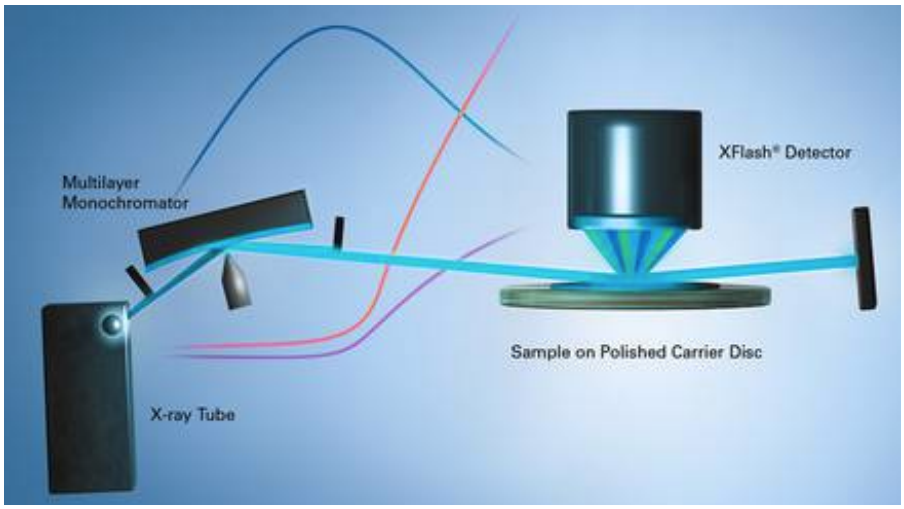


**Figure 11: Working principle of the S2 PICOFOX TXRF spectrometer [72].**

### 7.2.2 Sample Preparation

To generate a hydrophobic surface on the sample carriers, 5 µL of SERVA, a hydrophobic silicon solution, is directly pipetted on the quartz glass sample carriers and dried in an oven of 60°C. This coating prevents aqueous drops from spreading out. For the preparation of the samples, it is of high importance that the concentrations of the REEs are comparable with the concentration of the internal standard. 100 µL of 1000 mg/L gallium (Ga) standard is added to a certain amount (mainly 100 µL or 200 µL, depending on the europium concentration) of the rare earth aqueous solution in an eppendorf tube. This mixture is diluted to 1 mL with Milli-Q water and stirred with a vortex-mixer. 10 µL of the prepared solution is put on the pre-coated quartz plate and dried in an oven at 60°C for 30 min.

## 7.3 Irradiance Measurements

The set-up of for the irradiance measurements is shown in Figure 12 [75]. The irradiances are measured via a cosine corrector that is linked with the spectrometer of the type Ocean Optics QE 65000. This spectrometer is connected to the computer, which includes the SpectraSuite software platform. SpectraSuite allows clear analyze of spectral data through the SpectraSuite wizard that guides the operator through the irradiance measurements. The spectrometer absolute irradiance calibration is carried out by the DH2000 calibration light source. This is a deuterium tungsten halogen light source that produces a powerful and stable output from 230 to 2000 nm [76].

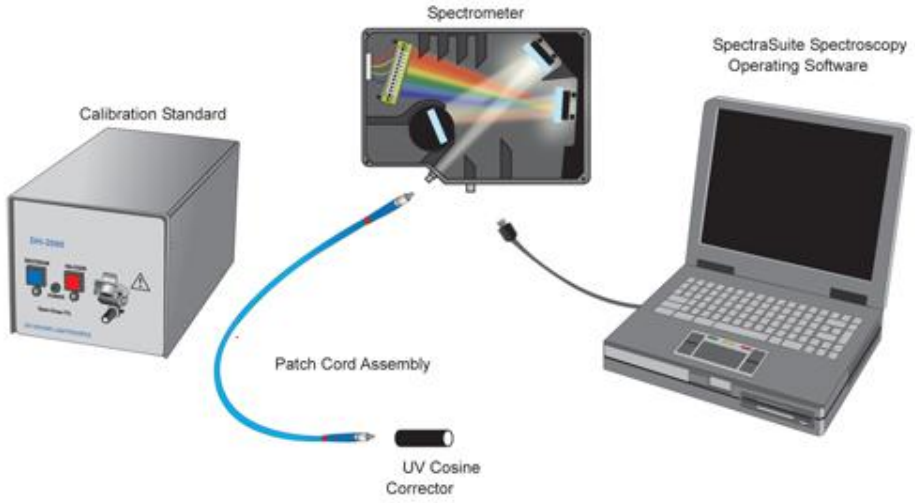


**Figure 12: Set-up for the irradiance measurements [75].**

### 7.3.1 Working Principle

The lamp from which the irradiance needs to be measured is put in a dark box at a specific distance from the cosine corrector. The radiation is collected in the cosine corrector and the light is transmitted through an optical fiber to the spectrometer. The light from the fiber enters the spectrometer via an entrance slit where a filter limits the bandwidth of light entering the spectrometer. In the spectrometer the incoming light falls on a mirror, which reflects the light as a collimated beam towards the grating. The grating splits and diffracts the light into several beams that fall on a focusing mirror. This mirror focuses first-order spectra, i.e. a spectrum produced by a diffraction grating where the difference in the path length of the light from adjacent slits of the grating is one wavelength [77], on the detector plane and sends higher orders to light traps. The detector is cooled and transforms the data

into digital information that is passed to the software. The software program SpectraSuite compares the sample information to the calibration and subsequently displays the spectrum [78] [79].

## 7.4 Ultraviolet-Visible Spectroscopy

The absorption of light by a compound is related with the excitation and promotion of electrons to higher energy orbitals. Only absorption of light with a particular energy will cause the transition of an electron to a higher energy level [80]. The UV-Visible (UV-Vis) spectrometer measures at which wavelengths absorption takes place, together with the quantitative degree of the absorption, in both the near and visible part of the spectrum [81]. A schematic view of the working principle of the UV/VIS spectrometer is visible in Figure 13 [81]. Spectra were carried out with a UV-VIS spectrophotometer of the type Shimadzu UV1601 that covers an optical range of 190 nm to 1100 nm [82].

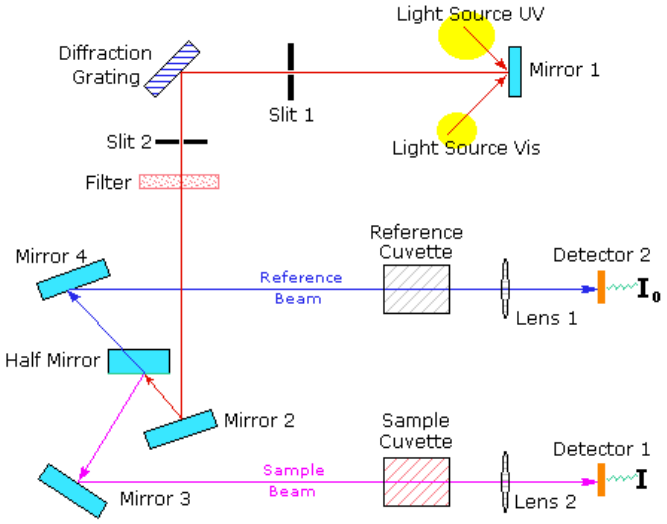


**Figure 13: Working principle of the UV/VIS spectrophotometer [81].**

The light source consists of a combination of a UV light source, namely a deuterium lamp (190 nm to 360 nm), together with a light source that covers the visible spectrum, more precisely a tungsten halogen lamp (360 nm to 1100 nm) [82]. The light beam is split by a diffracting grating into its individual wavelengths. The half mirror splits each wavelength beam into two equivalent beams of equal intensity; the incident beam (referred to as the reference beam on Figure 13) and the transmitted beam (referred to as the sample beam on Figure 13). The reference sample consists of the solvent in which the sample compounds are dissolved. The sample and reference are held in an optically transparent cuvette through

which the respective beams pass through. For each wavelength, the intensity of the incident beam ($I_0$) is measured and compared to the intensity of the transmitted beam ($I$). The absorbance $A$ is determined by equation (21).

$$A = \log \frac{I}{I_O} \tag{21}$$

$I$ equals $I_0$ if the compounds in the sample do not absorb light and hence $A$ = 0. The final absorption spectrum is a plot of the absorbance as function of the wavelength.
The wavelengths at which absorption takes place are correlated with the functional groups present in a molecule, whereas the concentrations of the absorbing compounds are proportional to the absorbance according to the Lambert-Beer law, expressed in equation (22).

$$A = \varepsilon \; c \; l \tag{22}$$

$A$ stands for the absorbance [/], ε for the molar extinction coefficient [$M^{-1}$. $cm^{-1}$], $c$ for the sample concentration [M] and $l$ for the length of the optical light path through the cuvette [cm]. By making a calibration graph with known concentrations, the concentration of unknown sample solutions can be determined.

In the experimental part, UV/Vis spectroscopy was only used to determine the position of the absorption bands, while the concentrations were determined with ICP-MS or TXRF. The samples consisted of 10 mM REE in an aqueous HCl solution of pH = 2. Consequently, the reference consisted of pure HCl solution of pH = 2.

## 7.5 X-ray Diffractometer

The crystal structure of the precipitate is determined at respectively room temperature and 100K on an X-ray diffractometer of the type Agilent SuperNova by Jeroen Jacobs. This diffractometer uses Mo Kα radiation (λ = 0.7107 Å) as X-ray source and is equipped with an Atlas CCD detector. The software programmes, CrysAlisPro and Olex2, were used to interpret and integrate the obtained images. The crystal structure was solved with the ShelxS structure solution program using Direct Methods and refined with the ShelxL package using full-matrix least squares minimization on $F^2$.

## 7.6 Experimental Set-Up

Every experiment in chapter nine is carried out as indicated below, unless it is explicitly stated otherwise. The general procedure consists of three major steps:

- preparing the mixtures,
- illuminating the mixtures and taking samples at regular time intervals,
- determining the concentration of the samples.

The detailed laboratory practice is as follows. First, the aqueous solutions are prepared by adding a well-defined quantity of 1 M HCl or 1 M NaOH to distilled water in order to attain the desired pH. Next, the REE are added as chloride hexahydrate salts and are dissolved in the acidic or basic solution together with the precipitating agent. Subsequently the scavenger is added immediately before illuminating the solution in order to avoid possible interactions before illumination. At this point, the first sample is taken and defined as 'sample at illumination time zero'. The solution is placed in a sample beaker and a LPML is immersed in the solution as can be seen in Figure 14

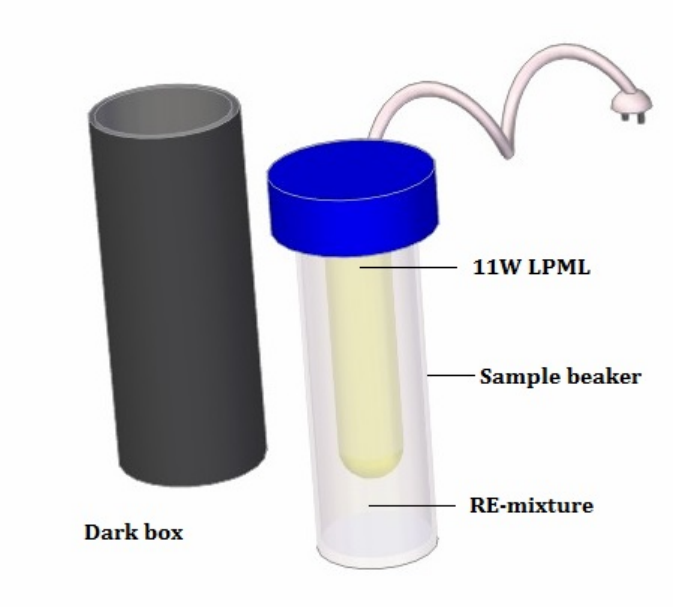


**Figure 14: Set-up photochemical experiment immersed lamp.**

The sample beaker is put in a secondary container that serves as a dark box. This is done in order to minimize interferences with other light sources and for safety reasons as well. The LPML induces the photochemical reactions by its spectral output at 185 nm and 254 nm. Samples are taken from the solution at regular time intervals. These samples are filtered in order to ensure the absence of precipitation. The REE-concentrations of the samples are

measured by ICPMS or TXRF. Herefrom the concentration of the precipitated divalent europium can be calculated and consequently the selectivity and efficiency of the separation can be determined. Please note that 50 mL of the RE mixture is not illuminated but stored in in a dark closet simultaneously. By comparing the illuminated against to the non-illuminated solutions, it is possible to determine if the observations are caused solely by illumination.

# 8. Health, Safety and Environment

Health, safety and environment (HSE) are essential and crucial parameters that need to be taken into account when performing an experimental master thesis. Several measures and prevention principles are taken into consideration to define the constraints of HSE, to minimize the risks and to create a sustainable work environment.

First of all, a HSE lab-introduction and briefing are organised by the promoter and the daily supervisor. This is followed by the HSE-test in order to ensure the full comprehension of the HSE-manual. Furthermore, risk analyses are set up before the start of activities in the laboratory. Next to the collective protective equipment that is available in the lab, specific precautionary measures are taken for the photochemical experiments. UV lamps with power varying from 11 W up to 60 W are used. They should be handled with care since the deep UV light is harmful (mainly for skin and eyes). The lamps are placed inside a dark box that blocks the light and protects the surrounding area from the damaging UV light. The lamps are accommodated with a light switch, so they are only switched on when they stand in the closed dark box. This is to prevent any irradiation of UV light on other chemicals or persons. To stop the experiment, first the power is switched off, and then the box can be opened to reach the sample beaker. All experiments are conducted at room temperature and atmospheric pressure, under a fume hood. Particular protective eyewear is available in the lab next to the conventional laboratory coat and gloves that are mandatory as personal protective equipment. Additionally, high quantities of organic scavengers or acids are used for the photochemical separation experiments. These compounds are often highly flammable. For instance, formic acid, isopropanol, ethanol and HCl are repeatedly used during the photochemical experiments and are categorized as risk class E3. Consequently, they should be handled with care. The particular risks associated with the chemicals were identified in the risk assessments.

# 9. Results and Discussion

In this section, the results of the photochemical separation experiments are presented and discussed in detail. The objective of this master thesis is to investigate a variety of parameters which have a considerable effect on the selectivity and/or efficiency of the photochemical separation. A distinction is made between two pre-eminent types of parameters, i.e. (1) chemical parameters and (2) parameters related to the light source. The chemical influences that were considered are: the concentration of the precipitating agent, the type of scavenger, the pH of the aqueous solution and the molar ratio of the REEs in the mixture. Next to these chemical effects, influences related to the light source will accordingly affect the selectivity and efficacy of the photochemical separation technique. The spectral output and irradiances of various lamps were examined, together with the distance and uniformity of irradiation.

It should be determined to which extend these influences are significant. In order to vary the diverse parameters in a representative way, three 'standard mixtures' were defined, in which the different variables were set to a default value or set point. Hence, when investigating the influence of a certain parameter in the later experiments, the concerning parameter was alternated while the rest of the variables were kept to the default value of the standard mixtures (unless expressly stated otherwise).

It is essential to discuss the results of the photochemical reduction of the standard mixtures extensively and in detail in order to enable full understanding of the technique. For this reason, the tables, containing the REE concentrations as function of the illumination time, have currently been inserted in the central text. They will however be included in appendices for the following experiments so as to not overload the report. In general, every experiment was carried out once, except for the concentrations determined with TXRF, which were measured twice in the first experiments. From these results, the dispersion of these measurements was calculated, resulting in an average relative standard deviation (RSD) of 1 %. Considering the low RSD, it was decided to measure the concentrations only once instead of twice in the latter experiments.

## 9.1 Standard mixtures

### 9.1.1 Variables

As previously explained, three standard mixtures are defined in which the different variables are set to a fixed set point. The detailed composition is shown in Table 2. Please note that the light-influencing parameters are not yet considered. Illumination of the reference mixtures is performed by a immersed 11W LPML. From now on, whenever the pH is mentioned, it refers to the pH of the solution after the addition of scavenger unless it is explicitly stated otherwise.

**Table 2: Composition of the standard mixtures.**

| Standard | Rare earths | | Aqueous solution | | | Precipitating agent | | Scavenger | |
|---|---|---|---|---|---|---|---|---|---|
| Mixture | REE | C(mM) | Acid | pH | V(mL) | Type | C(mM) | Type | Vol% |
| 1 | $SmCl_3.6H_2O$ | 10 | HCl | 1 | 300 | $(NH_4)_2SO_4$ | 50 | HCOOH | 20 |
| | $EuCl_3.6H_2O$ | 10 | | | | | | | |
| 2 | $GdCl_3.6H_2O$ | 10 | HCl | 1 | 300 | $(NH_4)_2SO_4$ | 50 | HCOOH | 20 |
| | $EuCl_3.6H_2O$ | 10 | | | | | | | |
| 3 | $YCl_3.6H_2O$ | 10 | HCl | 1 | 300 | $(NH_4)_2SO_4$ | 50 | HCOOH | 20 |
| | $EuCl_3.6H_2O$ | 10 | | | | | | | |

As can be seen in Table 2, the standard mixtures are only different with regard to the REEs determining the binary mixture. The compositions of the standard mixtures are based on concentrations and ratios found in literature [4] [46] [48], together with practical considerations. The three mixtures contain europium, as this is the essential element for the photochemical reduction due to its stable divalent oxidation state, and an additional trivalent rare earth element being samarium(III), gadolinium(III) or yttrium(III) for respectively standard mixture one, two and three.

The reason why samarium and gadolinium are chosen as second element of the mixture is because these are adjacent REEs of europium in the Periodic System. The REE and especially the neighboring REE have very similar ionic radii and chemical properties, resulting in low separation factors for the conventional separation method of solvent extraction. By choosing adjacent REE mixtures, it can be determined whether the higher expected selectivity can be experimentally obtained with the photochemical separation technique in comparison to the traditional solvent extraction technique.

Furthermore, since europium and yttrium are commonly used together in lamp phosphors, as discussed in chapter three, this couple of rare earths is present in an important and valuable waste stream [83]. Therefore, the separation and purification of a mixture of europium and yttrium is an economically relevant issue.

The concentrations of the REEs in the aqueous solutions were measured with TXRF and shown in Table 3, Table 4 and Table 5 for respectively standard mixture one, two and three. Subsequently, these results are plotted in accordingly Figure 15, Figure 16 and Figure 17.

**Table 3: Concentrations of Eu/Sm versus illumination time.**

| Illumination time (h) | $C_{aq, Sm}$ (mmol/L) | $C_{aq, Eu}$ (mmol/L) | Observation |
|---|---|---|---|
| 0 | 9.6 | 9.8 | (Scavenger added) |
| 1 | 9.3 | 9.8 | No precipitation |
| 2 | 9.6 | 8.7 | Precipitation |
| 3 | 9.1 | 7.7 | Precipitation |
| 4 | 9.5 | 7.0 | Precipitation |
| 6 | 9.2 | 5.4 | Precipitation |
| 7 | 9.4 | 3.7 | Precipitation |
| 24 | 9.1 | 0.4 | Precipitation |

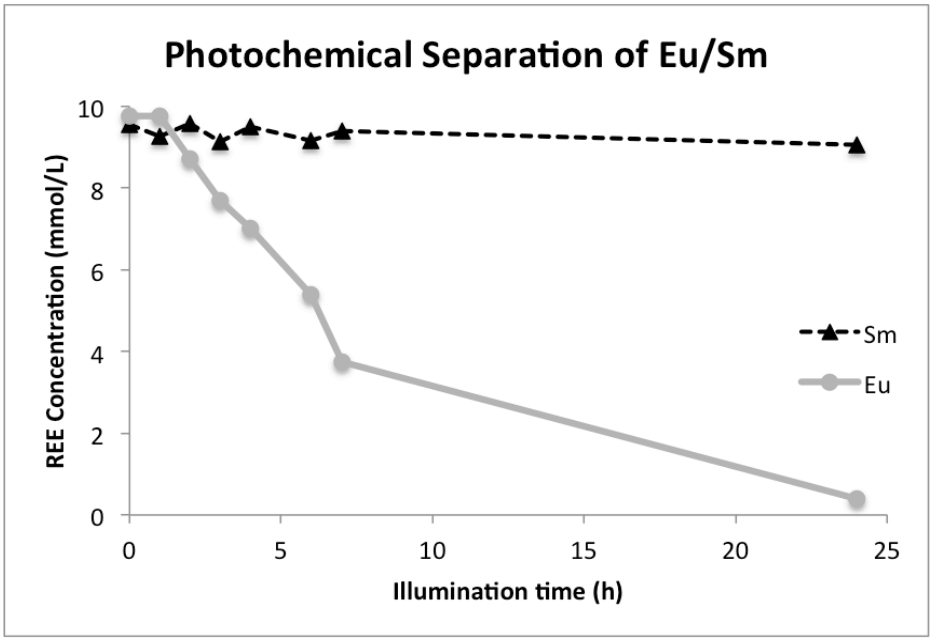


**Figure 15: Photochemical separation of Eu/Sm with 11 W LPML. 10 mM $EuCl_3 \cdot 6H_2O$, molar ratio Eu/Sm = 1, 50 mM $(NH_4)_2SO_4$, 20 vol% HCOOH, pH = 1.**

**Table 4: Concentrations of Eu/Gd versus illumination time.**

| Illumination time (h) | $C_{aq, Gd}$ (mmol/L) | $C_{aq, Eu}$ (mmol/L) | Observation |
|---|---|---|---|
| 0 | 10.4 | 10.7 | (Scavenger added) |
| 1 | 10.4 | 10.7 | No precipitation |
| 2 | 10.2 | 10.2 | No precipitation |
| 3 | 9.5 | 9.2 | No precipitation |
| 4 | 9.7 | 8.2 | Precipitation |
| 6 | 9.7 | 7.6 | Precipitation |
| 7 | 9.9 | 6.0 | Precipitation |
| 24 | 10.0 | 0.4 | Precipitation |

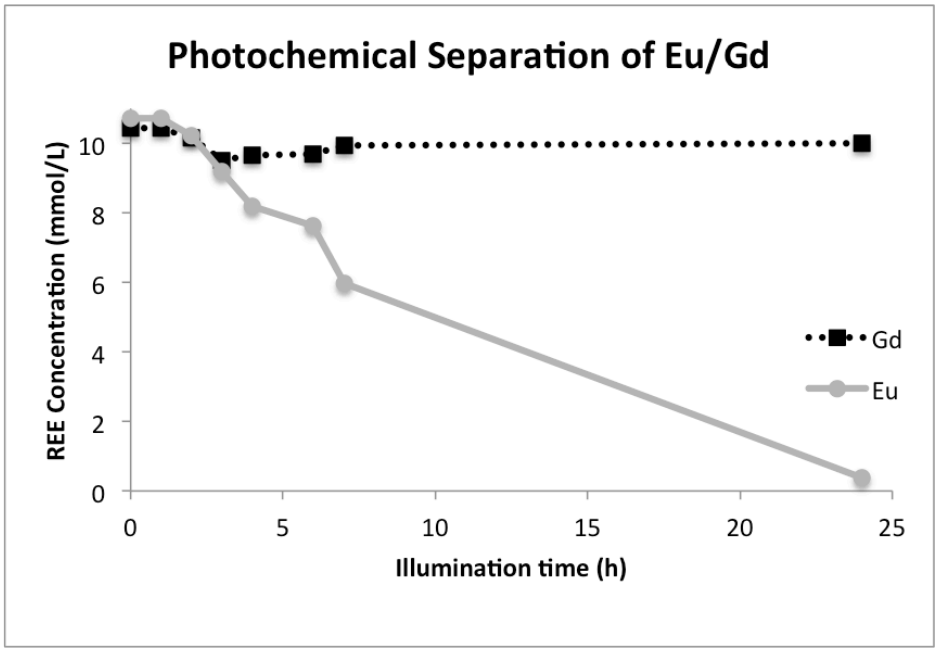


**Figure 16: Photochemical separation of Eu/Gd with 11 W LPML. 10 mM $EuCl_3 \cdot 6H_2O$, molar ratio Eu/Gd = 1, 50 mM $(NH_4)_2SO_4$, 20 vol% HCOOH, pH = 1.**

**Table 5: Concentrations of Eu/Y versus illumination time.**

| Illumination time (h) | $C_{aq, Y}$ (mmol/L) | $C_{aq, Eu}$ (mmol/L) | Observation |
|---|---|---|---|
| 0 | 8.3 | 7.5 | (Scavenger added) |
| 1 | 8.5 | 6.9 | No precipitation |
| 2 | 8.4 | 6.4 | No precipitation |
| 3 | 8.1 | 5.3 | Precipitation |
| 4 | 8.1 | 5.3 | Precipitation |
| 5 | 8.3 | 4.6 | Precipitation |
| 6 | 8.5 | 4.1 | Precipitation |
| 7 | 8.2 | 3.9 | Precipitation |
| 24 | 7.8 | 0.3 | Precipitation |

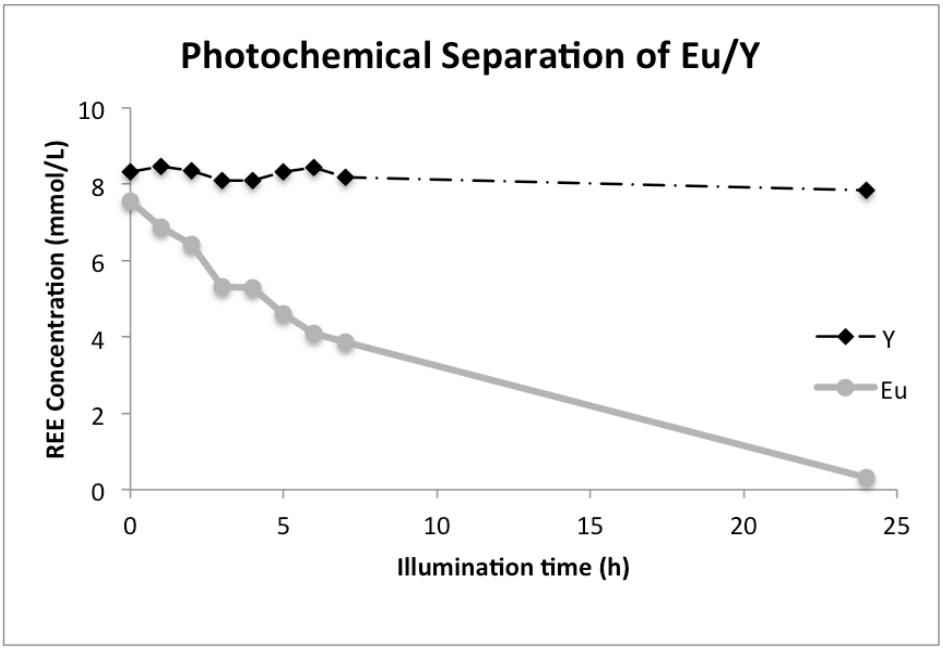


**Figure 17: Photochemical separation of Eu/Y with 11 W LPML. 10 mM $EuCl_3 \cdot 6H_2O$, molar ratio Eu/Y = 1, 50 mM $(NH_4)_2SO_4$, 20 vol% HCOOH, pH = 1.**

A first minor remark is that the start concentrations of the REE are lower than the 10 mM stated in Table 2 (except for mixture two), considering that 20 vol% of scavenger was added. The three mixtures have a slightly different start concentration, which can be associated to difficulties in accurate weighting of the REE when preparing the mixtures, due to the hygroscopic character of the chloride hexahydrate salts.

It was determined that the europium concentration in the aqueous phase has decreased in the three mixtures, indicating that europium(III) was selectively reduced and precipitated as $EuSO_4$. The selective reduction of europium is due to the spectral output of the LPML via the water-to-europium charge transfer band (188 nm line) and the sulfate-to-europium charge transfer band (254 nm line). No precipitation was visible in the non-illuminated dark samples. The concentration of samarium, gadolinium and yttrium remained relatively constant, only 5 % of Sm, 4 % of Gd and 6 % of Y(on molar basis) was removed after 24 h of illumination.

The removal of europium in the different mixtures is compared in Figure 18. Only the reduction of europium is illustrated, excluding the relatively constant concentration of the other REE in solution. Please mind the relative concentration scale in which the europium concentrations are compared to the starting concentration (on molar basis). This visual representation enables us to compare the influence on the europium reduction more precisely.

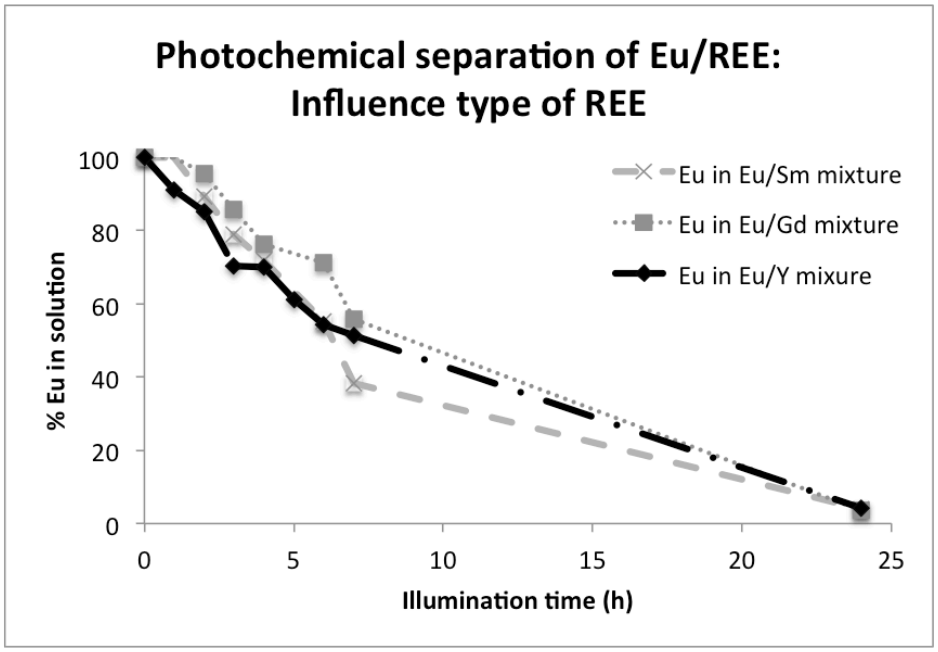


**Figure 18: Overview of removal of Eu in a Eu/Sm, Eu/Gd and Eu/Y mixture with 11 W LPML. 10 mM $EuCl_3 \cdot 6H_2O$, molar ratio Eu/REE = 1, 50 mM $(NH_4)_2SO_4$, 20 vol% HCOOH, pH = 1.**

Figure 18 shows that the differences in separation selectivity and efficiency for the three mixtures are minor. In other words, the same reduction level of europium is achieved, i.e. 96 % Eu(III) removal after 24 h for the three mixtures, and the europium removal rate in the

Eu/Sm and Eu/Y mixtures are practically the same. The Eu/Gd indicates a slightly slower precipitation, but this is practically negligible. This could be attributed to possible light absorption by Gd(III).

It is observed that **gadolinium** shows low intensity absorption bands in the 270-280 nm range [84]. The absorption bands correspond with f-f transitions and are Laporte forbidden. Consequently, they have much lower extinction coefficients than the allowed CT-bands [17]. The Gd(III) absorbance matches the (very weak) spectral lamp output at the wavelengths involved. Hence, it is possible that Gd(III) absorbs a small fraction of the irradiated light. Therefore, a slower reduction reaction could be attributed to this effect but it is expected to be negligible due to the very low extinction coefficients compared to the charge transfer bands.
Please note that **samarium** has almost a half full 4f-subshell ($4f^6$) and can exist in the divalent state, though not in water ($Sm(III) + e^- \rightarrow Sm(II)$; $E^0 = -1.55V$) [44]. Gadolinium and yttrium on the other hand have no stable divalent state. According to literature [58], there is very little spectral interference from other lanthanide species at the wavelengths involved, so that only Eu(III) can be reduced under the applied experimental conditions.
**Yttrium** does not show any spectral absorbance at the concerning wavelengths of the 11 W LPML. Accordingly, no losses in reduction efficiency nor selectivity could be attributed to the presence of yttrium. In the later experiments, the focus will be placed on the Eu/Y mixture, considering its economical relevance and the fact that spectral interference of yttrium can be excluded.

The precipitate of standard mixture 3 (Eu/Y) was dissolved in an acidic HCl solution of pH = 2 and the Eu and Y concentrations were measured with TXRF. An important observation is that practically no yttrium was present. More precisely, virtually 100 % pure $EuSO_4$ precipitate was obtained so no co-precipitation of yttrium was observed. Since the purity of the precipitate is very high, we could state that the selectivity of the photochemical separation technique is outstanding and a major asset of the technique.

From this experiment, it is possible to conclude that the photochemical separation technique works well on lab scale. For all of the three mixtures, 96 % of the trivalent europium has been removed after 24 h of illumination by precipitation as divalent europium under the given circumstances. The two main factors that need to be optimized are in essence the kinetics (considering that 24 h of irradiation is unusually long when aiming at

industrial applications). Secondly, the final purity needs to be enhanced. It was already expected from a thermodynamic point of view that a certain fraction of divalent europium could not be removed from the solution by precipitation, considering the precipitation equilibrium of $EuSO_4$ (see section 9.2). 96 % of removal is already quite high. Nevertheless, RE-applications often have very high purity requirements. For previously mentioned reasons, it is essential to get a better understanding of the reaction mechanism and to investigate the particular aspects that influence the kinetics and thermodynamics.

## 9.2 The influence of the concentration of the precipitating agent

The role of the sulfate-precipitating agent has already thoroughly been discussed in section 6.2 and was further investigated experimentally. The aim of the experiment was to determine the influence of the concentration of the precipitating reagent $(NH_4)_2SO_4$ on the photochemical separation of a RE mixture containing Eu/Y. Standard mixture three was made in fourfold, while all the variables in Table 2 were kept constant except for the concentration of precipitating agent $(NH_4)_2SO_4$. The four different mixtures contained respectively 10 mM, 50 mM, 150 mM and 250 mM of $(NH_4)_2SO_4$, corresponding with a $SO_4^{2-}$/Eu molar ratio of 1, 5, 15 and 25 .

The concentrations of the solutions were measured with TXRF and are listed in Appendix A. The removal of europium as function of the illumination time is illustrated in Table 6 and graphically summarized in Figure 19. The latter only shows the europium precipitation in the mixture, omitting the constant concentration of yttrium (no yttrium was removed in the last sample for none of the mixtures, see Appendix A).

**Table 6: % Eu(III) removed as function of the $Eu^{3+}/SO_4^{2-}$ molar ratio and illumination time.**

| **Molar ratio** | **Eu(III) removal(%)** | | |
|---|---|---|---|
| **$Eu^{3+}/SO_4^{2-}$** | **after 2 h** | **after 8 h** | **after 24 h** |
| 1 | 14 | 60 | 87 |
| 5 | 19 | 80 | 94 |
| 15 | 49 | 86 | 97 |
| 25 | 53 | - | 97 |

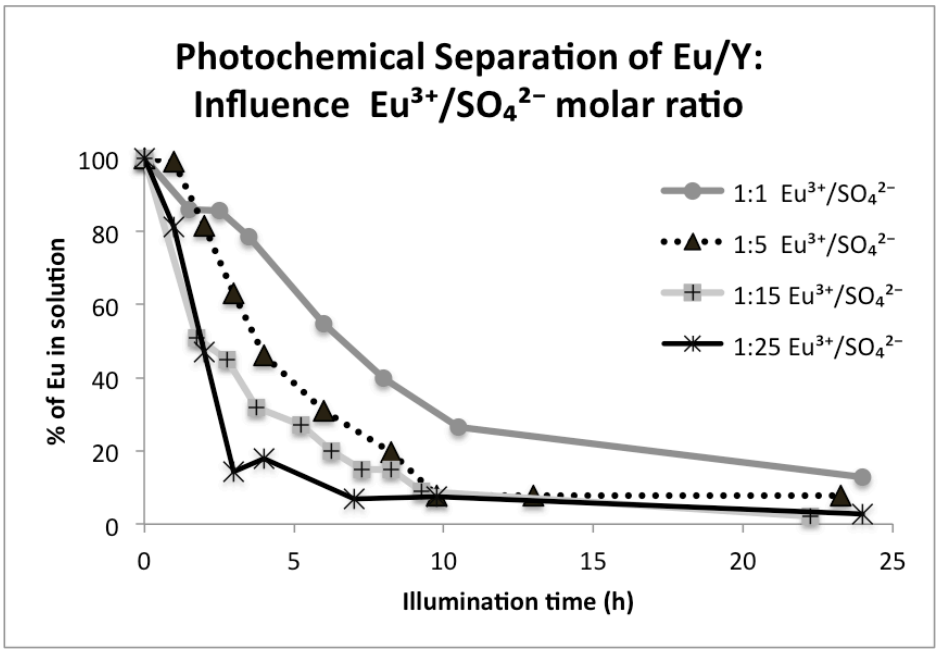


**Figure 19: Overview % Eu in solution in Eu/Y mixture for [$(NH_4)_2SO_4$] = 10 mM, 50 mM, 150 mM, 250 mM with 11 W LPML. 10 mM $EuCl_3 \cdot 6H_2O$, molar ratio Eu/Y = 1, 20 vol% HCOOH, pH = 1.**

In terms of kinetics, Table 6 and Figure 19 show a faster europium reduction for higher sulfate concentration. An excess of sulfate increases the probability of divalent europium meeting a sulfate ion in the solution, resulting in higher precipitation rates.

From thermodynamic point of view, Table 6 indicates that after 24 h of illumination, a better separation is obtained for the higher sulfate ratios than for the solution with 10 mM and 50 mM sulfate. Equation (23) illustrates the precipitation equilibrium. $EuSO_4$ has a solubility product of 1.5 $10^{-9}$ in water [85]. Please note that this value is only an approximation since the solubility product depends on the temperature and the composition of the aqueous phase (pH, dissolved salts, organic compounds, ... )[49].

$$EuSO_4 \rightleftharpoons Eu^{2+} + SO_4^{2-} \qquad (23)$$

$$K_{sp} = \left[Eu^{2+}\right] . \left[SO_4^{2-}\right] = 1.5\ 10^{-9} \qquad (24)$$

From equilibrium equation (23) and Le Chatelier's Principle, it is clear that the higher $[SO_4^{2-}]$, the more europium(II) can be removed from the solution by precipitation. This corresponds with the experimental results in Table 6.

As stated before, it was already expected from a thermodynamic point of view that a certain fraction of divalent europium could not be removed from the solution by precipitation, considering the solubility product of $EuSO_4$. The marginal concentration of divalent europium that remains in the solution can be calculated as followed. The equilibrium concentration of $Eu^{2+}$ that remains in solution is expressed by equation (25).

$$\left[Eu^{2+}\right] = \frac{K_{sp}}{\left[SO_4^{2-}\right]} \tag{25}$$

The fraction of europium that cannot be removed from the solution, is indicated by the ratio of the equilibrium concentration of $Eu^{2+}$ to the initial concentration of trivalent europium $[Eu^{3+}]_{initial}$ in solution, see equation (26).

$$\frac{\left[Eu^{2+}\right]}{\left[Eu^{3+}\right]_{initial}} = \frac{K_{sp}}{\left[SO_4^{2-}\right].\left[Eu^{3+}\right]_{initial}} \tag{26}$$

This is the lower limit of the fraction of europium that remains in the solution. For an equimolar amount of europium and sulfate and 10mM of initial $Eu^{3+}$, this results in approximately 0.4 %. This means that a maximum of 99.6 % of the europium can be removed by precipitation on molar basis.

Please note that several additional factors should be taken into consideration. First, the sulfate concentration is not constant but decreases due to photochemical decomposition and the formation of precipitate. Additionally, the initial concentrations of europium and sulfate are diluted by the addition of scavenger. Thirdly, the concentrations of europium and sulfate can diverge due to possible complex formation with the scavenger. Finally, the fact that samples are taken from the solution and not from the precipitate will influence the concentrations as well. These parameters will have an influence on the fraction of europium that remains in solution so that the theoretical value calculated by equation (26) will not be reached. The europium removal after 24 h of illumination versus the $SO_4^{2-}$/Eu molar ratio is illustrated in Figure 20.

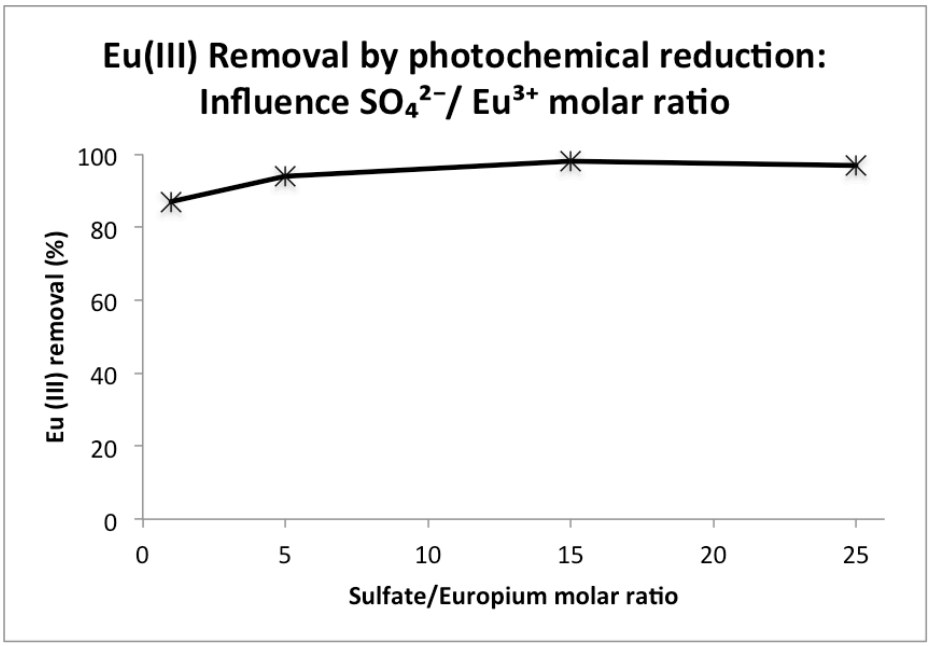


**Figure 20: Influence of the $SO_4^{2-}$/Eu molar ratio (1, 5, 15, 25) on europium removal in Eu/Y mixture after 24 h of illumination with a 11 W LPML. 10 mM $EuCl_3 \cdot 6H_2O$, molar ratio Eu/Y = 1, 20 vol% HCOOH, pH = 1.**

To conclude, a higher $SO_4^{2-}$/Eu molar ratio promotes a faster and higher removal of europium until an optimal limit is reached. This limit is visible as the plateau in Figure 20. This plateau value is the maximum percentage of europium that can be removed in practice (whereas higher ratios yield the same recovery). Consequently, in order to minimize the load of chemicals, the minimal sulfate concentration required to reach optimal recovery should be determined experimentally. A molar ratio of 15 meets these requirements for this experiment (when avoiding interpolation).

## 9.3 The influence of the scavenger

As stated before, the role of the scavenger is to neutralize the formed hydroxyl radicals and thereby minimize the backward oxidation reaction. For the photo-reduction of europium in aqueous media, a scavenger needs to have a carbon atom with at least one hydrogen atom directly attached to it, and preferably functional groups (R) that are radical-stabilizing (equation (27)).

$$R_3CH + OH^{\cdot} \rightarrow R_3C^{\cdot} + H_2O \qquad (27)$$

The most commonly applied scavengers are formic acid and isopropanol, which react according to equation (28) and (29).

$$(CH_3)_2CHOH + OH^{\cdot} \rightarrow (CH_3)_2C^{\cdot}OH + H_2O \quad (28)$$

$$HCOOH + OH^{\cdot} \rightarrow C^{\cdot}OOH + H_2O \quad (29)$$

The intention of this experiment is to determine whether these two scavengers lead to a significant difference with regard to the photochemical separation of the standard mixtures. The three standard mixtures are made in duplicate, whereby formic acid is added to the first set and isopropanol is added to the second (identical) set. An important remark is that formic acid is a strong acid, so that the scavenger influence is not independent from the pH influence. This is illustrated by Table 7, which shows the pH of the RE-solution before and after the addition of the scavenger formic acid.

**Table 7: pH of aqueous solution before and after addition of formic acid.**

| Initial pH of the solution | pH after addition of formic acid |
|---|---|
| 1.1 | 0.8 |
| 2.0 | 1.1 |
| 3.1 | 1.2 |
| 4.0 | 1.2 |
| 5.1 | 1.2 |
| 6.1 | 1.2 |
| 7.0 | 1.3 |
| 7.9 | 1.3 |

It is obvious that using formic acid considerably decreases the pH. However, abstraction can be made of the pH aspect by examining reference mixtures with the same pH after the addition of scavenger. This implies that standard mixtures, to which formic acid is added, have an initial pH = 4.0 and final pH = 1.2. Equivalently, for the second set of reference mixtures, the initial pH = 1.1 and the pH after addition of isopropanol is 1.2 as well.

Surprisingly, standard mixture one and two (Eu/Sm and Eu/Gd) showed precipitation for both the illuminated and the dark stored samples where isopropanol was added, indicating that the precipitation is not due to illumination. Both precipitates were collected and the

composition was investigated by X-ray crystallography. Both precipitates consisted of a REE(III) centre with coordination number nine: five coordinating water molecules and two bidentate sulfate ions. The asymmetric unit consists of one water molecule and an ammonium cation. It is remarkable that no europium was found in the divalent state after illumination.

The Eu/Y mixture, on the other hand, proved to be suited for selective removal of only europium when isopropanol was added, since no decrease in the yttrium concentration was observed. The concentrations are listed in Appendix B. The europium removal is visible in Figure 21 for both of the scavengers at final pH 1.

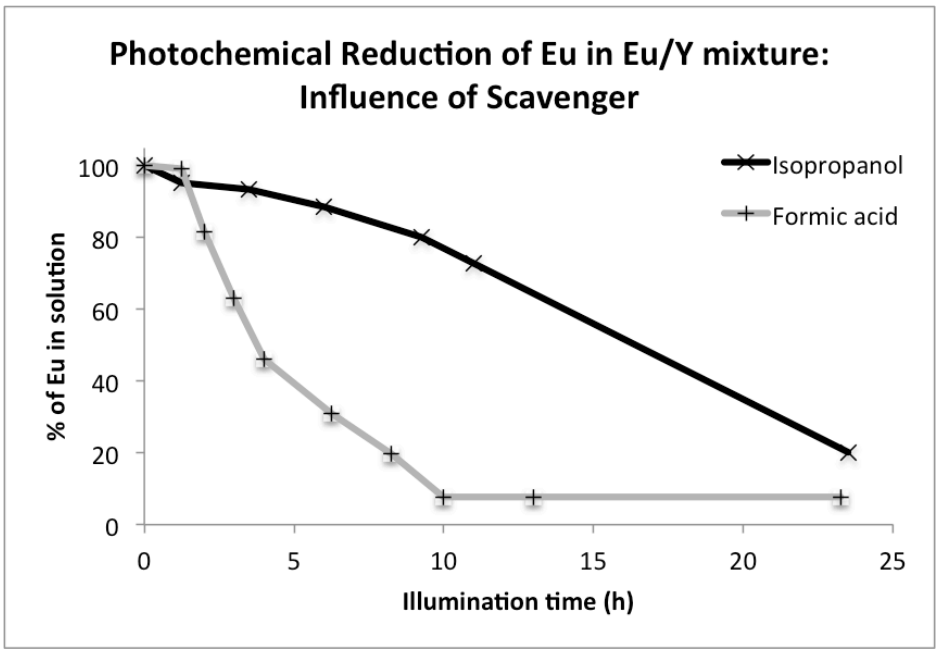


**Figure 21: Influence of the scavenger on europium removal in Eu/Y mixture with a 11 W LPML. 10 mM $EuCl_3 \cdot 6H_2O$, molar ratio Eu/Y = 1, 50 mM $(NH_4)_2SO_4$, 20 vol% scavenger isopropanol/formic acid, pH = 1.**

In order to fully understand the effect of isopropanol on the Eu/Sm and Eu/Gd mixtures, several solutions were made and stored without illuminating them. The REEs (Table 8) were added in 10 mM in a HCl aqueous solution of pH 1, together with 50 mM of precipitating agent and 20 vol% of isopropanol. After 24 h the mixtures were observed visually. The observations are summarized in Table 8.

**Table 8: Composition of the non-illuminated solutions.**

| Composition | Observation |
|---|---|
| Eu/Sm | Precipitation |
| Eu/Gd | Precipitation |
| Eu/Y | No Precipitation |
| Sm | Precipitation |
| Eu | Precipitation |
| Gd | No precipitation |
| Y | No precipitation |

The same mixtures without addition of isopropanol were also stored and no precipitation was visible in these mixtures. It can be deduced from these observations that the precipitation in the mixtures of Table 8 is caused by isopropanol. Furthermore, the precipitation formation is not related to the illumination of the samples. The phenomenon causing this is called the anti-solvent effect. The dielectric constant and consequently the solubility of a system can be changed by the addition of an anti-solvent: a liquid miscible with the solvent, which reduces the solute solubility in this new, mixed solvent [86]. The addition of an organic solvent with low dielectric constant will result in a larger decrease of the dielectric constant of the mixture, compared to the addition of a solvent with higher dielectric constant. The addition of an organic scavenger, such as formic acid and 2-propanol causes the decrease of the dielectric constant of the medium. This results in an increasing electrostatic attraction between the oppositely charged species, $RE^{3+}$ and $SO_4^{2-}$, and a decrease in the solubility of the rare earth(III) sulfates [48] [86]. The properties of the used scavengers are listed in Table 9 [87].

**Table 9: Scavengers and their properties.**

| Anti-solvents | Chemical Formula | Dielectric Constant $\varepsilon_r$ |
|---|---|---|
| Formic acid | HCOOH | 58.5 |
| Isopropanol | $C_3H_7OH$ | 17.9 |

Please note that formic acid has a too high dielectric constant to cause precipitation of trivalent rare earths. Isopropanol on the other hand, has a lower dielectric constant, so that

the solubility of the rare earth(III) sulfates decreases and precipitation of trivalent rare earth sulfates is observed. The reason why precipitation is only observed for the solutions containing europium and samarium is probably due to the following trend in solubility: $Eu_2(SO_4)_3 < Sm_2(SO_4)_3 < Gd_2(SO_4)_3 < Y_2(SO_4)_3$ [88].

Let's now focus on standard mixture three which was not susceptible to the anti-solvent effect with addition of isopropanol. Figure 21 illustrates the faster reaction when using formic acid. The same final removal of europium can be achieved with isopropanol, although longer illumination times will be required. The faster reaction is due to the fact that formic acid provokes an additional reducing effect by the equations (30) and (31). The formed radicals further react to form more stable compounds according to equation (32) and (33).

$$HCOOH \xrightarrow{260\ nm} C^{\cdot}OOH + H^{\cdot} \quad (30)$$

$$C^{\cdot}OOH + Eu^{3+} \rightarrow Eu^{2+} + CO_2 + H^{+} \quad (31)$$

$$H^{\cdot} + H^{\cdot} \rightarrow H_2 \quad (32)$$

$$H^{\cdot} + OH^{\cdot} \rightarrow H_2O \quad (33)$$

Consequently, formic acid induces a faster reduction reaction. Its disadvantages however are that it is not considered as a green product and especially that it induces a difficult pH control since it is a strong acid. The latter is not the case for isopropanol. Additionally, the organic radical formed when using isopropyl alcohol as scavenger (equation (28)), can also cause a further reduction of Eu(III) [48], [58] (equation (34)).

$$(CH_3)_2 CO^{\cdot}H + Eu^{3+} \rightarrow Eu^{2+} + H^{+} + (CH_3)_2 CO \quad (34)$$

The difference with formic acid is that this reaction is not caused by illumination, while the additional reducing effect of formic acid is induced by light of 260 nm. The faster reaction of formic acid corresponds with observations found in literature [46] [48].

We can conclude that the addition of scavenger is essential to neutralize reactive hydroxyl radicals, which cause an undesirable back reaction, namely the oxidation of divalent europium. In general, the choice of scavenger depends on the radical produced and is limited by the solubility of the reagents. It is also important that the scavenger does not interfere with the primary photoreduction equation [57]. Alternative scavengers (for instances ethanol, acetaldehyde, isopropyl formate) need to be examined in order to

overcome the limitations of the currently employed scavengers (pH-control for formic acid and anti-solvent effect with isopropanol). The photoreduction of Eu(III) occurred more rapidly with formic acid as scavenger, since $C^{\cdot}OOH^-$ radicals formed by photolysis of formic acid at 260 nm act as an extra reducing agent for Eu(III). Isopropanol cannot be used as scavenger for every RE mixture since it promotes the formation of RE(III)sulfate precipitation due to the so-called anti-solvent effect. Isopropanol has no additional photochemical reducing effect, but allows higher pH. This will lead to better results in terms of illumination times as will become clear in the next experiments (section 9.4).

## 9.4 The influence of the pH of the aqueous solution

The purpose of the experiment is to determine the influence of the pH on the photochemical separation of a Eu/Y-mixture. In order to investigate the influence of pH, it is essential to use a neutral scavenger that allows the preparation of an aqueous solution with varying pH. Since isopropanol does not alter the pH substantially (Table 10), isopropanol was used as scavenger instead of the usual formic acid.

**Table 10: pH of aqueous solution before and after addition of isopropanol.**

| Initial pH of the solution | pH after addition of isopropanol |
|---|---|
| 0.0 | 0.1 |
| 1.1 | 1.2 |
| 2.0 | 2.3 |
| 3.1 | 3.3 |
| 4.1 | 4.4 |
| 5.1 | 5.2 |
| 6,1 | 6.0 |
| 7.0 | 6.9 |
| 8.2 | 7.9 |

Mixtures of 10 mM $EuCl_3.6H_20$ and 10 mM $YCl_3.6H_20$ were prepared in pH-solutions of 0 up to 8. For pH 0 to pH 5, a 1M HCl-solution was diluted with distilled water to obtain the desired pH. The pH 6-solution was pure distilled water, while the pH 7 and 8 -solutions were prepared by adding small amounts of a 1M NaOH-solution to distilled water. 50 mM of $(NH_4)_2SO_4$ was added as a precipitating agent and prior to illumination 20 vol% of

isopropanol-scavenger was added. In Table 10, the pH-values before and after scavenger addition are listed.

The composition of the precipitate of the mixture with pH 2 was further examined. Single crystals were obtained by evaporating the solution at room temperature and the crystals were subsequently investigated by X-ray crystallography. The crystal structure is visible in Figure 22 and the detailed crystal data can be found in Appendix C.

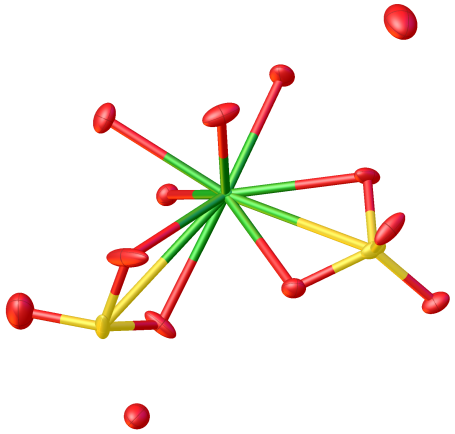

**Figure 22: Crystal structure of $EuSO_4$ precipitate at pH 2. With the green color stands for europium(II), red for oxygen and yellow for sulfur.**

The concentrations were measured with TXRF and are listed in Appendix D. The results of the lower pH range, i.e. pH = 0 to pH = 4, are summarized in Figure 23.

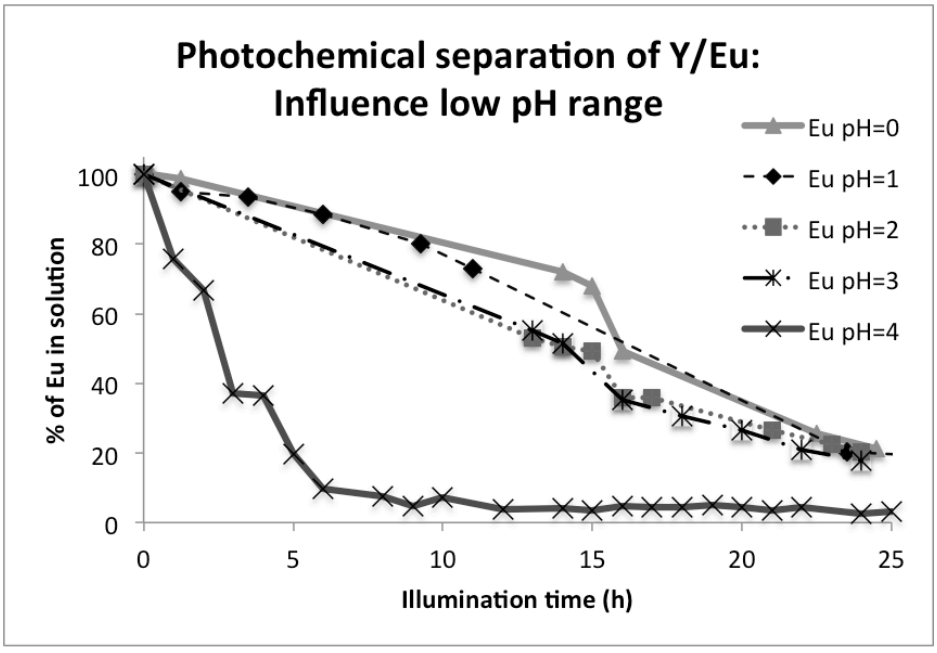


**Figure 23: Overview % Eu in solution in Eu/Y mixture for pH = 0–4 with 11 W LPML. 10 mM $EuCl_3 \cdot 6H_2O$ molar ratio Eu/Y = 1, 50 mM $(NH_4)_2SO_4$, 20 vol% isopropanol.**

Figure 23 illustrates that a decrease in acidity of the solution, from pH = 0 to pH = 4, yields a faster reduction of europium. This is also illustrated in Table 11, which indicates the Eu(III) percentage that is removed by precipitation after 14 and 24 h. Hence, there is an increasing separation efficiency with increasing pH for the Eu/Y mixture. For the pH 1-experiment, no sample was taken after exactly 14 h. To avoid interpolation, this value is excluded from the table.

**Table 11: Removal of europium after 14 and 24 h of illumination versus pH.**

| | pH | | | | |
|---|---|---|---|---|---|
| | **0** | **1** | **2** | **3** | **4** |
| % Eu removed after 14 h | 29 | - | 50 | 49 | 97 |
| % Eu removed after 24 h | 80 | 80 | 80 | 82 | 98 |

The faster reduction at higher pH can be explained by the photochemical reactions shown in equation (35) and equation (36). Light with a wavelength of 188 nm only promotes the forward reduction reaction (equation (35)) while the backward oxidation of europium occurs at 366 nm (equation (36)). The radicals, originating from the scavenger, do probably induce the backward reaction as well, but the specific mechanism is not fully understood yet. Equation (35) illustrates that an increase in $H^+$ concentration favours the oxidation according to the principle of Le Chatelier. Hence, at lower acidity of the aqueous solution, the oxidation reaction (36) cannot take place and the reduction reaction will be promoted so that faster separation can be obtained.

$$\left[Eu\left(H_2O\right)_n\right]^{3+} \underset{\longleftarrow}{\overset{188\ nm}{\longrightarrow}} \left[Eu\left(H_2O\right)_{n-1}\right]^{2+} + OH^{\bullet} + H^+ \qquad (35)$$

$$2Eu^{2+} + 2H^+ \xrightarrow{366\ nm} 2Eu^{3+} + H_2 \qquad (36)$$

Please note that after 72 h of illumination, 98.7 % and 98.8 % of Eu(III) has precipitated as Eu(II) for respectively pH = 2 and pH = 4. This means that a lower pH will only slow down the photochemical reaction. The same reduction level of europium can be achieved by applying longer illumination times. As stated in section 9.2, the fraction of europium that cannot be removed from the solution is determined by the precipitation equilibrium of $EuSO_4$.

Additionally, divalent europium is more thermodynamically stable in less acidic media as can be deducted from the Pourbaix diagram of water in Figure 24 [89].

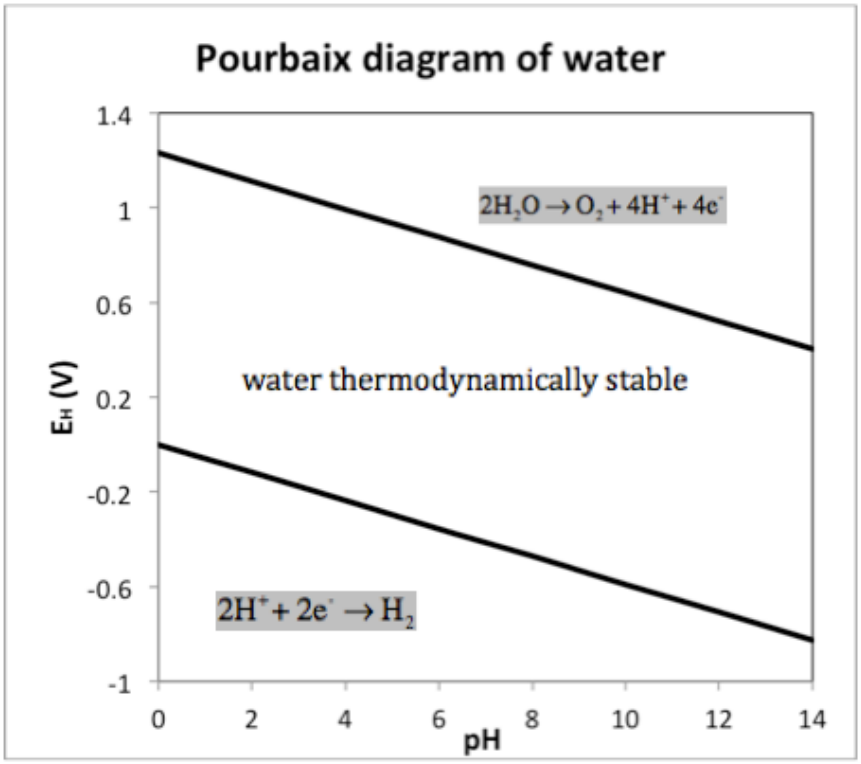


**Figure 24: Pourbaix diagram of water at standard conditions.**

The lower limit of the stability region of water is determined by the reduction reaction in equation (37).

$$2H^+ + 2e^- \rightarrow H_2 \qquad (37)$$

The Nernst equation can be written as in equation (38). With $E^0$ is the standard electric potential, $R$ the universal gas constant, $T$ the absolute temperature, $n$ the number of moles of electrons transferred in the balanced equation, $F$ the Faraday constant, $[H^+]$ the proton concentration and $p$ is the partial pressure [89].

$$E_{H^+/H_2} = E^\circ_{H^+/H_2} + \frac{RT}{nF} \ln\left(\frac{[H^+]^2}{p_{H_2}}\right) \qquad (38)$$

At standard conditions and unit partial pressure of $H_2$, this reduces to equation (39)

$$E = -0.059\ \mathrm{pH} \qquad (39)$$

As stated before, the standard redox potential of Eu(III) + $e^-$ → Eu(II) in water is $E_0$ = -0.34V. When entering this value in equation (39), an optimal pH of 5.8 is obtained. This means that from thermodynamic point of view, Eu(II) is stable at pH 5.8 or higher (up to the pH at

which hydrolysis takes place). At lower pH, the photochemical reduction can kinetically still take place but divalent europium will remain stable for a shorter time compared to higher pH. This will consequently result in a slower removal by precipitation. This corresponds with the observation that higher pH induces a faster reduction of europium. In conclusion, due to the higher stability of divalent europium at higher pH, the reduction reaction is enhanced and consequently a faster reaction is obtained.

Figure 25 illustrates the percentage of europium that is removed as function of the illumination time at higher pH, namely from pH = 5 to pH = 8. Since the concentration of yttrium has altered significantly at higher pH, the % of yttrium in the solution is visualized in Figure 26.

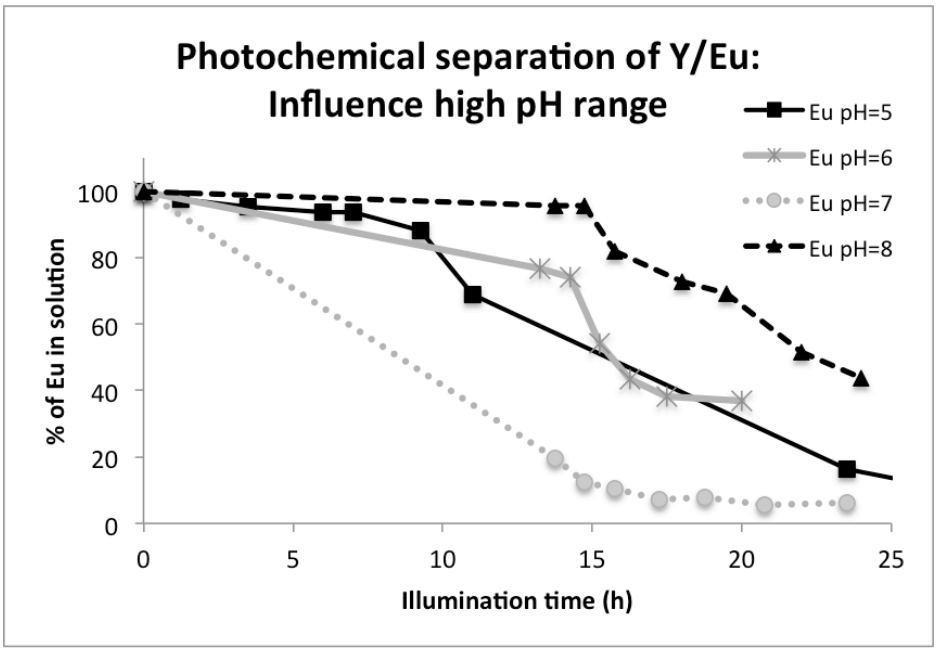


**Figure 25: Overview % Eu in solution in Eu/Y mixture for pH = 5–8 with 11 W LPML. 10 mM $EuCl_3 \cdot 6H_2O$, molar ratio Eu/Y = 1, 50 mM $(NH_4)_2SO_4$, 20 vol% isopropanol.**

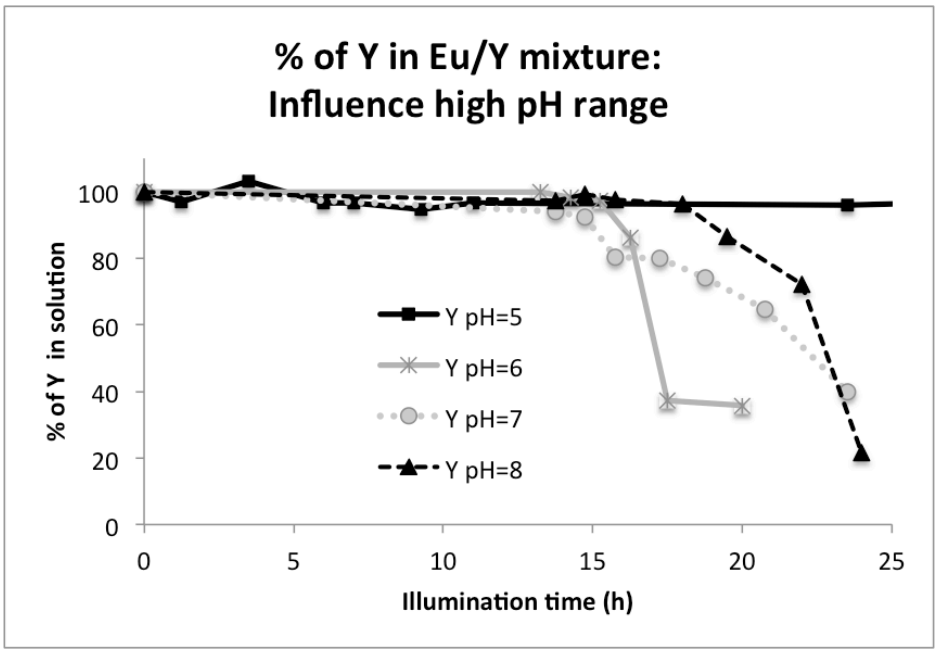


**Figure 26: Overview % Y in solution in Eu/Y mixture for pH = 5–8 with 11 W LPML. 10 mM $EuCl_3 \cdot 6H_2O$, molar ratio Eu/Y = 1, 50 mM $(NH_4)_2SO_4$, 20 vol% isopropanol.**

No straightforward relation regarding the europium reduction at higher pH can be deducted from Figure 25. On the other hand, Figure 26 indicates the removal of yttrium at pH = 6, pH = 7 and pH = 8. For pH = 5, no yttrium was removed from the solution but this mixer shows a slower europium reduction than pH = 4. It should be stressed that the solutions at pH = 6, pH = 7 and pH = 8 that were stored in a dark closet instead of being illuminated, revealed precipitation as well. The concentrations of these 'dark samples' were measured with TXRF and the removal of europium and yttrium after 48 h is shown in Table 12.

**Table 12: Removal of REE in the dark samples at different pH values after 48 h.**

| pH | % Eu removed after 48 h | % Y removed after 48 h |
|---|---|---|
| 6 | 12 | 21 |
| 7 | 21 | 29 |
| 8 | 22 | 25 |

Table 12 clearly demonstrates that Eu(III) and Y(III) were both removed from the aqueous solution of the dark samples by precipitation. In the line of the expectations, the removal of europium was reduced at higher pH values, for the reason that insoluble trivalent rare earth hydroxides are formed according to equation (40).

$$M^n + H_2O \rightleftharpoons M(OH)^{(n-1)+} + H^+ \qquad (40)$$

In general for the lanthanides, the tendency for hydrolysis increases with the increase of atomic number and the contraction of the ionic radius. The varying basicities of the REEs are illustrated by the pH at which the precipitation takes place. Precipitation pHs are a function of the solution conditions. The solubility constants $K_{sp}$ of $Eu(OH)_3$ and $Y(OH)_3$ together with the pH at which they are formed, are displayed in Table 13. As already mentioned, the precipitation pH is a function of the solution conditions, so that the absolute values in the table below need to be considered with caution. Table 13 illustrates that the pH difference at which yttrium and europium undergo hydrolysis is insignificant.

**Table 13: Properties of $Eu(OH)_3$ and $Y(OH)_3$.**

| | **Hydrolysis pH** | **$K_{sp}$** |
|---|---|---|
| $Eu(OH)_3$ | 6.75 [90] | $9.4 \times 10^{-27}$ [91] |
| $Y(OH)_3$ | 6.78 [92] | $1.0 \times 10^{-23}$ [48] |

This corresponds with the observations that at pH = 7 and pH = 8, hydrolysis occurs. As mentioned before, the values in Table 13 are influenced by the solution conditions such as salt concentration and the presence of organic compounds. This could explain why hydroxide precipitation can already be observed at pH = 6. It is however still unclear why the removal of yttrium occurs faster at pH = 6 than at pH = 8.

In conclusion, the pH has a significant influence on the photochemical reduction of europium in a Eu/Y mixture. An increase in pH from pH = 0 to pH = 4 yields a faster reduction, longer illumination times are required to reach the same removal of Eu(III) at lower pH. The optimal reduction conditions are obtained at pH = 4 due to more favourable conditions for the forward reaction and disadvantageous conditions for the undesired backreaction. Furthermore, divalent europium is more stable in less acidic media (cf. Pourbaix). At pH = 6 and higher, hydrolysis occurs, meaning that both $Eu(OH)_3$ and $Y(OH)_3$ are formed and precipitated together. Hence, no selective separation is obtained. When aiming at industrial applications, short illumination times are desired considering the feasibility of the process, the effectiveness of the separation in a certain time, the energy costs, etc. Optimization of the pH is a key factor when targeting commercial separation of RE mixtures.

## 9.5 The influence of the molar ratio of REE

As already stated in chapter three, $Y_2O_3$:Eu is a useful phosphor in many lightning applications. Yttria ($Y_2O_3$) is a perfect host lattice for Eu(III); yttrium is substituted by europium in an $Y_2O_3$ lattice. It is one of the main red-emitting phosphors that are widely used in lightning industry. Therefore, the separation of a Eu/Y mixture is economically relevant. Usually five to ten atom percentage (at.%) of yttrium is substituted by europium [83]. It is possible to go up to 50 at.% of europium in the phosphors, but this is economically not viable. Less than three atom percentage of $Eu^{3+}$ is not suitable because the charge transfer band of europium will not be intense enough to absorb all the UV radiation in a phosphor lamp.

Up till now, the experimental part of this master thesis only investigated equimolar binary mixtures in order to verify and substantiate the theoretical fundamentals and proof of principle. However, with this new set of experiments, we investigated the selective photochemical reduction of europium on synthetic mixtures of yttrium and europium whereby the Eu/Y ratio was varied according to the commercial composition of phosphors. The imitation of industrially applied mixtures is essential, as a 1:1 Eu/Y ratio will in practice almost never be found in a non-laboratory environment. Six different mixtures were made; all parameters of standard mixture three (see Table 2 for the composition) were kept constant, with exception of the Eu/Y molar ratio. The REE ratios of the mixtures are listed in Table 14.

**Table 14: Eu/Y mixtures with different molar ratio.**

| Ratio Eu:Y | [Eu(III)] (mM) | [Y(III)] (mM) | Literature Reference |
|---|---|---|---|
| 1:1 | 10 | 10 | - |
| 1:10 | 10 | 100 | [93] |
| 1:14 | 10 | 140 | [94] |
| 1:15 | 10 | 150 | [95] |
| 1:18 | 10 | 180 | [27] |
| 1:20 | 10 | 200 | [96] |

The concentrations of the different mixtures were measured with TXRF and can be found in Appendix E. Table 15 illustrates the removal of europium after a specific illumination time. The results are graphically summarized in Figure 27.

**Table 15: % Eu(III) removed in function of the Eu/Y ratio and illumination time.**

| Eu/Y ratio | Eu(III) removed | | |
|---|---|---|---|
| | after 7 h (%) | after 22.5 h (%) | after 50 h (%) |
| 1:1 | 49 | 96 | 99 |
| 1:10 | 35 | 78 | 97 |
| 1:14 | 23 | 64 | 95 |
| 1:15 | 20 | 58 | - |
| 1:18 | 10 | - | - |
| 1:20 | - | - | - |

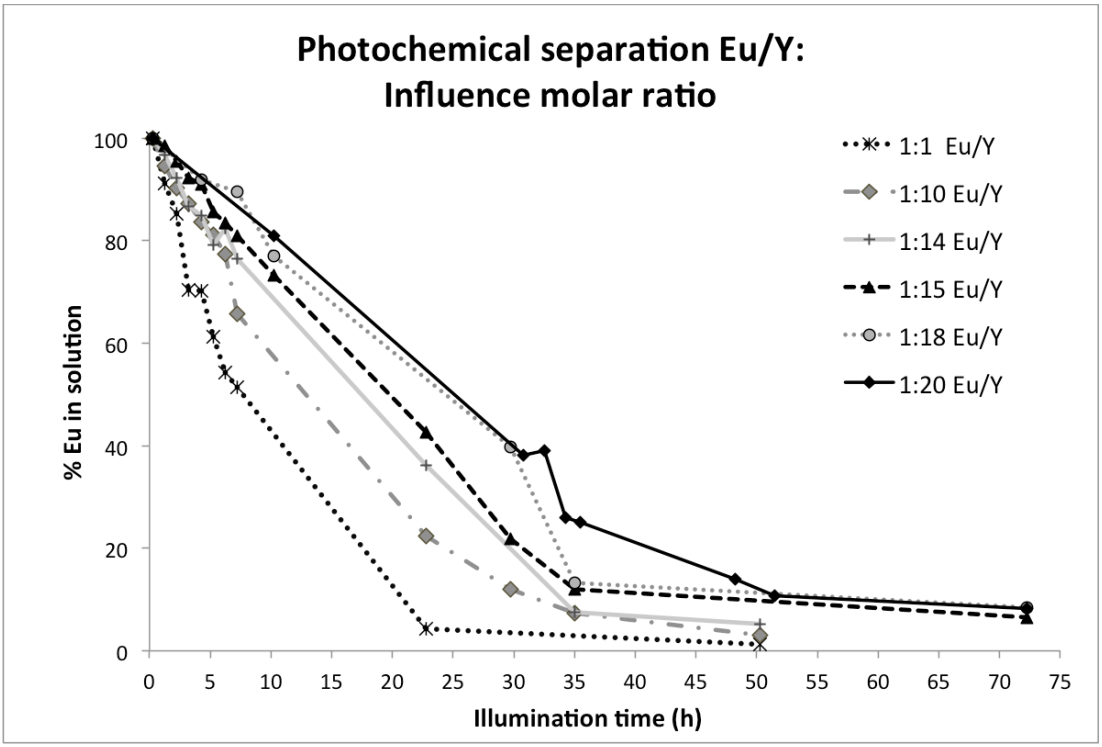


**Figure 27: Overview % Eu in solution in Eu/Y mixture for ratio 1:1, 1:10, 1:14, 1:15, 1:18, 1:20 with 11 W LPML. 10 mM $EuCl_3.6H_2O$, pH = 1, 50 mM $(NH_4)_2SO_4$, 20 vol% HCOOH.**

The concentration of yttrium did not alter significantly (0 %, 5 %, 12 %, 3 %, 2 %, 2 % of Y was respectively removed in the last sample) during illumination, while europium, on the contrary, was reduced and subsequently precipitated for all of the mixtures. Table 15 illustrates that a high concentration of yttrium delays the europium precipitation: the more yttrium is present in a solution in comparison with europium, the slower the precipitation rate. This could be explained by a kinetic effect: the high concentration of yttrium lowers the

probability of divalent europium meeting a sulfate ion in the solution, resulting in less electron transfer reactions from sulfate to europium and hence a slower precipitation reaction. Due to the slower reaction, longer illumination times have to be applied. The high concentration of yttrium provokes a slower precipitation rate, but does not alter the thermodynamic equilibrium. For all the applied ratios, more than 90 % of the europium had eventually precipitated after 72 h of illumination.

Apart from one study [48] regarding a Eu/Gd mixture with a 27-fold excess of Gd(III), not much research has been done considering the effect of molar ratio. In this particular study [48], De Morais & Ciminelli applied molar ratios of $HCOOH/Eu^{3+}$ = 600 and $SO_4^{2-}/Eu^{3+}$ = 10. An important factor is that a short illumination time of three hours with two non-immersed 15 W LPML with emission peak at 254 nm was applied to these experiments. The authors concluded that the experiments with a high gadolinium concentration did not lead to precipitation of $EuSO_4$ and that for this reason, no separation was possible. On that account, the authors stated that the use of photochemical reduction in aqueous phase is limited to diluted and relatively pure solutions. This conclusion is clearly contradicted by the observations of our own Eu/Y experiment, in which we demonstrated that highly concentrated mixtures can definitely be separated if only sufficient long illumination times were applied. However, a Eu/Gd 1:30 mixture has been tested for longer illumination times to gather more comparable data with respect to the literature reference.
A 1:30 mixture of Eu/Gd in an aqueous HCl solution of pH 1 with 20 vol% HCOOH scavenger and 50 mM $(NH_4)_2SO_4$ was illuminated for 87 h. Samples were taken at regular time intervals and the concentrations, analyzed on TXRF, are listed in Table 38 in Appendix E and the removal of REE is graphically summarized in Figure 28.

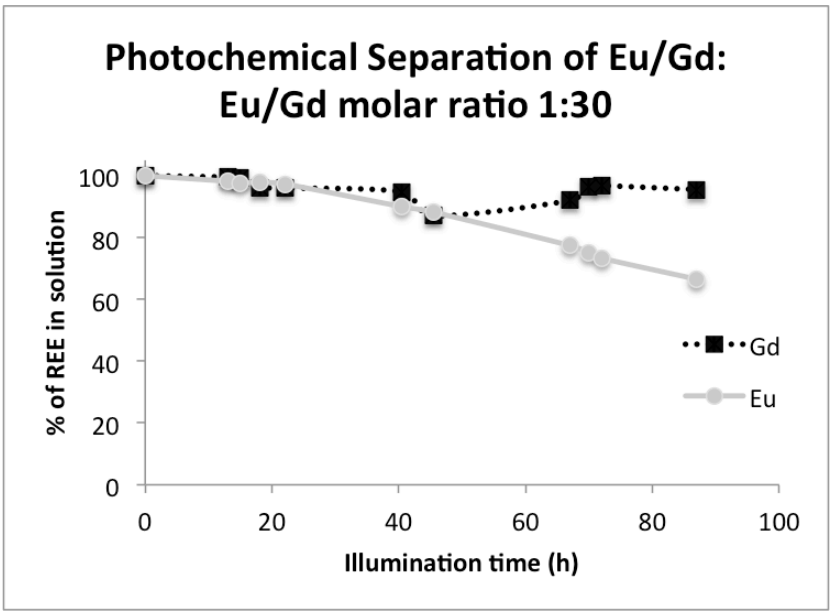


**Figure 28: % of REE in solution in Eu/Gd mixture for Eu/Gd ratio 1:30 with a 11 W LPML. 10 mM $EuCl_3 \cdot 6H_2O$, pH = 1, 50 mM $(NH_4)_2SO_4$, 20 vol% HCOOH.**

De Morais & Ciminelli applied an illumination time of only three hours (with two 15W instead of one 11 W lamp) and no separation was obtained. This corresponds with the observations of Figure 28 in which only 1.8 % of Eu was removed after 13 h. The final conclusion of De Morais can however indisputably be rejected on the basis of Figure 28: even for a Eu/Gd mixture with higher applied ratio (i.e. 1:30) than the 1:27 mixture of De Morais & Ciminelli, selective precipitation of europium was obtained. After 87 h of illumination, 33.5 % of Eu(III) was removed. Conclusively, it can be confirmed that separation for high concentrated RE mixtures, Eu/Y and Eu/Gd, is possible.

To summarize, the high concentration of other REEs only delays the europium precipitation and does not inhibit the separation, but significantly increase the illumination time. These results therefore indicate difficulties in applying the photochemical separation technique to more realistic mixtures. Since commercial concentrations are a key-factor when aiming at industrial applications, it is essential to further investigate the parameters that can reduce the illumination time. This would make the photochemical separation technique more economically accessible for the recycling of commercial phosphor mixtures. For this purpose, the influence of light source parameters, in particular irradiance, are investigated in the next section. Optimization of the light source parameters could decrease illumination times and (partly) solve the issue.

## 9.6 Light sources and their properties

Up to now, only the influence of chemical parameters on the photochemical separation of RE was investigated. The chemical influences that were investigated are the concentration of precipitating agent, the pH of the aqueous solution, the type of scavenger and the molar ratios of REEs. Next to these chemical effects, influences related to the properties of the light source will accordingly affect the selectivity and efficiency of the photochemical separation technique.

First of all, the selectivity of the rare earth separation is determined by the *spectral output* of the lamp. The wavelength(s) at which the light source emits, is crucial for the selectivity of the separation. This is visualized by the spectrum of the lamp that gives the spectral irradiance in function of the wavelength. The *spectral irradiance* is given in $\mu W/(cm^2.\ nm)$ and is a measure for the light power. The $\mu W/cm^2$ is the power density at the wavelength $\lambda$ (nm). Therefore '$cm^2$ 'refers to the illuminated area and 'nm' refers to the wavelength of interest [97].

Another main characteristic of the light source is its *irradiance* in a certain wavelength range. So, instead of considering the irradiance at each wavelength separately as for the spectral irradiance, the total amount of irradiation is obtained by integration over the appropriate range of frequencies in the spectrum. Hence, irradiance is the power of the radiation, per unit area and will be expressed in $\mu W/cm^2$.
An important observation is that the irradiance will vary depending on the distance from the light source. From this point of view, submerging the light source into the RE mixture will induce less irradiance losses compared to illumination from a certain distance. On the other hand, submerged lamps induce difficulties in set-up and reactor configuration, not to forget the additional safety requirements. For instance, additional design difficulties considering mixing and protection of the lamp need to be taken into account.

Finally, the *homogeneity* of irradiation needs to be taken into consideration. A light source that uniformly radiates light in all directions will give different results than light sources emitting a focused beam in a specific direction. The optimal location and set-up of the lamps versus the mixture should be determined in accordance with the homogeneity parameter.

At first, an overview of the used lamps is given. The previous experiments were all carried out with U-shaped submerged 11 W LPMLs. Next to these submerged lamps, a U-lamp of 11 W with reflector, two 40 W linear lamps and a 60 W U-lamp are used for the following experiments. Subsequently, the light-related parameters will be discussed for the individual lamps. Finally, the results of the experiments in which the same RE mixtures are irradiated by the different lamps during 96 h will be presented and discussed.

### 9.6.1 Immersed 11 W LPML

The *spectral output* of the two U-shaped submerged 11 W LPML was already briefly discussed in section 6.2. The lamps are fixed in a quartz housing in order to be submerged into the RE mixture and have a dominant spectral output at 185 nm and 254 nm. The irradiance profile was visualized previously in Figure 9. Please notice that the output at wavelengths below 200 nm cannot be detected due to limitations of the measuring set. The reactions take place at 188 nm (charge transfer band from $H_2O$ to $Eu^{3+}$, equation (35)), 240 nm (charge transfer band from $SO_4^{2-}$ to $Eu^{3+}$, equation (16)) and 366 nm (photochemical back reaction according to equation (10)).

The *spectral irradiances* of both 11 W LPML are measured in function of the distance and the angle of illumination. Irradiances are measured at 0, 5, 10 and 15 cm from the light source. The direction of the lamp emission is expressed by angles (Figure 29): 0° means that the irradiance is measured perpendicular to the U-shape tubes so that the light of both tubes is captured. Consequently, 90° represents the parallel position to the U-shape tubes of the lamp, so mainly the light of one of the tubes is captured. 45° is obviously an intermediate angle.

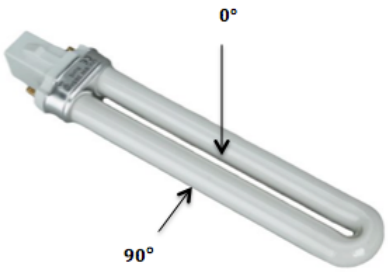


**Figure 29: U-Lamp angle definition.**

A distinction is made between the lamps, since one of them contains some traces of wear, namely soot deposition, and the other does not. Figure 30 displays the irradiance measurements for the lamp without soot deposition as function of the distance from the

light source. Figure 31 shows the equivalent for the 11 W LPML with soot deposition. The irradiances for the forward reduction reaction are determined by integrating the spectral irradiances over the wavelengths 200 to 260 nm. Analogously for the backward reaction, the spectral irradiances are integrated over the wavelength range of 360 to 370 nm.

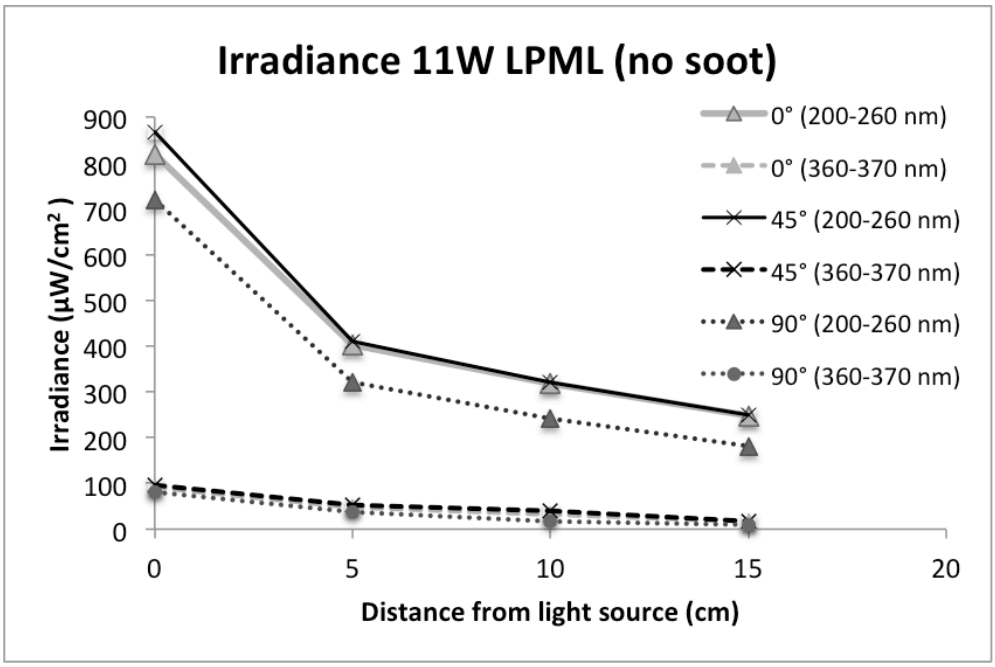


**Figure 30: Irradiances 11 W LPML (without soot deposition). Forward reaction wavelengths range: 200–260 nm. Backward reaction wavelengths range: 360–370 nm.**

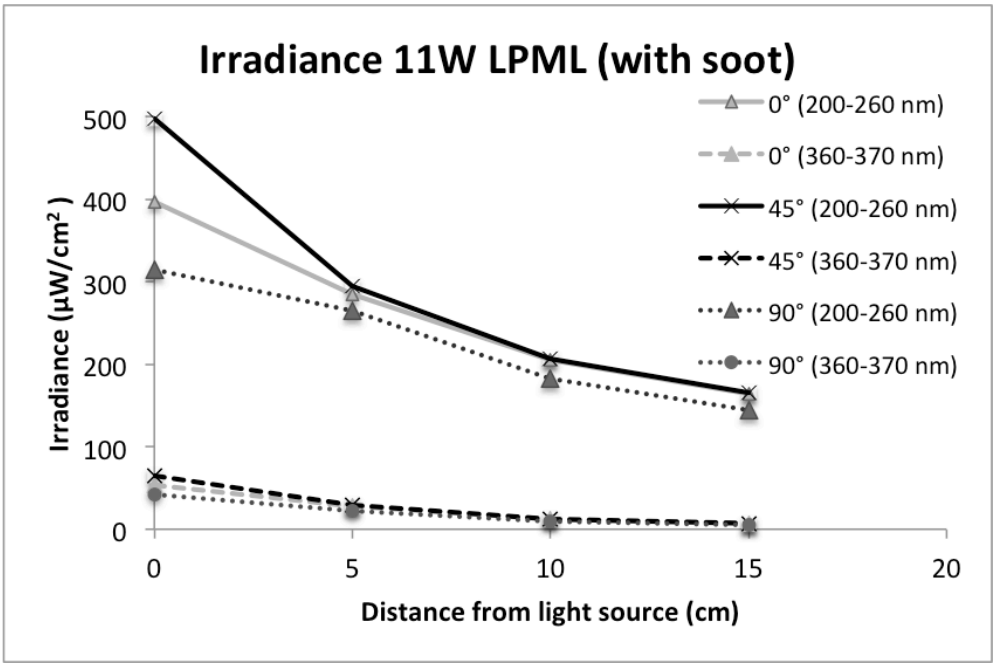


**Figure 31: Irradiances 11 W LPML (with soot deposition). Forward reaction wavelengths range: 200–260 nm. Backward reaction wavelengths range: 360–370 nm.**

It is observed that in the first place, the larger the distance from the light source, the lower the irradiance. In general, the biggest loss of lamp power takes place in the first 5 centimetres. The irradiance at distance zero is considered as representative for this set-up, since the lamps are submerged. The backward reaction exhibits much smaller irradiances than the forward reaction for both lamps. The irradiation in different directions is quite uniform at higher distances. On the other hand, from 0–5 cm there is some variation in homogeneity of irradiation. However, since these lamps are submerged into the solution, the non-uniformity of irradiation will be partially diminished since the RE-volume flows around the lamp. When comparing Figure 30 and Figure 31, it is clear that there is a significant difference in irradiance between the two lamps. This will be further investigated in section 9.7.

### 9.6.2 Non-immersed lamps

Next to the 11 W lamps, four other non-submerged lamps are considered. The LPMLs comprise a lamp of 11 W with reflector (referred to as the reflector lamp), two 40 W lamps and a 60 W lamp. These lamps are not immersed in the sample solution, as instead illumination is done from the top as can be seen in Figure 32. The lamp is fixed at a distance of approximately 5 cm above quartz plates that cover 4 or 5 beakers containing 90 mL RE-solution. For that reason, the irradiance at a distance of 5cm of the light source is considered as representative for this set-up.

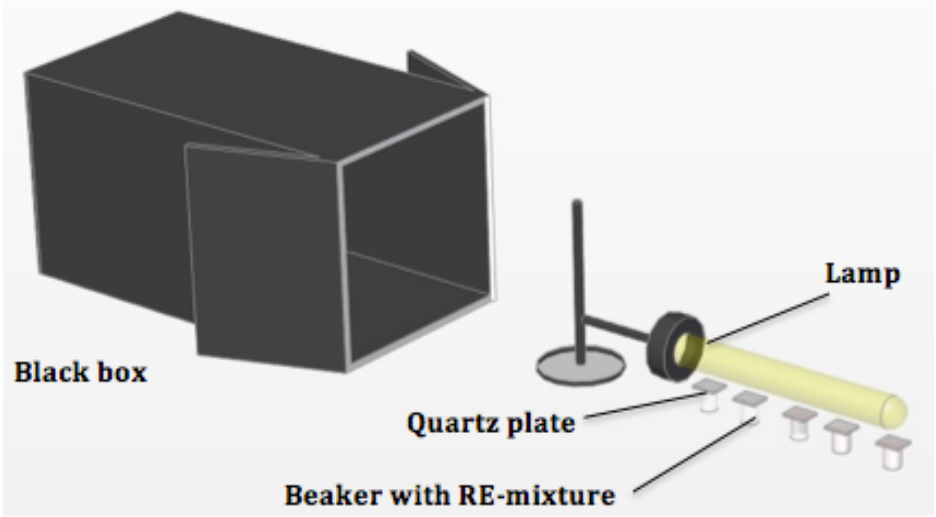


**Figure 32: Set-up photochemical experiment non-immersed lamp.**

The wattage of the U-shaped **reflector lamp** is also 11 W and a reflector can be mounted on the lamp in order to redirect the light toward the mixtures. Anyhow, the effect of the reflector is limited since the irradiances for the lamp in the UV with reflector are roughly 3 to 8 % higher than the irradiances of the same lamp without reflector. The U-lamp transmits the spectral output at 185 nm and 254 nm just like the 11 W lamps.

Two linear **40 W lamps** are available as well. The first 40 W lamp is a high ozone-generating lamp, which allows for the transmission of energy at both 185 nm and 254 nm wavelengths. Secondly an ozone-free 40 W linear lamp that transmits up to 90 % of its energy at the 254 nm wavelength in which a doped fused quartz is used to block the emission of 185 nm energy.

The last LPML that is used has the highest wattage of **60 W** and emits only at the 254 nm wavelength. This light source is also a U shaped lamp.

The *homogeneity* of irradiation has been measured for the various lamps. Since these lamps are placed horizontally above the RE mixtures, the uniformity of irradiation is no longer compared by angles but now the irradiances are measured in the middle and at both extremities of the lamps. The highest irradiances are obtained in the middle of each lamp. The 60 W lamp shows the highest variation in irradiances (The RSD of the irradiances measured for the forward reaction at both extremities and in the middle of the lamp equals 26 % for the forward reaction), while the other lamps emit light more uniformly (~RSD 15 %).

The *irradiances* of the immersed and non-immersed lamps can be found in Appendix F. Figure 33 compares the integrated spectral irradiances of the various lamps for the forward (200–260 nm) reaction and Figure 34 for the backward reaction (360–370 nm) as function of the distance from the light source. Please notice the logarithmic scale and the fact that the vertical axis does not start at zero in Figure 33.

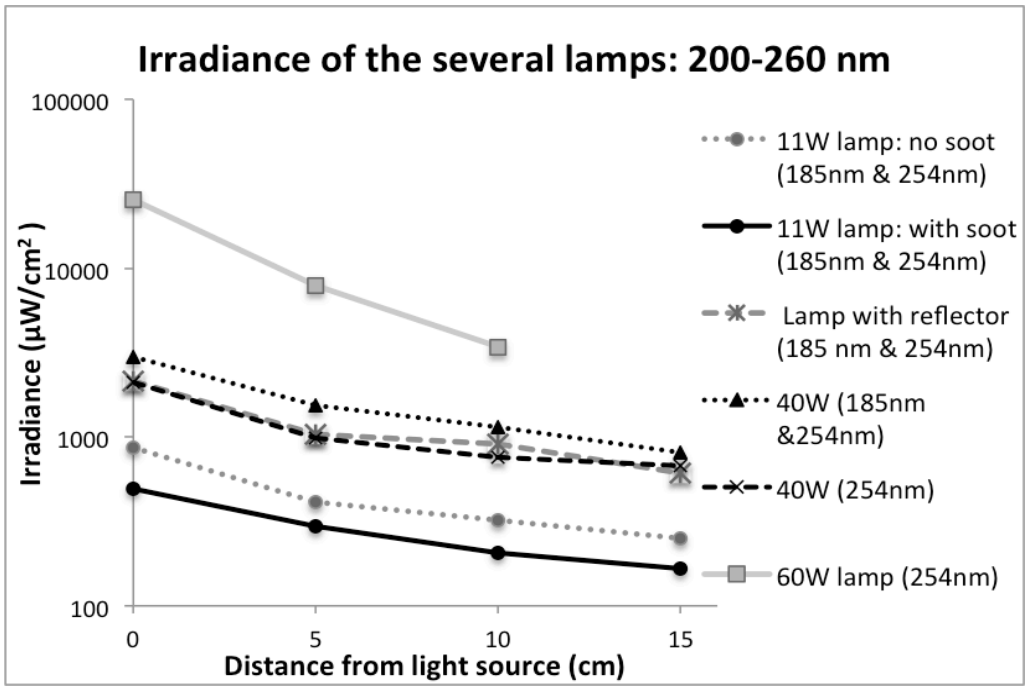


**Figure 33: Irradiances of the various lamps as function of the distance. Wavelengths range: 200–260nm.**

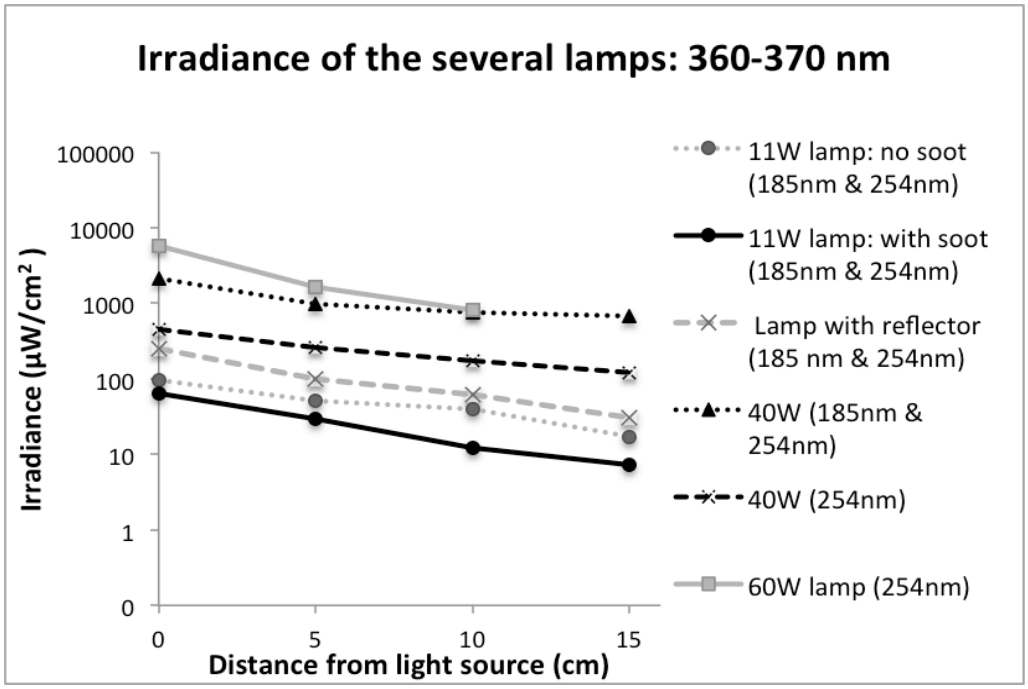


**Figure 34: Irradiances of the various lamps as function of the distance. Wavelengths range: 360–370 nm.**

An important distinction needs to be made between the lamps with both the 188 nm and the 254 nm line (namely the submersed 11 W LPMLs, the lamp with reflector and the ozone-generating 40 W lamp) and on the other hand, the 60 W and ozone-free 40 W lamp without emission at 185 nm. Both wavelengths can provoke photochemical reduction, via the water-to-europium charge transfer band (188 nm line) and the sulfate-to-europium charge transfer band (254 nm line). The 40 W lamps illustrate that higher irradiances are obtained for the lamp that emits at both wavelengths (Figure 33). The 40 W lamp with only the 254 nm line has a similar irradiance behaviour as the lamp with reflector.

All the lamps emit at the wavelength range that will induce the oxidation of europium (Figure 34). The 60 W and ozone generating 40 W lamp induce particularly high irradiances for the backward reaction. This is a major disadvantage, as partial re-oxidation of europium(II) will occur.

## 9.7 The influence of the irradiance of the 11 W immersed lamps

Now that the irradiances of the various lamps are discussed and characterized, its influence on the photochemical reduction is investigated. A first estimation of the effect of the irradiance is obtained by determining the difference in separation efficiency for the two (the bright and blackened) 11 W-immersed lamps. As stated before, there is a significant difference in irradiance between these lamps. This is due to soot accumulation (on the lamp with the most burning hours) by cause of wear and attrition, therefore the lamp is referred to as the blackened lamp. The irradiances of both lamps are compared in Figure 35.

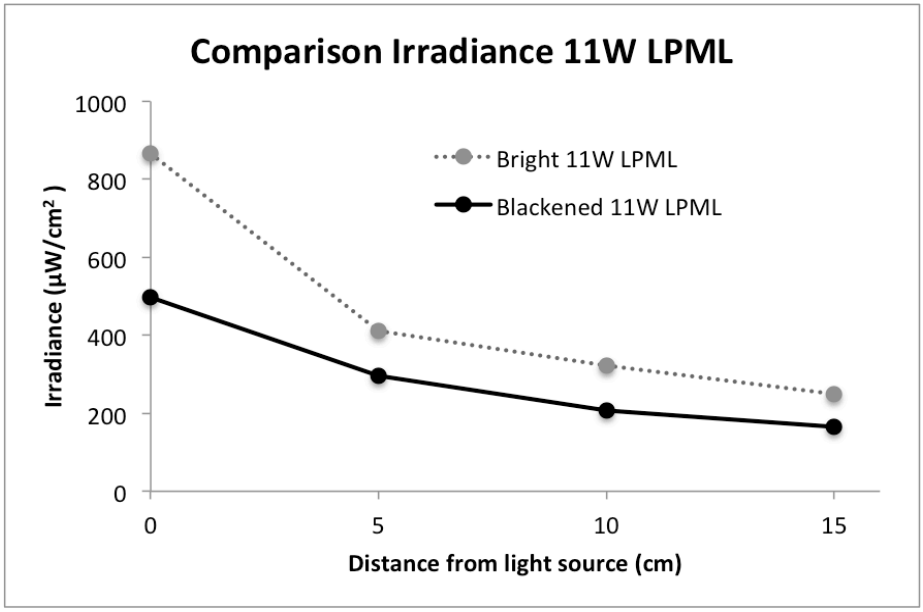


**Figure 35: Comparison Irradiance 11 W LPML with -and without soot deposition (at 45°).**

It is clear that the soot deposition significantly decreases the irradiance of the blackened lamp compared to the bright lamp. This was already observed visually during the execution of the experiments. In order to get a first estimation of the effect of the irradiance on the photochemical separation, the same mixture was illuminated with the two 11 W lamps. Standard mixture three (Eu/Y) with isopropanol as scavenger instead of formic acid with pH = 2, was illuminated by both lamps. The removal of europium as function of the illumination time is visible in Figure 36. The REE concentrations are listed in Appendix G. The yttrium concentration stayed approximately constant, namely 0 % (blackened lamp) and 1 % (bright lamp) removal of yttrium in the last sample compared to the initial concentration.

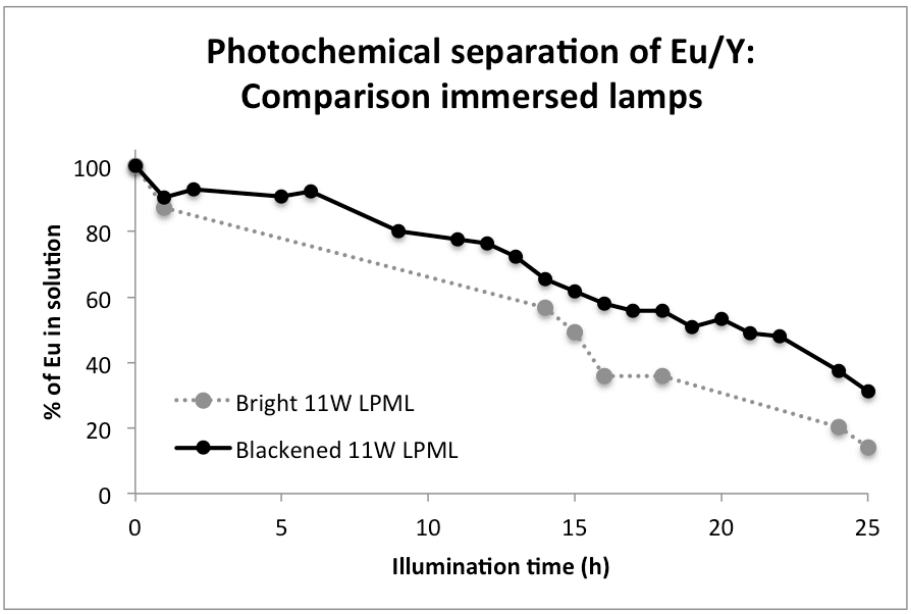


**Figure 36: Comparison Eu(III) reduction in Eu/Y mixture with the two 11 W LPML. 10 mM $EuCl_3 \cdot 6H_2O$, molar ratio Eu/Y = 1, pH = 2, 50 mM $(NH_4)_2SO_4$, 20 vol% isopropanol.**

As can be seen in Figure 36, the LPML with soot deposition shows a slower reduction of trivalent europium. It is indisputable that the irradiance of the light source has a major impact on the photochemical reduction. On that account, it was attempted to always use the same lamp for a specific set of experiments for determining the influence of a certain chemical parameter so that the difference in irradiation did not play any role. The influence of irradiance will be examined in more detail in the following section.

## 9.8 The influence of the irradiance of the various light sources

It is clear from the previous experiment that the higher the irradiance of the light source, the faster the europium reduction takes place. The irradiation influence on the photochemical reduction is now further investigated by illuminating the same mixtures with all the available lamps, except for the 40 W ozone-generating lamp. Figure 33 and Figure 34 show that there is a wide range in irradiation intensity. First, the composition of the four illuminated mixtures is specified and then the resulting concentrations are listed in the tables respectively for every lamp. A comparative graph between the various lamps is finally made in which the removal of europium is displayed for a single mixture. These experiments were monitored during a long period: a sample was taken every hour during the first 25 h and also after 48, 72 and 96 h of illumination.

Four different mixtures were prepared in order to illuminate them separately by the different lamps. The compositions of the different mixtures are given in Table 16. Europium and yttrium were added as chloride hexahydrate salts. 50 mM ammonium sulfate and 20 vol% scavenger were added to every mixture. $pH_{initial}$ and $pH_{final}$ refers to the pH of the aqueous solution before and after addition of scavenger respectively.

**Table 16: Composition of the mixtures A, B, C and D.**

| Parameters | Mixture A | Mixture B | Mixture C | Mixture D |
|---|---|---|---|---|
| [Eu]:[Y] (mM) | 10:10 | 10:100 | 10:10 | 10:10 |
| $pH_{initial}$ | 2.0 | 2.0 | 2.0 | 4.1 |
| $pH_{final}$ | 1.1 | 1.1 | 2.3 | 4.4 |
| Scavenger | HCOOH | HCOOH | Isopropanol | Isopropanol |

Only two mixtures (C and D) could be illuminated with the 11 W LPML since these lamps are submerged into the solutions and only two lamps are available. The other mixtures were already illuminated by the immersed lamps in previous experiments. Additionally, there was only space to illuminate three of the four mixtures with the lamp with reflector, so no data is available for mixture C for this light source. Simultaneously, a dark experiment was executed by storing the same mixtures in a dark place without UV-illumination.

The concentrations of the various mixtures as a function of the illumination time are listed in Appendix H. These results are plotted in Figure 37 to Figure 40. Please notice that the data points are not visualised by an explicit marker. This is intentionally done as the large

numbers of samples, especially during the first 25 hours, would lead to overlapping markers and consequently make the graph crowded and unclear.

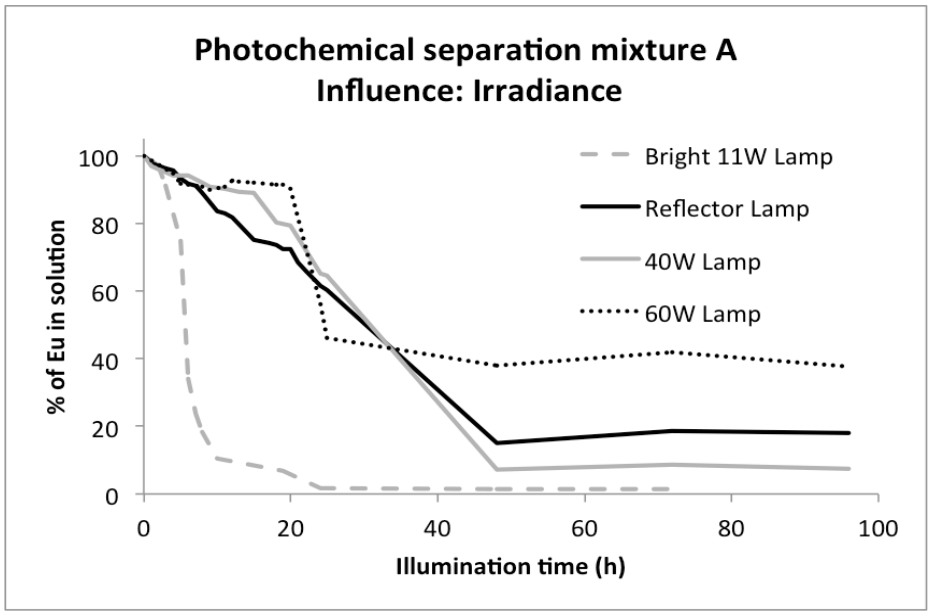


**Figure 37: Overview photochemical separation of Eu/Y by different light sources (11 W immersed lamp/ 11 W reflector lamp/40 W lamp/60 W lamp). Eu/Y ratio 1:1, 10 mM $EuCl_3 \cdot 6H_2O$, pH = 1, 50 mM $(NH_4)_2SO_4$, 20 vol% HCOOH.**

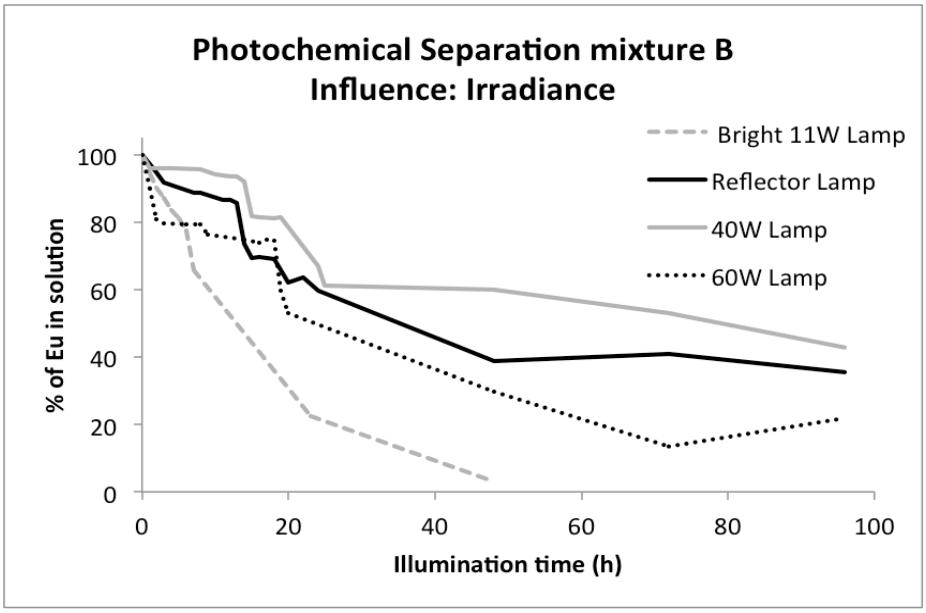


**Figure 38: Overview photochemical separation of Eu/Y by different light sources (11 W immersed lamp/ 11 W reflector lamp/40 W lamp/60 W lamp). Eu/Y ratio 1:10, 10 mM $EuCl_3 \cdot 6H_2O$, pH = 1, 50 mM $(NH_4)_2SO_4$, 20 vol% HCOOH.**

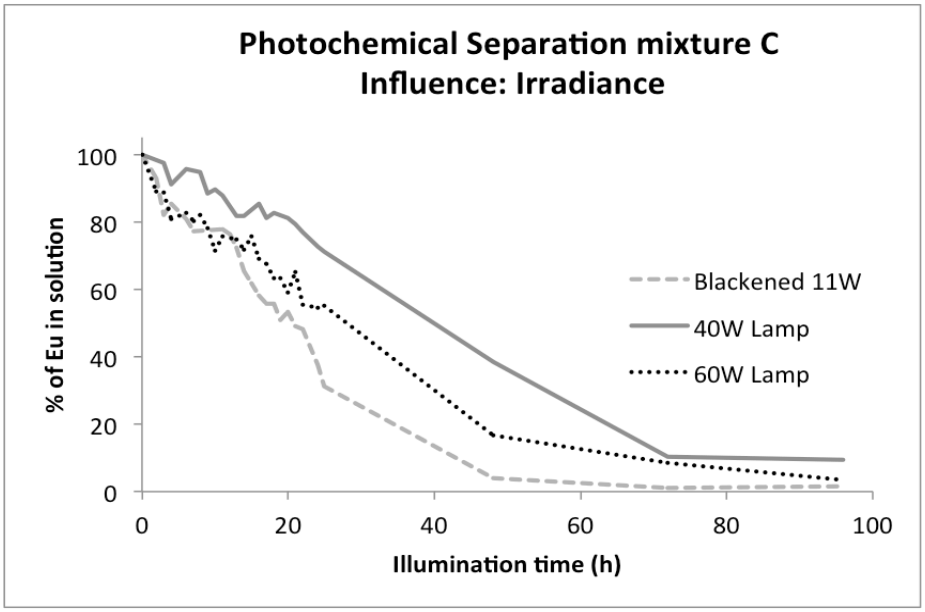


**Figure 39: Overview photochemical separation of Eu/Y by different light sources (11 W immersed lamp/40 W lamp/60 W lamp). Eu/Y ratio 1:1, 10 mM $EuCl_3 \cdot 6H_2O$, pH = 2, 50 mM $(NH_4)_2SO_4$, 20 vol% isopropanol.**

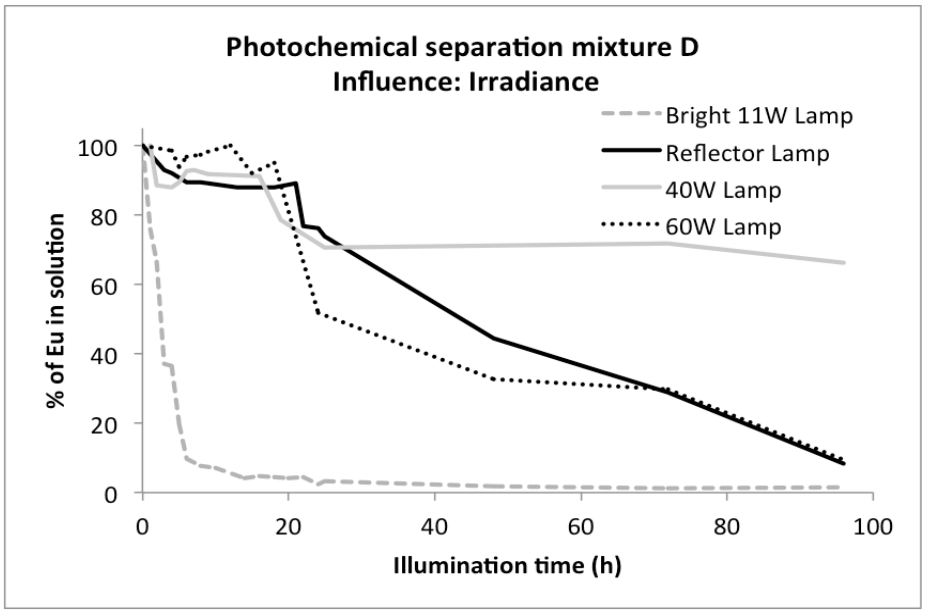


**Figure 40: Overview photochemical separation of Eu/Y by different light sources (11 W immersed lamp/Reflector lamp/40 W lamp/60 W lamp). Eu/Y ratio 1:1, 10 mM $EuCl_3 \cdot 6H_2O$, pH = 4, 50 mM $(NH_4)_2SO_4$, 20 vol% isopropanol.**

First of all, no precipitation was observed in the non-illuminated samples. From the experiment in section 9.7, we could reasonably expect faster reactions for higher irradiances. However, a distinction should also be made between lamps with both spectral

bands (at 185 and 254 nm) and lamps which emit only at 254nm. The first illuminate two CT-bands, while the latter only exploit the sulfate-to-europium CT-band. Hence, a slower reaction rate is expected for the latter. As a matter of fact, distinctions in set-up and lamp characteristics need to be taken into consideration next to the elementary irradiance of the light source in order to draw correct conclusions.

As can be deduced from the comparative graphs, the **11 W lamp** leads to the fastest precipitation for every single mixture, even though it has the lowest irradiance at 200–260 nm (Figure 33). This observation is related to the fact that the 11 W lamps are submerged in the solution. Therefore, the distance of illumination is considered zero, while the other light sources are positioned approximately 5 cm above the RE-solution. As already stated, there is a very fast decrease in irradiance with the distance. At 0 cm (Figure 33), the bright 11 W LPML has an irradiance (866 $\mu W/cm^2$) that is somewhat comparable to the irradiance at 5 cm for the lamp with reflector (1045 $\mu W/cm^2$) and the 40 W lamp with only the 254 nm line (989 $\mu W/cm^2$) for the forward reaction. The light intensities of the 11 W lamp are therefore not substantially lower than these of the other two lamps.
Another related argument for the faster reduction is that the uniformity and homogeneity of the illumination is much higher in comparison to the non-submerged lamps. In other words, the RE-volume is equally illuminated from the inside out, as opposed to only from the top. In addition, together with the lamp with reflector, the 11 W lamps have the lowest irradiances for the backward reaction (Figure 34). This means that photochemical re-oxidation of Eu(II) is minimal and losses in separation efficiency are reduced. Finally, an important consideration here is that the 11 W mercury lamps illuminates the samples with the 185 nm line and with the 254 nm line. Both peaks can provoke photochemical reduction. This is a supplementary argument to support the fast reduction of europium with the 11 W lamps.

When observing the behaviour of the (non-submersed) **reflector lamp** as compared to the **40 W** and **60 W** lamp, the following conclusions can be made. During the first couple of hours, the lamp with reflector usually exhibits the fastest europium reduction (except for mixture B) next to the 11 W lamp. After 15 to 25 illumination hours, the 60 W lamp however shows an accelerated removal of europium, so that a faster reduction is obtained as compared to the reflector lamp. The 40 W lamp provokes the slowest precipitation (except for mixture A). These observations could be elucidated by the presence/absence of the 185 nm wavelength emission. It is important to be aware of the fact that the lamp with reflector

illuminates with both 185 nm and 254 nm wavelength, whereas the 40 W and 60 W lamp only include the 254 nm wavelength. The water-to-europium charge transfer band (corresponding to the 185 nm line) and the sulfate-to-europium charge transfer band (exploited by the 254 nm line) provoke photochemical reduction and this independently from each other. The presence of the 185 nm could confirm the faster reduction for the reflector lamp during the first illumination time. The higher irradiances of the 60 W lamp will dominate after longer illumination times and compensate the absence of the 185 nm line.

Some of the previously mentioned statements are visually summarized in Figure 41. The irradiances of the various lamps for the forward reduction reaction (200-260 nm) and backward oxidation reaction (360–370 nm) are shown. The removal of europium in mixture D, after 25 h of illumination, is visualised on the same figure in order to emphasise the effect of the irradiation on the Eu removal. Mind the logarithmic scale on the left axis and the non-logarithmic axis on the right axis.

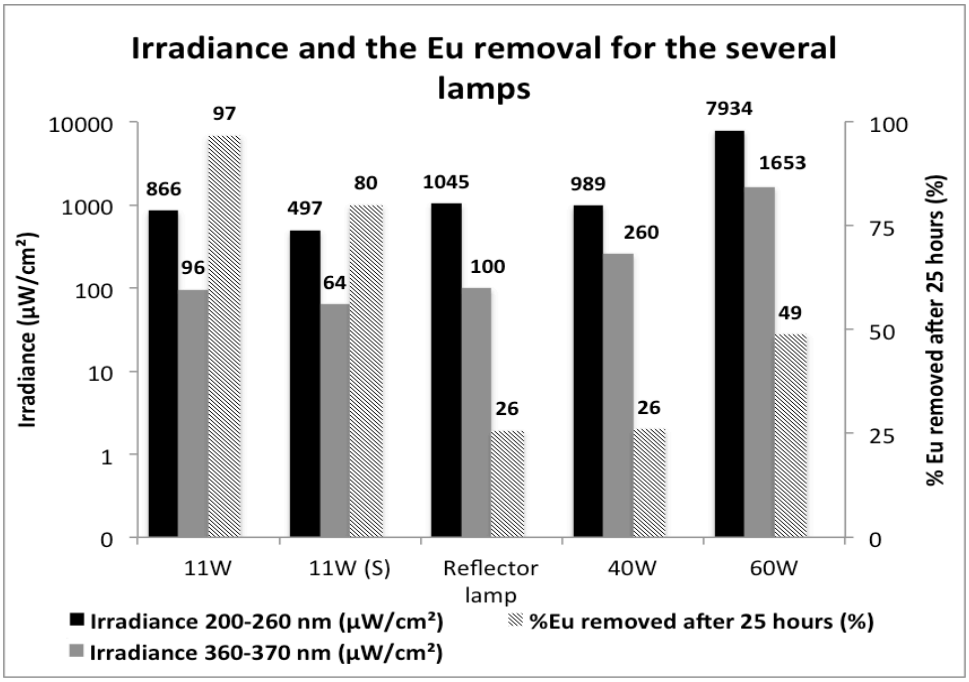


**Figure 41: The effect of the irradiance of the various lamps for the reduction reaction (200–260 nm) and the oxidation reaction (360–370 nm) on the Eu removal after 25 hours for mixture D. The irradiances are measured at 0/5 cm for the immersed/non-immersed lamps.**

Figure 41 illustrates that the lowest irradiances (96 and 64 µW/cm²), at the wavelengths inducing the re-oxidation of europium, are obtained for the 11 W immersed lamps. This promotes the highest europium removal for the immersed lamps (97 and 80 %). The

highest irradiances (260 and 1653 μW/cm$^2$) at 360–370 nm are achieved for the 40 W and 60 W lamps. Consequently, a slow reduction of europium is obtained for the 40 W lamp. The high irradiances of the 60 W for the forward reduction partly compensate this effect, so that still 49 % of europium is removed after 25 h.

By way of conclusion, it is fair to say that not only chemical parameters, but also spectral parameters have a great influence on the europium reduction. And even though it is clear that the irradiance has a major effect, this is not the only light related parameter that should be taken into account: the investigated light sources also differ in spectral output homogeneity of irradiation and in experimental set-up (including the distance from the light source).

Following conclusions can be drawn, based on the observations:

- The irradiance drops significantly with the distance from the light source. Therefore, submerged lamps show the fastest removal rates of europium since the light source is very close to the illuminated solution.
- Light sources that emit at both 185 nm and 254 nm provoke two independent reductions through a water-to-europium CT-band (at 188 nm) and a sulfate-to-europium CT-band (and 254 nm) respectively. This leads to higher precipitation yields for the same illumination times with comparison to light sources that only exploit the 254 nm band.
- A photochemical back-reaction is triggered by light output around 366 nm (see equation (10)). Light sources with lower irradiance at this wavelength cause faster reduction rates.
- Irradiance of lamps decreases as a function of time, hence the same (electrical) lamp power does not necessarily mean identical irradiance. Clearly, irradiance measurements are vital in order to allow comparison between different lamps and experimental set-up.

Characterization of the light source with respect to irradiance at both wavelengths of the forward and backward reaction is of major importance. Irradiance plays a key role in the kinetics of photochemical redox reactions, and maximizing the light power output is a challenge in order to achieve the highest possible irradiance and consequently the fastest reaction rate and lowest illumination times.

# 10. Further Research

As mentioned before, the photochemical separation technique is not yet optimized and is still in the research phase. No feasible practical application has been demonstrated as yet. Further investigations in different fields are required in order to determine the optimal operating conditions and to find and evaluate improvements, so as to overcome the existing barriers of the technique. Firstly, the parameters influencing the reaction itself need to be investigated and optimized. In a second phase, it is fundamental to characterize the ideal light source to induce the reaction in an energy-efficient way, which is essential before aiming at reactor design and scale-up possibilities.

## 10.1 Chemical parameters

First of all, the effect of the chemical parameters requires further investigation. This master thesis only covered a small part of the possible chemical influences. Potential new research routes might include, among others, the photochemical oxidation (e.g. $Ce^{3+}$ to $Ce^{4+}$) instead of the reduction of europium, the separation of RE mixtures in organic media instead of in aqueous solutions and the separation of more complex, non-binary mixtures.

Next to the reduction of europium, the photochemical technique can also induce oxidation reactions. Due to its electronic configuration, cerium can lose its single 4f electron to form stable $Ce^{4+}$ in water. Illumination at 250 nm induces the electron transfer from the cerium ion to the solvent. 4f-5d transitions are responsible for the photochemical oxidation (equation (41)) [98].

$$Ce^{3+}(H_2O) \xrightarrow{250\ nm} \left[Ce^{3+}(H_2O)\right]^{*} \rightarrow Ce^{4+} + H^{\bullet} + OH^{-} \qquad (41)$$

Due to the numerous commercial applications of cerium (e.g. pollution control catalyst, coatings, glass polishing,...), it is economically relevant to identify its photochemical recycling possibilities.

In non-aqueous media (e.g. methanol, ethanol, tetrahydrofuran (THF) and hexamethylfosforamide (HMPA)), additional non-trivalent REE are stabilized (such as $Sm^{2+}$, $Yb^{2+}$ and $Tb^{4+}$), so that the photochemical separation technique can be applied on a wider variety of mixtures [99]. Accordingly, it is more challenging to achieve high selectivity in organic solvents compared to aqueous media. The absorption bands are located at longer wavelengths (> 300 nm). On the one hand this is beneficial since it requires less energy, but on the other hand, it does not directly correspond with the dominant spectral output of the LPML. Other light sources should therefore be considered.

Commercial RE waste streams do not consist of perfect binary RE mixtures. For this reason, an investigation with regard to the influence of impurities and other REE on the separation selectivity and efficiency could be very meaningful. In this vision, 'separation trains' could be established. An industrial waste stream of fluorescent lamps [100] containing trivalent europium, gadolinium and cerium could for instance be separated by successively exploiting the selectively precipitation of the individual elements. First, the reduction of europium allows $EuSO_4$ formation, next Ce(III) is oxidized to Ce(IV) and removed as insoluble cerium(IV)iodate or cerium(IV)hydroxide. Gadolinium should remain unaffected by the irradiation and remain in solution. This would allow the mixture to be separated into individual fractions of rare earth elements.

## 10.2 Light source

It was clear from section 9.8 that the combination of uniform and high irradiances for the forward reaction, low irradiances for the backward reaction, illumination at both 185 nm and 254 nm wavelength and finally a short distance from the illumination source, are the parameters that encourage a fast reduction of europium. It is essential to promote further research to identify light sources that satisfy these conditions. The use of monochromatic illumination sources for instance, as compared to polychromatic light sources, allows the isolation of the optimal wavelength range so that the wavelengths for the forward reaction can be exploited while the wavelengths of the backreaction are eliminated. Less heat will be produced and dissipated and therefore, the loss in separation efficiency and selectivity will be reduced. UV filters can be used to this extent. High power UV-output within narrow

spectral bands could be obtained with lasers and LEDs, which could lead to a diminution in required illumination time due to a faster europium removal. Literature confirms that photochemical separation of rare earths with lasers has already successfully been carried out [67] [101]. This is not the case for LEDs. LEDs were only investigated in organic reactions. Excimer lasers have a major drawback, which is their high investment cost. Additionally, they are impractical in usage, especially for large volumes. LEDs on the other hand, are quasi-monochromatic light sources with a long lifetime, allowing flexible reactor configurations. Moreover, LEDs rapidly reach full luminosity so that no delay in start-up needs to be considered compared to the mercury lamps [102]. This allows periodical illumination and consequently lowers the energy consumption. Although UV-LEDs remain expensive, their cost price has decreased due to the extensive research and mass production in recent years.

## 10.3 Separation step

Another aspect that should be considered is the fact that the photochemical separation technique is based on a reduction process that is coupled with a separation step. In the experimental part of this master thesis, the separation relies on the precipitation as $EuSO_4$. The major drawback is that the highest achievable purity is limited by the solubility product of $EuSO_4$. In addition, co-precipitation of contaminants or impurities is enhanced by the presence of the sulfate precipitate and separation via precipitation is difficult to apply in a continuous process [61]. This was not observed in the own experiments, since only binary mixtures of REE were investigated without any form of contamination.

Therefore, other separation techniques must be investigated in order to overcome the limitations of the solubility equilibrium. Reversed-phase chromatography, ion-exchange chromatography and solvent extraction are separation techniques that are based on the fact that organic ligands preferentially bind to trivalent REE, as compared to divalent REE [61]. The coupling of these possible separation methods to the photochemical reduction needs to be considered and further investigated. This is especially the case for solvent extraction, considering how easily it can be implemented in a continuous configuration.

## 10.4 Reactor configuration

Next to the light source as such, the reactor set-up needs to be considered. It is however difficult to recommend a particular reactor configuration considering that the photochemical separation technique is still in an early stage of development. The set-up will depend on the optimized lab-scale results. For instance, the final reduction rate will determine the minimal residence time that is required to obtain the requested purity, and this will in its turn determine whether a continuous reactor can be applied or not. The reactor configuration will be influenced by the penetration depth of the light in a certain solvent as well. The type of light source will have a major impact on the reactor design: it is obvious that lasers, LEDs or lamps do not require the same conditions.

An important observation is that the irradiances of the light source decrease rapidly with the distance. From this point of view, submerging the light source into the RE mixture will induce less irradiance losses compared to illumination from a certain distance. On the other hand, submerged lamps induce difficulties in set-up and reactor configuration, not to forget the additional safety requirements. For instance, additional design difficulties related to mixing and protection of the lamp need to be considered.

# 11. Conclusion

The rare earths are a group of chemical elements with similar properties that tend to occur in the same ore deposits. An essential chemical property is that the rare earths are typically found in the trivalent oxidation state. These metals are considered as strategically important due to their usage in many high tech (smartphones, catalysts, military precision weapons,…) and sustainable (HEV's, wind turbine, etc.) modern applications. Rare earths are also used in phosphor coatings that are crucial for the conversion of UV radiation into visible light in fluorescent lamps. Mixtures containing yttrium and europium in the experimental part of the master thesis are based on waste streams of the red emitting phosphor from fluorescent lamps.

The rare earths encounter an increasing popularity in today's technologically developing society due to their usage in numerous applications. These metals are scarce as their name suggests while their demand continues to rise by cause of their economic and strategic relevance. The mining of RE containing ores is economically challenging since the elements are found in mixed and non-concentrated form. Not to forget that the mining procedure is energy-intensive and it includes possible environmental risks. World's largest rare earth producer China accounts for more than 90 % of the global rare earth supply. However, since it faces increasing domestic demands, China is currently restricting its export. Consequentially, the global market suffers from a critical shortage of rare earths. The limited availability has caused a positive encouragement in the search for sustainable recycling methods and alternative separation techniques, in the context of 'urban mining'. The EU, Japan and the US make funding available to boost scientific research in this domain. The photochemical separation technique is a promising technology that is part of this objective.

In this thesis, the various parameters that affect the photochemical separation of rare earth elements in an aqueous solution are examined. This innovative separation technique

consists of two main parts: the selective photochemical reduction of europium, followed by the chemical separation. The absorption of UV-light, originating from low-pressure mercury lamps (LPMLs) with main light output at 185 nm and 254 nm, induces the transfer of an electron from the ligands to the central europium ion via a ligand-to-metal charge-transfer (LMCT-band). Europium is hereby selectively reduced to the divalent state. Subsequently, the divalent europium is removed from the solution by precipitation as insoluble $EuSO_4$.
Strictly speaking, the selectivity of the separation arises from the specificity of the redox reaction through the LMCT-bands. Trivalent europium has a water-to-europium charge transfer band at 188 nm, which corresponds with the light output at 185 nm of the LPML. In addition, sulfate, next to its role as a precipitating agent, creates an extra sulfate-to-europium LMCT-band at 240 nm. Additives can therefore generate new absorption bands and thereby allow us to work at longer (i.e. more energy-efficient) wavelengths. The influence of chemical and spectral parameters was identified and evaluated in terms of separation efficiency and selectivity.

First of all, the experiments show without any doubt that the photochemical separation technique works. Up to 98 % removal of europium could be achieved and the collected $EuSO_4$ precipitate did not contain significant traces of yttrium. This clearly points out the high selectivity of the technique, which is a major asset. The highest achievable purity of the separation is dictated by the solubility equilibrium of $EuSO_4$. A higher $SO_4^{2-}$/Eu molar ratio promotes a faster and higher removal of europium until an optimal limit is reached. This was attained at molar ratio 15.
A so-called scavenger is added to the mixtures, i.e. an organic compound that neutralizes reactive hydroxyl radicals which are formed along with the photochemical reduction reaction. These radicals cause an undesirable back reaction via oxidation of divalent europium. Both isopropanol and formic acid were tested as scavenger. With regard to formic acid, shorter illumination times are required to achieve the same europium removal. This can be attributed to the absorption of light by formic acid at 260 nm, thereby forming reactive radicals which cause an additional reduction of trivalent europium. The main disadvantage of this scavenger is its strong acidity, which causes the need to work at low pH (0–1). Isopropanol on the other hand has no additional photochemical reducing effect, but allows higher pH. This leads to better results in terms of illumination times since the pH of the aqueous phase influences the speed of the photochemical reaction and europium(II) is

better stabilized in less acidic solution (in accordance with the Pourbaix diagram).
An increase in pH from 0 to 4 leads to faster reactions. This observation has been linked to the presence of protons at low pH, which promote the unwanted oxidation of divalent to trivalent europium. pH values larger than or equal to 6 cause hydrolysis, which leads to hydroxide precipitation of all the rare earths, so that no selective separation can be achieved. The most efficient separation was therefore obtained at pH 4.
Next to the ideal equimolar mixtures, industrial simulated europium/yttrium-mixtures with different molar ratios were also investigated. The higher the excess of yttrium, the slower the europium removal takes place. However, longer illumination times yield the same removal percentage (> 90 %) and selectivity (~ 100 %) for europium. Consequently, the excess of yttrium only induces a kinetic effect that entails an additional difficulty with regard to the reduction of illumination times.

It is clear that the reaction kinetics are an important issue. Illumination times of 24 h to achieve the required purities are unacceptable when aiming at industrial applications. A possible way to tackle this problem is to use stronger lamps with higher irradiance. This leads to faster reactions and allows shorter residence times, which is a necessary condition to switch from batch to continuous systems in the future. High and homogeneous irradiances, corresponding to the absorption band of the forward reaction (185 nm and 254 nm), accelerate the reaction. Analogously, low irradiances for the photochemical backward reaction (at 366 nm), increase the efficiency of the separation. The use of LEDs or other energy-efficient light sources could significantly increase the potential of the photochemical separation technique. It is obvious that the spectral output of the light source also determines the selectivity of the separation: the absorption bands of the mixture should be located at the dominant emitted wavelengths of the light source to obtain the highest achievable selectivity. This research has clearly indicated that the photochemical technique has great potential to be used in the recycling of europium in waste streams of lamp phosphors and could thus provide an answer to the current scarcity of europium.

While the photochemical separation process has proven successful, the technique is still in an early stage of development. Research should be encouraged to reveal the set of chemical and spectral parameters that influence the reaction and to which extend these influences act. This allows us to determine the ideal light source and the most favourable operating conditions to carry out a particular separation. Alternative separation steps, other than sulfate precipitation, to remove europium(II) need to be considered as well. The reactor

design and feasibility of the technique will depend on this preliminary research.

We can conclude that the photochemical separation technique is a radically different approach towards current rare earth separation. The technique has already shown serious potential, but at the same time certain barriers still exist and need to be overcome. The use of relatively large amounts of organic scavenger, the high cost of certain light sources, the fact that the separation technique is restricted to RE mixtures containing a stable non-trivalent state and especially the long illumination times are the major obstacles of the photochemical technique. Despite the fact that no feasible applications have been demonstrated yet, there is no doubt of the potential interest it could have. The main asset is unquestionably the high spectral selectivity and specificity. Additionally, possible energy savings and the reduction of required chemicals compared to conventional techniques such as solvent extraction or (electro)chemical reduction could be realized. That's why the potential for commercial profitability is high and it is crucial to further develop the technology in order to bring it to market. This technology could provide for an environmentally friendly and innovative answer to the rare earth supply problem in the future.

# 12. Appendices

# Appendix A

The concentrations of the experiment in section 9.2 were measured with TXRF and are shown in Table 17, Table 18, Table 19 and Table 20 for respectively 10 mM, 50 mM, 150 mM and 250 mM $(NH_4)_2SO_4$.

**Table 17: Concentrations of Eu/Y with 10 mM $(NH_4)_2SO_4$ versus illumination time.**

| Illumination time (h) | $C_{aq, Y}$ (mmol/L) | $C_{aq, Eu}$ (mmol/L) | Observation |
|---|---|---|---|
| 0 | 8.3 | 9.0 | (Scavenger added) |
| 1.5 | 8.6 | 7.8 | No precipitation |
| 2.5 | 7.9 | 7.7 | No precipitation |
| 3.5 | 7.9 | 7.1 | No precipitation |
| 6 | 8.5 | 4.9 | Precipitation |
| 8 | 8.6 | 3.6 | Precipitation |
| 10.5 | 8.9 | 2.4 | Precipitation |
| 24 | 8.5 | 1.2 | Precipitation |

**Table 18: Concentrations of Eu/Y with 50 mM $(NH_4)_2SO_4$ versus illumination time.**

| Illumination time (h) | $C_{aq, Y}$ (mmol/L) | $C_{aq, Eu}$ (mmol/L) | Observation |
|---|---|---|---|
| 0 | 8.1 | 8.1 | (Scavenger added) |
| 1 | 8.0 | 8.0 | No precipitation |
| 2 | 8.4 | 6.6 | Precipitation |
| 3 | 8.3 | 5.1 | Precipitation |
| 4 | 7.8 | 3.7 | Precipitation |
| 6 | 8.1 | 2.5 | Precipitation |
| 8 | 8.4 | 1.6 | Precipitation |
| 10 | 8.4 | 0.6 | Precipitation |
| 13 | 8.0 | 0.6 | Precipitation |
| 23 | 8.2 | 0.6 | Precipitation |

**Table 19: Concentrations of Eu/Y with 150 mM $(NH_4)_2SO_4$ versus illumination time.**

| Illumination time (h) | $C_{aq, Y}$ (mmol/L) | $C_{aq, Eu}$ (mmol/L) | Observation |
|---|---|---|---|
| 0 | 7.6 | 7.6 | (Scavenger added) |
| 1.75 | 7.7 | 3.9 | Precipitation |
| 2.75 | 7.2 | 3.4 | Precipitation |
| 3.75 | 6.7 | 2.4 | Precipitation |
| 5.25 | 6.6 | 2.0 | Precipitation |
| 6.25 | 7.8 | 1.5 | Precipitation |
| 7.25 | 8.2 | 1.2 | Precipitation |
| 8.25 | 7.2 | 1.1 | Precipitation |
| 9.25 | 8.2 | 0.7 | Precipitation |
| 22.25 | 7.8 | 0.2 | Precipitation |

**Table 20: Concentrations of Eu/Y with 250 mM $(NH_4)_2SO_4$ versus illumination time.**

| Illumination time (h) | $C_{aq, Y}$ (mmol/L) | $C_{aq, Eu}$ (mmol/L) | Observation |
|---|---|---|---|
| 0 | 7.5 | 7.5 | (Scavenger added) |
| 1 | 8.0 | 6.1 | Precipitation |
| 2 | 7.8 | 3.5 | Precipitation |
| 3 | 8.2 | 1.1 | Precipitation |
| 4 | 7.7 | 1.3 | Precipitation |
| 7 | 7.9 | 0.5 | Precipitation |
| 9.75 | 8.8 | 0.6 | Precipitation |
| 24 | 7.5 | 0.2 | Precipitation |

# Appendix B

The concentrations of the experiment in section 9.3 were measured with TXRF and are listed in Table 21 and Table 22 for respectively formic acid and isopropanol as scavenger.

**Table 21: Concentrations of Eu/Y with HCOOH scavenger versus illumination time.**

| Illumination time (h) | $C_{aq, Y}$ (mmol/L) | $C_{aq, Eu}$ (mmol/L) | Observation |
|---|---|---|---|
| 0 | 8.1 | 8.1 | (Scavenger added) |
| 1.25 | 8.0 | 8.0 | No precipitation |
| 2 | 8.4 | 6.6 | Precipitation |
| 3 | 8.3 | 5.1 | Precipitation |
| 4 | 7.8 | 3.7 | Precipitation |
| 6.25 | 8.1 | 2.5 | Precipitation |
| 8.25 | 8.4 | 1.6 | Precipitation |
| 10 | 8.4 | 0.6 | Precipitation |
| 13 | 8.0 | 0.6 | Precipitation |
| 23.25 | 8.4 | 0.6 | Precipitation |

**Table 22: Concentrations of Eu/Y with isopropanol scavenger versus illumination time.**

| Illumination time (h) | $C_{aq, Y}$ (mmol/L) | $C_{aq, Eu}$ (mmol/L) | Observation |
|---|---|---|---|
| 0 | 9.4 | 9.0 | (Scavenger added) |
| 1.25 | 7.6 | 8.6 | No Precipitation |
| 3.5 | 6.3 | 8.4 | No Precipitation |
| 6 | 6.8 | 8.0 | No Precipitation |
| 9.25 | 7.5 | 7.2 | Precipitation |
| 11 | 7.6 | 6.6 | Precipitation |
| 23.5 | 6.4 | 1.8 | Precipitation |
| 27.75 | 6.1 | 1.7 | Precipitation |
| 30 | 7.4 | 1.6 | Precipitation |

# Appendix C

The dataset considering the X-ray crystallography of the precipitate (pH = 2) from section 9.4 is listed below.

## Crystallographic data

| | |
|---|---|
| Chemical formula | $EuO_{13}S_2$ |
| Molar mass | 424.08 g $mol^{-1}$ |
| Lattice system | Monoclinic |
| Space group | $P2_1/c$ |
| a | 6.5785(4) Å |
| b | 18.7231(9) Å |
| c | 8.7123(5) Å |
| β | 97.340(5)° |
| V | 1064.31(10) $Å^3$ |
| Z | 4 |
| ρ | 2.647 g $cm^{-3}$ |
| F(000) | 796.0 |
| Crystal size | 0.2 x 0.2 x 0.2 $mm^3$ |

## Data collection specifications

| | |
|---|---|
| T | 100.01(10) K |
| X-ray source (λ) | Mo Kα (6.346 $mm^{-1}$) |
| Reflections measured | 7529 |
| Unique reflections | 2179 |

## Statistic specifications

| | |
|---|---|
| $R_{int}$ | 0.0248 |
| $R_1$ (all data) | 0.0301 |
| $wR_2$ (all data) | 0.0747 |

# Appendix D

The concentrations of experiment 9.4 were measured with TXRF and are shown in Table 23 to Table 31 for respectively pH = 0, pH = 1, pH = 2, pH = 3, pH = 4, pH = 5, pH = 6, pH = 7 and pH = 8

**Table 23: Concentrations of Eu/Y at pH = 0 versus illumination time.**

| Time (h) | $C_{aq,\,Eu}$ (mmol/L) | $C_{aq,Y}$ (mmol/L) | Observation |
|---|---|---|---|
| 0 | 8.3 | 6.7 | Scavenger added |
| 14 | 5.9 | 6.2 | Precipitation |
| 15 | 5.6 | 6.2 | Precipitation |
| 16 | 4.1 | 6.5 | Precipitation |
| 22.5 | 2.1 | 6.7 | Precipitation |
| 24 | 1.7 | 6.7 | Precipitation |

**Table 24: Concentrations of Eu/Y at pH = 1 versus illumination time.**

| Time (h) | $C_{aq,\,Eu}$ (mmol/L) | $C_{aq,Y}$ (mmol/L) | Observation |
|---|---|---|---|
| 0 | 9.0 | 7.9 | (Scavenger added) |
| 1.25 | 8.6 | 7.6 | No Precipitation |
| 3.5 | 8.4 | 6.3 | No Precipitation |
| 6 | 8.0 | 6.8 | No Precipitation |
| 9.25 | 7.2 | 7.5 | Precipitation |
| 11 | 6.6 | 7.6 | Precipitation |
| 23.5 | 1.8 | 6.4 | Precipitation |
| 27.75 | 1.7 | 6.1 | Precipitation |
| 30 | 1.6 | 7.4 | Precipitation |

**Table 25: Concentrations of Eu/Y at pH = 2 versus illumination time.**

| Time (h) | $C_{aq, Eu}$ (mmol/L) | $C_{aq,Y}$ (mmol/L) | Observation |
|---|---|---|---|
| 0 | 7.6 | 8.9 | (Savenger added) |
| 13 | 4.0 | 8.7 | Precipitation |
| 14 | 3.8 | 8.5 | Precipitation |
| 15 | 3.7 | 7.9 | Precipitation |
| 16 | 2.7 | 7.9 | Precipitation |
| 18 | 2.7 | 8.1 | Precipitation |
| 21 | 2.0 | 8.0 | Precipitation |
| 23 | 1.7 | 8.4 | Precipitation |
| 24 | 1.5 | 8.8 | Precipitation |
| 72 | 0.1 | 7.9 | Precipitation |

**Table 26: Concentrations of Eu/Y at pH = 3 versus illumination time.**

| Time (h) | $C_{aq, Eu}$ (mmol/L) | $C_{aq,Y}$ (mmol/L) | Observation |
|---|---|---|---|
| 0 | 8.8 | 8.7 | (Scavenger Added) |
| 13 | 4.9 | 8.4 | Precipitation |
| 14 | 4.5 | 8.5 | Precipitation |
| 16 | 3.1 | 8.8 | Precipitation |
| 18 | 2.7 | 7.8 | Precipitation |
| 20 | 2.3 | 8.0 | Precipitation |
| 22 | 1.8 | 8.4 | Precipitation |
| 24 | 1.6 | 8.5 | Precipitation |

**Table 27: Concentrations of Eu/Y at pH = 4 versus illumination time.**

| Time (h) | $C_{aq,\,Eu}$ (mmol/L) | $C_{aq,Y}$ (mmol/L) | Observation |
|---|---|---|---|
| 0 | 8.6 | 6.9 | (Scavenger added) |
| 1 | 6.5 | 5.7 | Precipitation |
| 2 | 5.7 | 6.3 | Precipitation |
| 3 | 3.2 | 5.7 | Precipitation |
| 4 | 3.1 | 5.6 | Precipitation |
| 5 | 1.7 | 6.7 | Precipitation |
| 6 | 0.8 | 5.5 | Precipitation |
| 8 | 0.7 | 6.9 | Precipitation |
| 9 | 0.4 | 5.6 | Precipitation |
| 10 | 0.6 | 5.6 | Precipitation |
| 12 | 0.3 | 7.0 | Precipitation |
| 14 | 0.3 | 6.3 | Precipitation |
| 15 | 0.3 | 6.4 | Precipitation |
| 16 | 0.4 | 6.5 | Precipitation |
| 17 | 0.4 | 5.5 | Precipitation |
| 18 | 0.4 | 6.4 | Precipitation |
| 19 | 0.4 | 7.0 | Precipitation |
| 20 | 0.6 | 6.8 | Precipitation |
| 21 | 0.3 | 6.8 | Precipitation |
| 22 | 0.6 | 6.3 | Precipitation |
| 24 | 0.2 | 6.9 | Precipitation |
| 25 | 0.3 | 6.1 | Precipitation |
| 48 | 0.2 | 7.1 | Precipitation |
| 72 | 0.1 | 7.9 | Precipitation |
| 96 | 0.1 | 7,4 | Precipitation |

**Table 28: Concentrations of Eu/Y at pH = 5 versus illumination time.**

| Time (h) | $C_{aq, Eu}$ (mmol/L) | $C_{aq,Y}$ (mmol/L) | Observation |
|---|---|---|---|
| 0 | 8.6 | 6.6 | (Scavenger Added) |
| 1.25 | 8.3 | 6.4 | No Precipitation |
| 3.5 | 8.1 | 6.8 | No Precipitation |
| 6 | 8.6 | 6.4 | No Precipitation |
| 7 | 8.0 | 6.4 | No Precipitation |
| 9.25 | 7.5 | 6.3 | Precipitation |
| 11 | 5.9 | 6.4 | Precipitation |
| 23.5 | 1.4 | 6.3 | Precipitation |
| 27.75 | 0.8 | 6.4 | Precipitation |
| 30 | 0.7 | 6.4 | Precipitation |

**Table 29: Concentrations of Eu/Y at pH = 6 versus illumination time.**

| Time (h) | $C_{aq, Eu}$ (mmol/L) | $C_{aq,Y}$ (mmol/L) | Observation |
|---|---|---|---|
| 0 | 8.8 | 6.3 | (Scavenger added) |
| 13.25 | 6.8 | 6.3 | Precipitation |
| 14.25 | 6.5 | 6.2 | Precipitation |
| 15.25 | 4.8 | 6.2 | Precipitation |
| 16.25 | 3.8 | 5.5 | Precipitation |
| 17.5 | 3.4 | 2.4 | Precipitation |
| 20 | 3.2 | 2.3 | Precipitation |

**Table 30: Concentrations of Eu/Y at pH = 7 versus illumination time.**

| Time (h) | $C_{aq, Eu}$ (mmol/L) | $C_{aq,Y}$ (mmol/L) | Observation |
|---|---|---|---|
| 0 | 8.7 | 9.4 | (Scavenger added) |
| 13.75 | 1.7 | 8.8 | Precipitation |
| 14.75 | 1.1 | 8.7 | Precipitation |
| 15.75 | 0.9 | 7.5 | Precipitation |
| 17.25 | 0.6 | 7.5 | Precipitation |
| 18.75 | 0.7 | 6.9 | Precipitation |
| 20.75 | 0.5 | 6.0 | Precipitation |
| 23.50 | 0.5 | 3.7 | Precipitation |

**Table 31: Concentrations of Eu/Y at pH = 8 versus illumination time.**

| Time (h) | $C_{aq,\,Eu}$ (mmol/l) | $C_{aq,Y}$ (mmol/L) | Observation |
|---|---|---|---|
| 0 | 9.1 | 7.7 | (Scavenger added) |
| 13.75 | 8.7 | 7.5 | Precipitation |
| 14.75 | 8.7 | 7.7 | Precipitation |
| 15.75 | 7.5 | 7.5 | Precipitation |
| 18 | 6.6 | 7.4 | Precipitation |
| 19.5 | 6.3 | 6.7 | Precipitation |
| 22 | 4.7 | 5.6 | Precipitation |
| 24 | 4.0 | 1.7 | Precipitation |

# Appendix E

The REE concentrations from section 9.5 can be found in Table 32 to Table 37 for respectively Eu/Y ratio 1:1, 1:10, 1:14, 1:15, 1:18, 1:20. The 1:30 Eu/Gd concentrations are given in Table 38.

**Table 32: REE concentrations with Eu/Y ratio 1:1 versus illumination time.**

| Illumination time (h) | $C_{aq, Y}$ (mmol/L) | $C_{aq, Eu}$ (mmol/L) | Observation |
|---|---|---|---|
| 0 | 8.3 | 7.5 | (Scavenger added) |
| 1 | 8.5 | 6.9 | Precipitation |
| 2 | 8.4 | 6.4 | Precipitation |
| 3 | 8.1 | 5.3 | Precipitation |
| 4 | 8.1 | 5.3 | Precipitation |
| 5 | 8.3 | 4.6 | Precipitation |
| 6 | 8.5 | 4.1 | Precipitation |
| 7 | 8.2 | 3.9 | Precipitation |
| 22.5 | 7.8 | 0.3 | Precipitation |
| 50 | 8.3 | 0.1 | Precipitation |

**Table 33: REE concentrations with Eu/Y ratio 1:10 versus illumination time.**

| Illumination time (h) | $C_{aq, Y}$ (mmol/L) | $C_{aq, Eu}$ (mmol/L) | Observation |
|---|---|---|---|
| 0 | 108.4 | 10.3 | (Scavenger added) |
| 1 | 107.1 | 9.7 | No precipitation |
| 2 | 110.0 | 9.3 | No precipitation |
| 3 | 110.2 | 9.0 | No precipitation |
| 4 | 105.5 | 8.6 | No precipitation |
| 5 | 105.4 | 8.3 | No precipitation |
| 6 | 107.2 | 7.9 | No precipitation |
| 7 | 106.3 | 6.7 | No precipitation |
| 22.5 | 102.3 | 2.3 | Precipitation |
| 29.5 | 103.7 | 1.2 | Precipitation |
| 34.75 | 105.2 | 0.8 | Precipitation |
| 50 | 103.2 | 0.3 | Precipitation |

**Table 34: REE concentrations with Eu/Y ratio 1:14 versus illumination time.**

| Illumination time (h) | $C_{aq, Y}$ (mmol/L) | $C_{aq, Eu}$ (mmol/L) | Observation |
|---|---|---|---|
| 0 | 108.2 | 7.5 | (Scavenger added) |
| 1 | 100.7 | 7.3 | No Precipitation |
| 2 | 101.5 | 7.0 | No Precipitation |
| 3 | 101.1 | 6.5 | No Precipitation |
| 4 | 100.7 | 6.4 | No Precipitation |
| 5 | 96.9 | 6.0 | Precipitation |
| 6 | 102.6 | 6.2 | Precipitation |
| 7 | 100.3 | 5.8 | Precipitation |
| 22.5 | 110.1 | 2.7 | Precipitation |
| 34.75 | 106.1 | 0.6 | Precipitation |
| 50 | 95.5 | 0.4 | Precipitation |

**Table 35: REE concentrations with Eu/Y ratio 1:15 versus illumination time.**

| Illumination time (h) | $C_{aq, Y}$ (mmol/L) | $C_{aq, Eu}$ (mmol/L) | Observation |
|---|---|---|---|
| 0 | 159.2 | 10.6 | (Scavenger added) |
| 1 | 162.6 | 10.4 | No Precipitation |
| 2 | 157.4 | 10.1 | No Precipitation |
| 3 | 156.9 | 9.7 | No Precipitation |
| 4 | 155.5 | 9.6 | No Precipitation |
| 5 | 154.5 | 9.0 | No Precipitation |
| 6 | 160.2 | 8.8 | No Precipitation |
| 7 | 159.3 | 8.5 | Precipitation |
| 10 | 153.5 | 7.7 | Precipitation |
| 22.5 | 155.6 | 4.5 | Precipitation |
| 29.5 | 150.2 | 2.3 | Precipitation |
| 34.75 | 157.4 | 1.3 | Precipitation |
| 72 | 154.2 | 0.7 | Precipitation |

**Table 36: REE concentrations with Eu/Y ratio 1:18 versus illumination time.**

| Illumination time (h) | $C_{aq, Y}$ (mmol/L) | $C_{aq, Eu}$ (mmol/L) | Observation |
|---|---|---|---|
| 0 | 192.9 | 11.5 | (Scavenger added) |
| 4 | 185.6 | 10.5 | No Precipitation |
| 7 | 187.2 | 10.3 | No Precipitation |
| 10 | 176.9 | 8.8 | No Precipitation |
| 29.5 | 177.5 | 4.6 | Precipitation |
| 34.75 | 189.4 | 1.5 | Precipitation |
| 72 | 189.5 | 1.0 | Precipitation |

**Table 37: REE concentrations with Eu/Y ratio 1:20 versus illumination time.**

| Illumination time (h) | $C_{aq, Y}$ (mmol/L) | $C_{aq, Eu}$ (mmol/L) | Observation |
|---|---|---|---|
| 0 | 173.8 | 9.0 | (Scavenger added) |
| 10 | 168.7 | 7.3 | No Precipitation |
| 30.5 | 152.9 | 3.4 | Precipitation |
| 32.25 | 160.6 | 3.5 | Precipitation |
| 34 | 161.1 | 2.3 | Precipitation |
| 35.25 | 171.5 | 2.3 | Precipitation |
| 48 | 172.9 | 1.3 | Precipitation |
| 51.25 | 163.1 | 1.0 | Precipitation |
| 72 | 169.6 | 0.7 | Precipitation |

**Table 38: REE concentrations with Eu/Gd ratio 1:30 versus illumination time.**

| Illumination time (h) | $C_{aq, Gd}$ (mmol/L) | $C_{aq, Eu}$ (mmol/L) | Observation |
|---|---|---|---|
| 0 | 158.4 | 5.1 | (Scavenger added) |
| 13 | 157.7 | 5.0 | No precipitation |
| 15 | 157.1 | 5.0 | No precipitation |
| 18 | 152.3 | 5.0 | No precipitation |
| 22 | 152.1 | 5.0 | No precipitation |
| 40.5 | 150.1 | 4.6 | No precipitation |
| 45.5 | 138.0 | 4.5 | No precipitation |
| 67 | 145.7 | 4.0 | No precipitation |
| 70 | 152.7 | 3.8 | No precipitation |
| 72 | 153.3 | 3.8 | No precipitation |
| 87 | 151.3 | 3.4 | Precipitation |

# Appendix F

The measured irradiances of the various light sources are listed in Table 39 for the wavelengths inducing the forward reaction, respectively Table 40 for the backward reaction.

**Table 39: Irradiances of the various light sources in μW/cm² as function of the distance. Wavelengths range: 200-260 nm.**

| Distance (cm) | 0 | 5 | 10 | 15 |
|---|---|---|---|---|
| Bright 11 W lamp | 866 | 411 | 321 | 249 |
| Blackened 11 W lamp | 497 | 295 | 207 | 165 |
| Lamp with reflector | 2136 | 1045 | 904 | 612 |
| 40 W lamp(185 nm & 254 nm) | 3002 | 1553 | 1155 | 805 |
| 40 W lamp(254 nm) | 2098 | 989 | 759 | 675 |
| 60 W lamp | 25335 | 7934 | 3430 | - |
| LED | 40700 | - | - | - |

**Table 40: Irradiances of the various light sources in μW/cm² as function of the distance. Wavelengths range: 360-370 nm.**

| Distance (cm) | 0 | 5 | 10 | 15 |
|---|---|---|---|---|
| Bright 11 W lamp | 96 | 52 | 40 | 17 |
| Blackened 11 W lamp | 64 | 30 | 12 | 7 |
| Lamp with reflector | 247 | 100 | 62 | 30 |
| 40 W lamp(185 nm & 254 nm) | 2098 | 989 | 759 | 675 |
| 40 W lamp(254 nm) | 459 | 260 | 175 | 121 |
| 60 W lamp | 5686 | 1653 | 808 | - |
| LED | 0 | - | - | - |

# Appendix G

The europium and yttrium concentrations of the mixture illuminated in section 9.7 are listed in Table 41 and Table 42.

**Table 41: REE concentrations versus illumination time for the bright 11 W LPML.**

| Illumination time (h) | $C_{aq, Y}$ (mmol/L) | $C_{aq, Eu}$ (mmol/L) | Observation |
|---|---|---|---|
| 0 | 8.4 | 10.5 | (Scavenger added) |
| 1 | 8.2 | 9.1 | No precipitation |
| 14 | 8.0 | 5.9 | Precipitation |
| 15 | 7.8 | 5.2 | Precipitation |
| 16 | 7.8 | 3.7 | Precipitation |
| 18 | 8.2 | 3.8 | Precipitation |
| 24 | 8.1 | 2.1 | Precipitation |
| 25 | 8.3 | 1.5 | Precipitation |

**Table 42: REE concentrations versus illumination time for the blackened 11 W LPML.**

| Illumination time (h) | $C_{aq, Y}$ (mmol/L) | $C_{aq, Eu}$ (mmol/L) | Observation |
|---|---|---|---|
| 0 | 6.8 | 8.8 | (Scavenger added) |
| 1 | 6.1 | 7.9 | No precipitation |
| 2 | 5.6 | 8.1 | No precipitation |
| 3 | 5.9 | 7.2 | No precipitation |
| 4 | 6.3 | 7.5 | No precipitation |
| 5 | 5.1 | 7.9 | No precipitation |
| 6 | 6.8 | 7.1 | No precipitation |
| 7 | 6.2 | 6.8 | Precipitation |
| 8 | 5.5 | 6.7 | Precipitation |
| 9 | 5.4 | 7.0 | Precipitation |
| 10 | 6.5 | 7.0 | Precipitation |
| 11 | 6.4 | 6.8 | Precipitation |
| 12 | 6.0 | 6.7 | Precipitation |
| 13 | 5.0 | 6.3 | Precipitation |
| 14 | 5.7 | 5.7 | Precipitation |
| 15 | 5.8 | 5.4 | Precipitation |
| 16 | 7.0 | 5.1 | Precipitation |
| 17 | 6.7 | 4.9 | Precipitation |
| 18 | 6.7 | 4.9 | Precipitation |
| 19 | 7.2 | 4.5 | Precipitation |
| 20 | 7.2 | 4.7 | Precipitation |
| 21 | 6.2 | 4.3 | Precipitation |
| 22 | 5.8 | 4.2 | Precipitation |
| 24 | 5.9 | 3.3 | Precipitation |
| 25 | 5.4 | 2.7 | Precipitation |
| 48 | 7.2 | 0.4 | Precipitation |
| 72 | 7.0 | 0.1 | Precipitation |
| 96 | 6.9 | 0.2 | Precipitation |

# Appendix H

The Eu/Y concentrations of experiment 9.8 are listed in Table 43 to Table 55.

## Concentrations Mixture A

**Table 43: REE concentrations mixture A versus illumination time (reflector lamp).**

| Illumination time (h) | $C_{aq, Y}$ (mmol/L) | $C_{aq, Eu}$ (mmol/L) | Observation |
|---|---|---|---|
| 0 | 7.8 | 8.6 | (Scavenger added) |
| 1 | 7.0 | 8.4 | No precipitation |
| 3 | 7.5 | 8.3 | No precipitation |
| 4 | 7.5 | 8.3 | No precipitation |
| 5 | 7.1 | 8.1 | No precipitation |
| 6 | 7.5 | 7.9 | No precipitation |
| 7 | 7.3 | 7.9 | No precipitation |
| 8 | 7.2 | 7.7 | Precipitation |
| 9 | 7.3 | 8.0 | Precipitation |
| 10 | 7.0 | 7.2 | Precipitation |
| 11 | 6.8 | 7.2 | Precipitation |
| 12 | 7.1 | 7.1 | Precipitation |
| 13 | 7.2 | 7.5 | Precipitation |
| 14 | 6.4 | 6.4 | Precipitation |
| 15 | 6.9 | 6.5 | Precipitation |
| 16 | 5.7 | 6.2 | Precipitation |
| 17 | 6.5 | 6.4 | Precipitation |
| 18 | 7.0 | 6.3 | Precipitation |
| 19 | 6.4 | 6.2 | Precipitation |
| 20 | 6.1 | 6.2 | Precipitation |
| 21 | 6.1 | 5.9 | Precipitation |
| 22 | 5.8 | 5.7 | Precipitation |
| 24 | 6.1 | 5.3 | Precipitation |
| 25 | 5.6 | 5.2 | Precipitation |
| 48 | 6.2 | 1.3 | Precipitation |
| 72 | 7.1 | 1.6 | Precipitation |
| 96 | 7.0 | 1.6 | Precipitation |

**Table 44: REE concentrations mixture A versus illumination time (40 W lamp).**

| Illumination time (h) | $C_{aq, Y}$ (mmol/L) | $C_{aq, Eu}$ (mmol/L) | Observation |
|---|---|---|---|
| 0 | 7.8 | 8.6 | (Scavenger added) |
| 1 | 7.5 | 8.4 | No precipitation |
| 2 | 7.4 | 7.8 | No precipitation |
| 3 | 7.2 | 7.7 | No precipitation |
| 4 | 7.5 | 8.1 | No precipitation |
| 5 | 7.4 | 8.3 | No precipitation |
| 6 | 7.2 | 8.1 | No precipitation |
| 8 | 7.2 | 8.0 | No precipitation |
| 9 | 6.8 | 7.8 | No precipitation |
| 11 | 7.2 | 7.8 | No precipitation |
| 12 | 7.2 | 7.7 | No precipitation |
| 13 | 7.1 | 7.7 | No precipitation |
| 15 | 6.9 | 7.7 | No precipitation |
| 16 | 6.8 | 7.7 | No precipitation |
| 18 | 7.0 | 6.9 | No precipitation |
| 19 | 7.1 | 6.8 | No precipitation |
| 20 | 7.1 | 6.8 | No precipitation |
| 24 | 6.8 | 5.6 | Precipitation |
| 25 | 6.7 | 5.6 | Precipitation |
| 48 | 7.4 | 0.6 | Precipitation |
| 72 | 6.6 | 0.8 | Precipitation |
| 96 | 7.6 | 0.7 | Precipitation |

**Table 45: REE concentrations mixture A versus illumination time (60 W lamp).**

| Illumination time (h) | $C_{aq, Y}$ (mmol/L) | $C_{aq, Eu}$ (mmol/L) | Observation |
|---|---|---|---|
| 0 | 7.8 | 8.6 | (Scavenger added) |
| 1 | 7.2 | 7.7 | No precipitation |
| 2 | 7.1 | 7.9 | No precipitation |
| 3 | 7.0 | 8.0 | No precipitation |
| 4 | 7.1 | 8.2 | No precipitation |
| 6 | 7.1 | 7.9 | No precipitation |
| 8 | 7.0 | 7.8 | No precipitation |
| 9 | 6.5 | 7.8 | No precipitation |
| 12 | 6.8 | 8.0 | No precipitation |
| 13 | 7.0 | 8.0 | No precipitation |
| 15 | 6.8 | 7.9 | No precipitation |
| 16 | 7.0 | 7.7 | No precipitation |
| 18 | 6.5 | 7.9 | No precipitation |
| 19 | 7.5 | 7.9 | No precipitation |
| 20 | 7.0 | 7.8 | No precipitation |
| 24 | 7.0 | 4.8 | Precipitation |
| 25 | 6.0 | 4.0 | Precipitation |
| 48 | 5.9 | 3.3 | Precipitation |
| 72 | 7.4 | 3.6 | Precipitation |
| 96 | 6.3 | 3.2 | Precipitation |

## Concentrations Mixture B

**Table 46: REE concentrations mixture B versus illumination time (reflector lamp).**

| Illumination time (h) | $C_{aq, Y}$ (mmol/L) | $C_{aq, Eu}$ (mmol/L) | Observation |
|---|---|---|---|
| 0 | 67.2 | 7.6 | (Scavenger added) |
| 1 | 60.2 | 7.4 | No precipitation |
| 2 | 64.8 | 7.2 | No precipitation |
| 3 | 63.7 | 7.0 | No precipitation |
| 4 | 63.3 | 6.6 | No precipitation |
| 6 | 67.6 | 7.3 | No precipitation |
| 7 | 65.3 | 6.7 | No precipitation |
| 8 | 65.0 | 6.7 | No precipitation |
| 11 | 67.0 | 6.6 | No precipitation |
| 12 | 67.9 | 6.6 | No precipitation |
| 13 | 67.7 | 6.5 | Precipitation |
| 14 | 68.0 | 5.6 | Precipitation |
| 15 | 68.6 | 5.3 | Precipitation |
| 16 | 67.0 | 5.3 | Precipitation |
| 17 | 67.7 | 5.8 | Precipitation |
| 18 | 65.6 | 5.2 | Precipitation |
| 19 | 62.0 | 5.8 | Precipitation |
| 20 | 60.1 | 4.7 | Precipitation |
| 22 | 64.8 | 4.8 | Precipitation |
| 24 | 61.8 | 4.5 | Precipitation |
| 48 | 66.1 | 3.0 | Precipitation |
| 72 | 76.7 | 3.1 | Precipitation |
| 96 | 71.4 | 2.7 | Precipitation |

**Table 47: REE concentrations mixture B versus illumination time (40 W lamp).**

| Illumination time (h) | $C_{aq, Y}$ (mmol/L) | $C_{aq, Eu}$ (mmol/L) | Observation |
|---|---|---|---|
| 0 | 70.2 | 7.6 | (Scavenger added) |
| 1 | 71.0 | 7.3 | No precipitation |
| 2 | 71.0 | 7.1 | No precipitation |
| 3 | 63.0 | 7.0 | No precipitation |
| 4 | 61.5 | 7.3 | No precipitation |
| 6 | 63.3 | 7.5 | No precipitation |
| 8 | 63.4 | 7.3 | No precipitation |
| 10 | 64.2 | 7.1 | No precipitation |
| 11 | 65.9 | 6.9 | No precipitation |
| 12 | 71.0 | 7.1 | No precipitation |
| 13 | 70.0 | 7.1 | No precipitation |
| 14 | 66.7 | 7.0 | No precipitation |
| 15 | 64.4 | 6.2 | No precipitation |
| 16 | 76.2 | 6.2 | No precipitation |
| 17 | 72.7 | 6.2 | No precipitation |
| 18 | 70.5 | 6.2 | No precipitation |
| 19 | 72.0 | 6.2 | No precipitation |
| 24 | 60.1 | 5.1 | Precipitation |
| 25 | 66.2 | 4.7 | Precipitation |
| 48 | 68.9 | 4.5 | Precipitation |
| 72 | 69.1 | 4.1 | Precipitation |
| 96 | 62.7 | 3.2 | Precipitation |

**Table 48: REE concentrations mixture B versus illumination time (60 W lamp).**

| Illumination time (h) | $C_{aq, Y}$ (mmol/L) | $C_{aq, Eu}$ (mmol/L) | Observation |
|---|---|---|---|
| 0 | 70.2 | 7.6 | (Scavenger added) |
| 1 | 66.2 | 6.8 | No precipitation |
| 2 | 52.1 | 6.1 | No precipitation |
| 3 | 57.1 | 6.0 | No precipitation |
| 4 | 58.0 | 6.1 | No precipitation |
| 6 | 60.6 | 6.0 | No precipitation |
| 8 | 59.1 | 6.0 | No precipitation |
| 9 | 54.8 | 5.8 | No precipitation |
| 13 | 51.8 | 5.5 | No precipitation |
| 14 | 55.2 | 5.7 | No precipitation |
| 15 | 56.2 | 5.7 | No precipitation |
| 16 | 67.0 | 5.6 | No precipitation |
| 17 | 60.0 | 5.7 | No precipitation |
| 18 | 59.6 | 5.6 | No precipitation |
| 19 | 61.2 | 4.5 | No precipitation |
| 20 | 60.1 | 4.0 | No precipitation |
| 48 | 69.9 | 2.3 | Precipitation |
| 72 | 57.6 | 1.0 | Precipitation |
| 96 | 70.0 | 1.7 | Precipitation |

## Concentrations Mixture C

**Table 49: REE concentrations mixture C versus illumination time (Blackened 11 W LPML).**

| Illumination time (h) | $C_{aq, Y}$ (mmol/L) | $C_{aq, Eu}$ (mmol/L) | Observation |
|---|---|---|---|
| 0 | 6.8 | 8.8 | (Scavenger added) |
| 1 | 6.1 | 7.9 | No precipitation |
| 2 | 5.6 | 8.1 | No precipitation |
| 3 | 5.9 | 7.2 | No precipitation |
| 4 | 6.3 | 7.5 | No precipitation |
| 5 | 5.1 | 7.9 | No precipitation |
| 6 | 6.8 | 7.1 | No precipitation |
| 7 | 6.2 | 6.8 | Precipitation |
| 8 | 5.6 | 6.7 | Precipitation |
| 9 | 5.4 | 7.0 | Precipitation |
| 10 | 6.5 | 7.0 | Precipitation |
| 11 | 6.4 | 6.8 | Precipitation |
| 12 | 6.0 | 6.7 | Precipitation |
| 13 | 5.0 | 6.3 | Precipitation |
| 14 | 5.7 | 5.7 | Precipitation |
| 15 | 5.8 | 5.4 | Precipitation |
| 16 | 7.0 | 5.1 | Precipitation |
| 17 | 6.7 | 4.9 | Precipitation |
| 18 | 6.7 | 4.9 | Precipitation |
| 19 | 7.2 | 4.5 | Precipitation |
| 20 | 7.2 | 4.7 | Precipitation |
| 21 | 6.2 | 4.3 | Precipitation |
| 22 | 5.8 | 4.2 | Precipitation |
| 24 | 5.9 | 3.3 | Precipitation |
| 25 | 5.4 | 2.7 | Precipitation |
| 48 | 7.3 | 0.4 | Precipitation |
| 72 | 7.0 | 0.1 | Precipitation |
| 96 | 6.9 | 0.2 | Precipitation |

**Table 50: REE concentrations mixture C versus illumination time (40 W lamp).**

| Illumination time (h) | $C_{aq, Y}$ (mmol/L) | $C_{aq, Eu}$ (mmol/L) | Observation |
|---|---|---|---|
| 0 | 6.8 | 8.8 | (Scavenger added) |
| 1 | 6.0 | 8.0 | No precipitation |
| 3 | 5.6 | 8.5 | No precipitation |
| 4 | 5.7 | 8.0 | No precipitation |
| 5 | 5.9 | 7.6 | No precipitation |
| 6 | 5.7 | 8.4 | No precipitation |
| 7 | 6.1 | 7.8 | No precipitation |
| 8 | 6.2 | 8.3 | No precipitation |
| 9 | 5.5 | 7.7 | No precipitation |
| 10 | 6.3 | 7.8 | No precipitation |
| 11 | 6.1 | 7.7 | No precipitation |
| 13 | 5.7 | 7.1 | No precipitation |
| 14 | 5.9 | 7.2 | No precipitation |
| 15 | 6.1 | 7.7 | No precipitation |
| 16 | 6.0 | 7.5 | No precipitation |
| 17 | 5.5 | 7.1 | No precipitation |
| 20 | 6.2 | 7.1 | No precipitation |
| 21 | 6.2 | 6.9 | No precipitation |
| 22 | 6.3 | 6.7 | No precipitation |
| 24 | 6.3 | 6.4 | No precipitation |
| 25 | 6.2 | 6.2 | No precipitation |
| 48 | 6.8 | 3.4 | Precipitation |
| 72 | 6.6 | 0.9 | Precipitation |
| 96 | 7.3 | 0.8 | Precipitation |

**Table 51: REE concentrations mixture C versus illumination time (60 W lamp).**

| Illumination time (h) | $C_{aq, Y}$ (mmol/L) | $C_{aq, Eu}$ (mmol/L) | Observation |
|---|---|---|---|
| 0 | 6.8 | 8.8 | (Scavenger added) |
| 1 | 5.9 | 7.8 | No precipitation |
| 2 | 5.9 | 7.8 | No precipitation |
| 3 | 5.6 | 7.9 | No precipitation |
| 4 | 5.4 | 7.1 | No precipitation |
| 5 | 6.7 | 7.8 | No precipitation |
| 6 | 6.0 | 7.2 | No precipitation |
| 7 | 5.4 | 7.0 | No precipitation |
| 8 | 6.1 | 7.2 | No precipitation |
| 9 | 5.3 | 6.8 | No precipitation |
| 10 | 6.3 | 6.3 | Precipitation |
| 11 | 6.0 | 6.6 | Precipitation |
| 12 | 5.80 | 6.12 | Precipitation |
| 13 | 5.77 | 6.54 | Precipitation |
| 14 | 6.04 | 6.26 | Precipitation |
| 15 | 6.47 | 6.63 | Precipitation |
| 16 | 6.14 | 6.04 | Precipitation |
| 17 | 6.03 | 5.91 | Precipitation |
| 18 | 6.16 | 5.54 | Precipitation |
| 19 | 5.91 | 5.54 | Precipitation |
| 20 | 5.97 | 5.17 | Precipitation |
| 21 | 6.56 | 5.69 | Precipitation |
| 22 | 6.80 | 4.84 | Precipitation |
| 24 | 6.78 | 4.78 | Precipitation |
| 25 | 5.84 | 4.82 | Precipitation |
| 48 | 5.93 | 1.47 | Precipitation |
| 72 | 6.55 | 0.75 | Precipitation |
| 96 | 6.05 | 0.30 | Precipitation |

## Concentrations Mixture D

**Table 52: REE concentrations mixture D versus illumination time (Bright 11 W LPML).**

| Illumination time (h) | $C_{aq, Y}$ (mmol/L) | $C_{aq, Eu}$ (mmol/L) | Observation |
|---|---|---|---|
| 0 | 6.9 | 8.6 | (Scavenger added) |
| 1 | 6.7 | 6.5 | Precipitation |
| 2 | 6.3 | 5.7 | Precipitation |
| 3 | 7.0 | 3.2 | Precipitation |
| 4 | 6.0 | 3.1 | Precipitation |
| 5 | 6.7 | 1.7 | Precipitation |
| 6 | 5.9 | 0.8 | Precipitation |
| 8 | 6.9 | 0.7 | Precipitation |
| 9 | 6.0 | 0.4 | Precipitation |
| 10 | 6.6 | 0.6 | Precipitation |
| 12 | 7.0 | 0.3 | Precipitation |
| 14 | 6.3 | 0.4 | Precipitation |
| 15 | 6.4 | 0.3 | Precipitation |
| 16 | 6.5 | 0.4 | Precipitation |
| 17 | 6.5 | 0.4 | Precipitation |
| 18 | 6.4 | 0.4 | Precipitation |
| 19 | 7.0 | 0.4 | Precipitation |
| 20 | 6.8 | 0.4 | Precipitation |
| 21 | 6.8 | 0.3 | Precipitation |
| 22 | 6.3 | 0.4 | Precipitation |
| 24 | 6.9 | 0.2 | Precipitation |
| 25 | 6.1 | 0.3 | Precipitation |
| 48 | 6.1 | 0.2 | Precipitation |
| 72 | 5.9 | 0.1 | Precipitation |
| 96 | 6.4 | 0.1 | Precipitation |

**Table 53: REE concentrations mixture D versus illumination time (Lamp with reflector).**

| Illumination time (h) | $C_{aq, Y}$ (mmol/L) | $C_{aq, Eu}$ (mmol/L) | Observation |
|---|---|---|---|
| 0 | 6.9 | 8.6 | (Scavenger added) |
| 1 | 6.5 | 7.9 | No precipitation |
| 3 | 5.8 | 8.0 | No precipitation |
| 4 | 5.8 | 7.9 | No precipitation |
| 5 | 6.3 | 8.3 | No precipitation |
| 6 | 6.6 | 7.7 | No precipitation |
| 8 | 5.8 | 7.9 | No precipitation |
| 9 | 6.1 | 7.4 | No precipitation |
| 13 | 6.1 | 7.6 | No precipitation |
| 18 | 6.8 | 7.6 | No precipitation |
| 20 | 5.9 | 7.4 | No precipitation |
| 21 | 6.2 | 7.7 | No precipitation |
| 22 | 6.7 | 6.6 | No precipitation |
| 24 | 6.5 | 6.6 | Precipitation |
| 25 | 6.1 | 6.4 | Precipitation |
| 48 | 7.1 | 3.8 | Precipitation |
| 72 | 6.7 | 2.5 | Precipitation |
| 96 | 7.0 | 0.7 | Precipitation |

**Table 54: REE concentrations mixture D versus illumination time (40 W lamp).**

| Illumination time (h) | $C_{aq, Y}$ (mmol/L) | $C_{aq, Eu}$ (mmol/L) | Observation |
|---|---|---|---|
| 0 | 6.9 | 8.6 | (Scavenger added) |
| 1 | 6.5 | 7.6 | No precipitation |
| 3 | 7.0 | 7.6 | No precipitation |
| 4 | 7.9 | 7.7 | No precipitation |
| 5 | 6.8 | 8.0 | No precipitation |
| 6 | 7.0 | 8.0 | No precipitation |
| 8 | 7.0 | 7.9 | No precipitation |
| 9 | 7.1 | 8.3 | No precipitation |
| 10 | 7.0 | 8.3 | No precipitation |
| 15 | 6.5 | 7.9 | No precipitation |
| 18 | 6.1 | 6.8 | No precipitation |
| 24 | 5.8 | 6.1 | No precipitation |
| 25 | 6.1 | 6.4 | No precipitation |
| 48 | 6.6 | 6.2 | No precipitation |
| 72 | 6.1 | 5.7 | No precipitation |
| 96 | 6.5 | 6.4 | No precipitation |

**Table 55: REE concentrations mixture D versus illumination time (60 W lamp).**

| Illumination time (h) | $C_{aq, Y}$ (mmol/L) | $C_{aq, Eu}$ (mmol/L) | Observation |
|---|---|---|---|
| 0 | 6.9 | 8.6 | (Scavenger added) |
| 1 | 6.7 | 8.1 | No precipitation |
| 3 | 6.4 | 7.8 | No precipitation |
| 4 | 6.5 | 8.5 | No precipitation |
| 5 | 7.0 | 8.1 | No precipitation |
| 6 | 6.4 | 8.3 | No precipitation |
| 8 | 6.0 | 8.4 | No precipitation |
| 9 | 5.8 | 8.5 | No precipitation |
| 12 | 6.8 | 8.6 | No precipitation |
| 15 | 7.0 | 7.9 | No precipitation |
| 18 | 5.6 | 8.2 | No precipitation |
| 24 | 5.7 | 4.5 | Precipitation |
| 25 | 5.7 | 4.4 | Precipitation |
| 48 | 6.3 | 2.8 | Precipitation |
| 72 | 5.7 | 2.6 | Precipitation |
| 96 | 6.2 | 0.8 | Precipitation |

# References


[1] KU Leuven. Research platform for the advanced recycling and reuse of rare earths platform. http://kuleuven.rare3.eu/ (accessed May 14, 2014).

[2] EPA. *Rare Earth Elements: A Review of Production, Processing, Recycling, and Associated Environmental Issues;* Technical Report 600/R-12/572; EPA: Cincinnati, December 2012.

[3] Gupta, C. K.; Krishnamurthy, N. *Extractive Metallurgy of Rare Earths;* CRC Press: Florida, 2005; pp 1-484.

[4] Ciminelli, V.; Morais, C. A. Recovery of europium by chemical reduction of a commercial solution of europium and Gadolinium chlorides. *Hydrometallurgy* **2001,** *60*, 247-253.

[5] Binnemans, K.; Jones, P. T.; Blanpain, B.; Van Gerven, T.; Yang, Y.; Walton, A.; Buchert, M. Recycling of rare earths: a critical review. *J. Clean. Prod.* **2013**, *51*, 1-22.

[6] Azvedo, B. C.; Luo, Y.; Marçal, A. L.; Matos, M. G.; Zhang, Q. Europium complexes: fundamental and photonic applications. In *Europium Synthesis, Characteristics and Potential Applications;* Moustafa, M., Ed.; Nova Science: New York, 2013; pp 1-22.

[7] Argonne National Laboratory. Europium. http://www.vff-marenostrum.org/Nuntium-Novitatum/PDF/europium.pdf (accessed December 1, 2013).

[8] Emsley, J. Europium. *Nature's Building Blocks. An A-Z Guide to the Elements,* 2; Oxford University Press: Oxford, 2011; pp 139-141.

[9] Drake, M. J.; Weill, D. F. Europium Anomaly in Plagioclase Feldspar: Experimental Results and Semiquantitative Model. *Science* **1973,** *180,* 1059-1060

[10] Oostingh, K. *Analysis of Rare Earth Element concentrations in barite ($BaSO_4$).* MSc-Thesis, Utrecht University, Utrecht, 2011.

[11] Phosphors. In *Kirk-Othmer Encyclopedia of Chemical Technology*, Wiley & Sons: New York, 2007; Vol. 8, pp 256-258.

[12] U.S. Department of Energy. *Critical Materials Strategy;* DOE Report U.S. Government Printing Office: Washington, DC, 2011.

[13] Centralna banka Crne Gore. Sigurnosne oznake. http://www.cb-mn.org/index.php?mn1=novac&mn2=sigurnosne_oznake (accessed May 12, 2014).

[14] Jeona, D. Y.; Kanga, J. H.; Muresanb, L.; Nazarova, M. V.; Popovicib, E. J.; Tsukerblat, B. S. Lattice parameter and luminescence properties of europium activated yttrium oxide. *Solid State Commun.* **2005**, *33*, 183-186.

[15] OSRAM. Low pressure gas discharge for fluorescent and compact fluorescent

lamps. http://www.osram.com/osram_com/news-and-knowledge/fluorescent-lamps/professional-knowledge/low-pressure-gas-discharge/index.jsp (accessed November 19, 2013).
[16] EPA. Basic information about recycling mercury-containing light bulbs (Lamps). http://www.epa.gov/osw/hazard/wastetypes/universal/lamps/basic.htm (accessed November 19, 2013).
[17] *Physics and Chemistry of Luminescent Materials;* Ronda, C. R., Shea, L. E., Srivastava, M., Eds.; The Electrochemical Society: New Jersey, 2000.
[18] Kumar, R.; Ranjan, A.; Roy, S. Lightning: A new concept on re-utilization of fused fluorescent lamp. *Journal of Theoretical and Applied Information Technology* **2005***, 21*, 12-17.
[19] He, S. Emission and Excitation Mechanisms of Phosphors. In *Luminescence,* He, S.; Ronda, C.; WILEY-VCH. : Weinheim, 2008, 1-34
[20] Jüstel, T.; Ronda, C. C.; Srivastava, A. M.; Suijver, F. J.; Vergeer, P. In *Luminescence;* Ronda, C. C., Ed.; Wiley-VCH: Weinheim, 2008.
[21] Jones, E. D. *Light-Emitting Diodes (LEDs) for General Illumination;* Report for Optoelectronics industry development association (OIDA): Washington, DC, March 2001.
[22] *Encyclopedic Dictionary of Condensed Matter Physics*, Poole, C.P., Ed.; Elsevier Inc.: San Diego, 2004; Vol.1.
[23] Jeon, D. Y.; Kangb, J. H.; Shina, S. H.; Zang, D. S. Enhancement of cathodoluminescence intensities of $Y_2O_3$:Eu and $Gd_2O_3$:Eu phosphors by incorporation of Li ions. *J. Lumin*. **2005,** *114,* 275–280.
[24] Sommerer, T. J.; Srivastava, A. M. Fluorescent lamp phosphors. *Elec. Soc. Int.* **1998,** *7,* 28-31.
[25] Djerdj, I.; Furic, K.; Gajovic, A.; Su, D. S.; Tomasic, N. Influence of mechanomchemical processing to luminescence properties in $Y_2O_3$ powder. *J. Alloys Compd*. **2008***, 456*, 313-319.
[26] Jüstel, T.; Nikol, H.; Ronda, C. R. Rare earth phosphors: fundamentals and applications. *J. Alloys Compd.* **1998** *, 277*, 669–676.
[27] Ban, G.; Forest, H. Evidence for Eu Emission from Two Symmetry Sites in $Y_2O_3$:$Eu^{+3}$. *J. Electrochem. Soc.* **1969,** *116, 4974.*
[28] Mazza, M.; Blumenthal, D.; Schmitt, G.J. *Ensuring Japan's Citical Resource Security: Case studies in rare earth element and natural gas supplies*; Case-Study Report; AEI: Washington, DC, July 2013.
[29] Think Global Green. Rare-earth metals. http://www.thinkglobalgreen.org/rare-earthmetals.html (accessed November 4, 2013).
[30] Alonso, E.; Sherman, A. M.; Wallington, T. J.; Everson, M. P.; Field, F. R.; Roth, R.; Kirchain, R. E. Evaluating Rare Earth Element Availability: A Case with Revolutionary Demand from Clean Technologies. *Environ. Sci. Technol*. **2012**, *46,* 3406-3414.
[31] Falconnet, P. The economics of rare earths. *J. Less-Common Met.* **1985,** *111,* 9-15.
[32] Houses of Parliament. *Rare Earth Metals;* PostNote 368; The Parliamentary Office of Science and Technology: London, 2011, 1-4
[33] Bradsher, K. After China's Rare Earth Embargo, a New Calculus. *The New York Times*, Oct 29, 2010, p. B1.

[34] WTO, China files notice of appeal in rare earth disputes. http://www.wto.org/english/news_e/news14_e/ds432_433apl_25apr14_e.htm (accessed May 2, 2014).
[35] Jolly, D. China export restrictions on metals violate global trade law, panel finds. *The New York Times*, March 27, 2014, p. B3.
[36] Clapper, J. R. (2013). *Worldwide Threat Assesment of the US Intelligence Community;* Statement for the Record; US Intelligence Community: Virginia, March 2013, 1-30.
[37] Buchert, M.; Dittrich, S.; Liu , R.; Merz, C.; Schüler, D. (2011). *Study on Rare Earths and Their Recycling.* Final Report for The Greens/EFA Group in the European Parliament; Öko-Institut: Darmstadt, January 2011.
[38] Humphries, M. *Rare Earth Elements: The Global Supply Chain;* CRS Report for Congress; CRS: Washington, DC, December 2013.
[39] Long, K. R.; Van Gosen, B. S.; Foley, N. K.; Cordier, D. *The Principal Rare Earth Element Deposits of the United States—A Summary of Domestic Deposits and a Global Perspective*; Scientific Investigations Report; USGS: Virginia, 2010.
[40] Bras, B.; Meyer, L. Rare earth metal recycling. In *Sustainable system and Technology*, Proceedings of the IEEE International Symposium, Chicago, 16-18 May 2011.
[41] Cuia, D.; Huang, X.; Long, Z.; Wang, L.; Yu, Y.; Xiao, Y. Eliminating ammonia emissions during rare earth separation through control of equilibrium acidity in a HEH(EHP)-Cl system. *Green Chemistry* **2013,** *15,* 1889–1894.
[42] Miranda Jr., P.; Zinner, L. B. Separation of Samarium and gadolinium solutions by solvent extraction. *J. Alloys Compd.* **1997,** *249,* 116-119.
[43] Berthod, A.; Varda-Broch, S. Determination of liquid-liquid partition coefficients by separation methods. *J. Chromatogr.* **2004**, *1037,* 3-14.
[44] Benedict, U. *Book on the Physics and Chemistry of Rare Earths;* Gschneider, K. A., Eyring, L., Eds.; Elsevier Science: Amsterdam, 2000; Vol. 28, pp 320-323.
[45] Solvay. Key Message for the panel 'Separations'. Presented at Conference TMS Toronto [online], Toronto, 21-22 April. Investorintel. http://investorintel.com/wp-content/uploads/2013/05/TMS-panel-separations-A.Leveque.pdf (accessed January 29, 2014).
[46] Hirai, T.; Komasawa, I. Separation of Eu from Eu/Sm/Gd mixture by photoreductive stripping in solvent extraction process. *Ind. Eng. Chem. Res.* **1995,** *34*, 237-241.
[47] Sayed, S. A.; Rabie, K. A.; Salama, I. E. Studies on europium separation from a middle rare earth concentrate by in situ zinc reduction technique. *Sep. Purif. Technol.* **2005,** *46,* 145-154.
[48] Ciminelli, V. S. T.; de Morais, C. A. Europium recovery by photochemical reduction from Eu and Eu-Gd chloride solutions. *Sep. Sci. Technol.* **2002**, *37*, 3305-3321.
[49] Fisher, D. R.; Johnsen, A. M.; McNamara, K.; Soderquist, C. Z. An improved purification process for $^{153}$Gd produced in natural europium targets. Patent PCT/US2011/048269, February 23, 2012.
[50] Ciminelli, V. S. T.; Morais, C. A. Recovery of europium from a rare earth chloride solution. *Hydrometallurgy* **1998,** *49,* 167–177.
[51] Dumousseau, J.; Rollat, A.; Sab, J. Recovery of europium (II) values by electrolysis. U.S. Patent 4,938,852, July 3, 1990.
[52] Kang, X.-H.; Qiu, L.-F.; Wang, T.-S. A Study on Photochemical Separation of Rare

Earths: The Separation of Europium from an Industrial Concentrate Material of Samarium, Europium, and Gadolinium. *Sep. Sci. Technol.* **1991,** *26*, 199-221.
[53] Atanasyants, A. G.; Seryogin , A. N. The reaction of the electrochemical reduction Eu(III)+e+Eu(II) in hydrochloric solution. *Hydrometallurgy* **1997**, *37*, 367-374.
[54] Girginb, I.; Yörükoglua, A. Recovery of europium by electrochemical reduction from sulfate solutions. *Hydrometallurgy* **2002**, *63*, 85-91.
[55] Chung, K. W. Electrochemical reduction of Eu(III) for the recovery of Eu from rare earth materials solution using turbulent-induced cell. In *Materials Science*, Proceedings of the 2nd International Conference and Exhibition on Materials Science & Engineering, Las vegas, USA, October 7-9, 2013; Omics Group: Hyderabad, India, 2013.
[56] Atanasyants, A. G.; Seryogin, A. N. Electrochemical extraction of samarium from mixture of rare earth metals. *Hydrometallurgy* **1997,** *4,* 255-259.
[57] Donohue, T. Photochemical separation of metals in solution by precipitation following reduction or oxidation. U.S. Patent 4,172,775, October 30, 1979.
[58] Donohue, T. Photochemical separation of europium from lanthanide mixtures in aqueous solution. *Chem. Phys. Lett.* **1979**, 601-604.
[59] Yusov, A. B.; Shilov, V. P. *Photochemistry of f-element ions*. Russian Chemical Bulletin, International Edition; Institute of Physical Chemistry: Moscow, December 2000.
[60] Krupta, J. C.; Makhov, V.N. UV-VUV Lasers and Fast Scintillators. In *Physics of Laser Crystals;* Krupta, J., Kulagin, N. Eds.; Kluwer Academic Publishers: Dordrecht, The Netherlands, 2002; pp 23-35.
[61] Hoffmann, D. C.; Nitsche, H.; Schwantes, J. M.; Sudowe, R. Applications of solvent extraction in the high-yield multi-process reduction/separation of Eu from excess Sm. *J. Radioanal. Nucl. Chem.* **2008**, *276*, 543-548.
[62] Von Bergmann, H.; Stamn, U. Principles of Excimer Lasers. *In Excimer Laser Technology*; Basting, D., Marowsky, G. Eds.; Springer: Göttingen, 2004; pp 41-47.
[63] *McGraw-Hill Encyclopedia of Science and Technology*, 9th ed.; McGraw-Hill:New York, 2002; 20 vols.
[64] Heering W. UV sources Basics, Properties and Applications. *IUVA News* **2004**, *6*, 7-13.
[65] Flesch, P. Light and Light Sources: High-Intensity Discharge Lamps; Springer: Berlin, 2006; pp 10-169.
[66] Kołodyńska D.; Zbigniew H. Investigation of Sorption and Separation of Lanthanides on the Ion Exchangers of Various Types. In *Ion Exchange Technologies* [online]; Kilislioglu A. Ed.; InTech: Rijeka, 2012, pp 101-155. http://www.intechopen.com/books/ion-exchange-technologies/investigation-of-sorption-and-separation-of-lanthanides-on-the-ion-exchangers-of-various-types (accessed March 11, 2014).
[67] Donohue, T. Photochemical Separation of europium from lanthanide mixtures in aqueous solution. *J. Chem. Phys.* **1977,** *67*, 5402-5404.
[68] Kusaba, M.; Nakashima, N.; Izawa, Y.; Yamanaka, C.; Kawamura, W. Two-photon reduction of $Eu^{3+}$ to $Eu^{2+}$ via the f-f transitions in methanol. *Chem. Phys. Lett.* **1994**, 407-411.
[69] USGS. Introduction to ICP-MS. crustal.usgs.gov/laboratories/icpms/intro.html

(accessed December 12, 2013).
[70] ThermoFisher. From first principles: An introduction to the ICP-MS technique. http://www.thermo.com/eThermo/CMA/PDFs/Various/File_2512.pdf (accessed December 12, 2013).
[71] Pharmacopeia. Plasma spectrochemistry. http://www.pharmacopeia.cn/v29240/usp29nf24s0_c730.html (accessed December 12, 2013).
[72] Bruker. S2 PICOFOX. http://www.bruker.com/fileadmin/user_upload/8-PDF-Docs/X-rayDiffraction_ElementalAnalysis/TXRF/Brochures/bro_s2_picofox_en_rev3-2_lowres.pdf (accessed December 12, 2013).
[73] Wang, K.; Dung, N. D. T.; Whang, A. J. Prism-Based Sunlight Concentrator layout: A genetic Algorithm Solution. *J. Sol. Energy Eng.* **2013**, *136*, 1-6.
[74] Bruker. *S2 PCOFOX;* User Manual; Bruker AXS Microanalysis GmbH: Berlin, 2008.
[75] AzoOptics. Determining albedo with upwelling and downwelling measurement equipment. http://www.azooptics.com/Article.aspx?ArticleID=634 (accessed April 4, 2014).
[76] Ocean Optics. HG-1 mercury argon calibration light source installation and operation instructions. http://www.oceanoptics.com/technical/hg1.pdf (accessed April 4, 2014).
[77] HyperPhysics. Atomic Spectra. http://hyperphysics.phy-astr.gsu.edu/hbase/class/phscilab/spectra.html (accessed April 2, 2014).
[78] Ocean Optics. QE650000 Spectrometer: Scientific-Grade Spectroscopy in a Small Footprint; Technical Report; Ocean Optics Inc.: Dunedin, USA, 2009.
[79] Ocean Optics. *SpectraSuite: Spectrometer Operating Software;* Installation and Operation Manual; Ocean Optics Inc.: Dunedin, USA, 2009.
[80] Michigan State University. Visible and ultraviolet spectroscopy. http://www2.chemistry.msu.edu/faculty/reusch/virttxtjml/spectrpy/uv-vis/spectrum.htm (accessed May 15, 2014).
[81] Michigan State University. UV-Visible spectroscopy. http://www2.chemistry.msu.edu/faculty/reusch/virttxtjml/spectrpy/uv-vis/uvspec.htm#uv1 (accessed May 15, 2014).
[82] Shimadzu. *Shimadzu recording spectrophotometer 1601;* Instruction Manual; Shimadzu corporation: Kyoto, 1994.
[83] Haire, R. G.; Einsteinium. In *The Chemistry of the Actinide and Transactinide Elements,* 4th ed.; Edelsteln, N. M., Lestern, R. M., Fuger, J. Eds.; Springer: Dodrecht, The Netherlands, 2010; Vol. 6, pp 1607-1608.
[84] Binnemans, K.; Görller-Walrand, C., Adam, J. L. Spectroscopic properties of $Gd^{3+}$-doped fluorozirconate glass. *Chem. Phys. Lett.* **1997**, *280*, 333-338.
[85] *Gmelin Handbuch der Anorganischen Chemie;* Bergmann, H., Hein, H., Hinz, I., Merlet, P., Vetter, U., Eds.; Springler-Verlag: Berlin, 1981.
[86] Bernardo, A.; Giulietti, M. Crystallization by Antisolvent Addition and Cooling. In *Crystallization Science and Technology;* M. Andreeta, Ed.; InTech: Rijeka, Croatia, 2012; pp 380-387.
[87] Stenutz, R. Dielectric constants and refractive index. http://www.stenutz.eu/chem/ (accessed December 6, 2013).
[88] Jaffe, S.; Spedding, F. H. Conductances, Solubilities and ionization constants of some rare earth sulfates in aqueous solutions at 25°. *J. Am. Chem. Soc.* **1954**, *76*,

882-884.
[89] UC Davis. Electrochemistry: The Nernst equation. http://chemwiki.ucdavis.edu/Analytical_Chemistry/Electrochemistry/Electrochemistry_4%3A_The_Nernst_Equation (accessed May 23, 2014).
[90] Byrne H.; Klungness G.D. Comparative hydrolysis behavior of the rare earths and yttrium: the influence of temperature and ionic strength. *Polyhedron* **2000**, *19,* 99-107.
[91] Fisher, D. R.; Johnsen, A. M.; McNamara, K.; Soderquist, C. Z. A non-aqueous reduction process for purifying $^{153}$Gd produced in natural europium targets. *Appl. Radiat. Isot.* **2013**, *82*, 158-165.
[92] Britton, H. T. S. Electrometric studies of the precipitation of hydroxides. Part III. Precipitation in the cerite group of rare earths and of yttrium hydroxide by use of the hydrogen electrode**.** *J. Am. Chem. Soc.* **1925**, *127***,** 2142-2147.
[93] Nazarov, M.; Noh, D. Y. Phosphors based on europium doped oxides and oxysulfides. In *New generation of europium and terbium-activated phosphors: from syntheses to applications;* Pan Stanford Publishing: Singapore, 2011; pp 270-282.
[94] Singh, D.; Singh, L.R. Preparation of $Eu^{3+}$ doped $Y_2O_3$ and core-shell $Y_2O_3$: Eu-$Y_2NO_3$ nanoparticles: Photoluminescence study. *Indian J. Eng. Mater. Sci*. **2009**, *16*, 175-188.
[95] Kavetsky, A. G.; Meleshkov, S. P. Red-Emitting Phosphors. In *Polymers, Phosphors, and Voltaics for Radioisotope Microbatteries;* Bower, E.; Barbanel, Y. A.; Shreter, Y. G.; Bohnert, G. W., Eds.; CRC Press: Florida, 2002; pp 142-148.
[96] Sigma-Aldrich. Yttrium oxide-Europium doped. http://www.sigmaaldrich.com/catalog/product/aldrich/756490?lang=fr&region=BE (accessed November 11, 2013).
[97] Photovoltaic Education Network. Spectral Irradiance. http://pveducation.org/pvcdrom/properties-of-sunlight/spectral-irradiance (accessed April 21, 2014).
[98] Donohue, T. Photochemical separation of cerium from rare earth mixtures in aqueous solution. *Chem. Phys. Lett*. **1978**, *61*, 601-604.
[99] Jørgensen, K. Electron transfer spectra of lanthanide complexes. *Mol. Phys.* **1962,** *5,* 271-277.
[100] Chalmers publication library. Leaching and solvent extraction of rare earth metals from fluorescent lamp waste. http://publications.lib.chalmers.se/publication/192063-leaching-and-solvent-extraction-of-rare-earth-metals-from-fluorescent-lamp-waste (accessed May 14, 2014)
[101] Donohue, T. Laser purification of the rare-earths. *Opt. Eng.* **1979**, *18*, 181-186.
[102] Conner, D. Test results for LED, CFL, and incandescent lamp evaluation. http://www.designingwithleds.com/test-results-for-led-cfl-and-incandescent-lamp-evaluation/ (accessed May 14, 2014).